A METHOD TO DETERMINE FLOOD GENERATING MECHANISM FOR DAM SAFETY ASSESSMENT

Ross D. Zhou, P. Eng, Hatch Ltd., Niagara Falls, Ontario, Canada
C. Richard Donnelly, P. Eng, Hatch Niagara Falls, Ontario, Canada

ABSTRACT:

In any dam safety assessment, it is necessary to establish the inflow design flood (IDF) to ensure that the dam has adequate capacity to handle flood flows up to a point where there is no unacceptable risk to the public if the dam should fail too wordy, clarify. In Ontario, and many other areas in Canada and USA, the inflow design flood may be generated either by high intensity summer storm events or, more commonly, by rain on snowmelt (or simply snowmelt) events depending on the size and location of watershed, local meteorological conditions and other hydrological parameters. In order to determine the critical flood generating mechanism for a dam site, a detailed hydrological model is usually needed in order to simulate both types of flood events. Based on the simulation model, the higher flood generated is selected as the inflow design flood. This procedure can require a significant amount of effort and, therefore, cost.

This paper provides details of a simple, but effective, methodology based on hydrological principles commonly used in dam safety assessments to accurately identify the critical flood generating mechanism for a given dam site using watershed and local meteorological characteristics without going through the detailed hydrological modeling processes. This procedure will allow hydrologists and hydro-technical engineers to focus on the evaluation of the critical flood generating events leading to reduced time and efforts in the performance of hydrological analyses of accurate and reliable dam safety assessments.

RÉSUMÉ

Lors de l'évaluation de la sécurité d'un barrage, on doit établir le débit d'évacuation de la crue pour lequel le barrage est conçu afin de s'assurer que la capacité du barrage est adéquate pour soutenir le débit des crues dans une mesure suffisante pour ne pas exposer le public à des risques inacceptables en cas de rupture du barrage. En Ontario et dans bon nombre d'autres régions du Canada et des États-Unis, le débit d'évacuation de la crue pour lequel le barrage est conçu peut être généré par des événements pluvio-hydrologiques estivaux de forte intensité ou, plus couramment, par des événements de précipitations sur la neige (ou simplement par la fonte des neiges), selon la taille et l'emplacement du bassin hydrologique, les conditions météorologiques locales et d'autres paramètres hydrologiques. Pour déterminer les mécanismes de formation des crues critiques pour un site de barrage, on doit habituellement avoir recours à un modèle hydrologique détaillé afin de simuler les deux types d'événements de crues. En fonction du modèle de simulation, la crue générée la plus élevée est sélectionnée comme le débit d'évacuation de la crue pour lequel le barrage est conçu. Cette procédure peut nécessiter des efforts considérables et, conséquemment, entraîner des coûts élevés.

Le présent document décrit une méthode simple, mais efficace fondée sur des principes hydrologiques couramment employés lors des évaluations de la sécurité des barrages afin de déterminer avec précision le mécanisme de formation des crues critiques pour un site de barrage donné. Cette méthode s'appuie sur les caractéristiques du bassin hydrologique et les conditions météorologiques locales, sans toutefois recourir aux procédés de modélisation hydrologique détaillée. Elle permet aux hydrologues ainsi qu'aux ingénieurs hydrotechniciens de se concentrer sur l'évaluation des événements de formation des crues critiques, ce qui réduit le temps et les efforts nécessaires à la réalisation d'analyses hydrologiques pour l'évaluation précise et fiable de la sécurité des barrages.

1. INTRODUCTION

The determination of inflow design flood (IDF) is a critical requirement in any dam safety assessment. Hydrologists and engineers are often asked to estimate the magnitude and the associated runoff hydrograph of the inflow design flood for a dam based on available meteorological information, watershed size and characteristics and, if available, historical stream flow records. The spillway capacity of the dam will then be evaluated using the inflow design flood. If the spillway capacity is not large enough to pass the IDF, major modifications may be required to meet the dam safety requirement. The cost of spillway enlargements that might be required can be very significant. The accuracy of inflow design flood estimates, therefore, affects the decision of the dam owner.

In Ontario, historical flood records show that inflow design flood can result either from summer storm generated runoff events or from spring snowmelt flood events or from both mechanisms. In the determination of inflow design flood, hydrologists and engineers have to know which flood generating mechanism will result in the critical flood conditions for a dam site before the flood magnitude estimation can be made.

However, there is, currently, no well established procedure for the determination of the critical flood generating mechanism. For this reason, hydrologists and engineers have to analyze both conditions and then select the higher flood as the IDF in a dam safety assessment. It is well known that flood hydrological analyses are quite time consuming.

It would therefore be helpful if a simple, theoretical or 'physically' based, but effective procedure is available for identification of the critical flood generating mechanism allowing the hydrologists and engineers to focus on the critical flood generating mechanics to make estimations only for this condition thereby reducing the time and effort expended to complete a dam safety assessment.

This paper presents a simple procedure to fill this need. Following this step by step procedure allows the most likely flood generating process for a particular dam site to be established. Section 2 reviews the current knowledge for this topic and discusses the potential application of these concepts. Section 3 develops the basic set of equations used in the procedure and discusses the limitation of the method. Section 4 discusses the unique watershed performance of some of the watersheds in Ontario and the implications of this performance on flood generating processes. Section 5 uses an example to show the usefulness of the proposed method. Finally section 6 discusses the conclusions obtained from the development of the procedure.

2. CURRENT KNOWLEDGE IN THIS AREA

Flood typology is among the most active research area in catchment hydrology. It is known that the flood generating processes are complex and controlled by a number of variables including precipitation pattern, snowmelt, properties of the catchment and the state of the catchment and the interactions among these variables (Merz and Blöschl, 2003).

The National Research Council Canada (NRCC) (1989) pointed out that the factors affecting the importance of snowmelt contributions relative to storm rainfall include basin size, accumulated snowpack on the ground at the time of flooding, basin storage and the return period of the event. NRCC uses basin size as the main indicator of dominating flood generating mechanism for different watersheds. NRCC pointed out that the annual maximum flood occurs as a result of storm rainfall for all return periods for small, especially small urban watersheds with minimum basin storage. For very large basins, with large distributed storage and moderate accumulated snowpack at the time of the spring thaw, the annual maximum flood is the result of snowmelt or rain on snowmelt events. NRCC also realized that, between the two extremes, lie many of the catchment basins for which the annual maximum flood can be the result of either storm induced or snowmelt resulted event. Carefully examining the above discussions will lead one to have the following question: how large should a watershed be to classify it as a large, medium and small catchment? And based on the current understanding of watershed behaviour, the above classification leaves some questions unanswered since it is known that under the same climate input and initial conditions, catchments with the same size may perform differently which means that

basin shape, main river length, size and slope, and the basin topographical conditions also play an important role in flood generation. Therefore, basin size is not the only indicator. Hydrologists and engineers can not use basin size alone to determine the type of flood for generating a critical flood for a particular catchment. The problem is more complex. A better physically based method is needed.

Stoddart and Watt (1970) suggested that two separate flood frequency analyses shall be undertaken, one for snowmelt floods and one for storm induced floods. However, this can only be done at sites where there are stream flow records. If the inflow design flood must be estimated based on hydrological modelling approach, the two flood frequency curve concept can not be applied. Another problem is that statistical analysis presents the results of the design flood events but it does not reveal the causes of the event and hence, it does not contribute to the understanding of the physical processes.

Using the two flood frequency curve concept, NRCC (1989) outlined four cases that may be important for consideration. Let μ_{rain}, μ_{snow} represent the mean annual maximum storm and snowmelt volumes and σ_{rain}, σ_{snow} represent the standard deviations of annual maximum storm and snowmelt volumes. Four cases exist:

- Case 1 ($\mu_{rain} > \mu_{snow}$ and $\sigma_{rain} \geq \sigma_{snow}$)
- Case 2 ($\mu_{rain} < \mu_{snow}$ and $\sigma_{rain} \leq \sigma_{snow}$)
- Case 3 ($\mu_{rain} > \mu_{snow}$ and $\sigma_{rain} < \sigma_{snow}$)
- Case 4 ($\mu_{rain} < \mu_{snow}$ and $\sigma_{rain} > \sigma_{snow}$)

NRCC discussed the possibility of flood generating mechanism for these cases. Although these discussions will provide some general guidelines to the practice in IDF estimation, the use of these guidelines may not lead to a clear distinguish between snowmelt flooding and rain storm induced flooding for a specific dam site. In these discussions, the importance of drainage size and the influence of watershed characteristics are not considered. But these factors can not be ignored.

Currently, much of the research focuses on the differences resulted in the performance of probability distributions due to the typology of floods. Blöschl and Sivapalan (1997) analyzed the relationship between the coefficient of variation (CV) of maximum annual floods and the drainage area for various flood generating processes. They concluded that there is a very complex relationship between CV and drainage area size and type of flood generating process that may help to explain the complicity. Using a statistical assessment will not be able to give a satisfactory explanation for the complex relationship between CV and drainage area.

Robinson and Sivapalan (1997) made a significant contribution in this area of research and to the understanding of the flood generating processes. They studied the interactions among storm, within-storm, between storm and seasonal variations of rainfall and catchment response time. They correctly pointed out that the watershed response time is one of the factors that is important in flood generating processes.

Merz and Blöschl (2003) analyzed the coefficient of variation (CV) of flood samples resulting from different flood types. The types of flood generating mechanisms examined in their study included: long-rain floods, short-rain floods, flash floods, rain-on-snowmelt floods, and snowmelt floods. They concluded that CV decreases with catchment area size except for flash floods for which CV increases with catchment area. Therefore, catchment area alone is not a good indicator of the flood generating mechanisms.

Haga and Matsumoto, et al. (2005) emphathized the importance of basin response time, especially the lag time, on flood generating behaviour and they used another factor, antecedent soil moisture condition, to qualify the effects of initial soil moisture conditions on the basin's response. They concluded that the consideration of basin antecedent soil moisture condition, the rainfall amount and intensity are essential for understanding the regional characteristics of lag times and basin's response.

Merz and Parajka (2006) examined the relationship between the runoff coefficient and the type of flood. They found that the main controls on flood event coefficients are the climate and runoff regime. The antecedent soil moisture and event characteristics have significant influences on the variation of runoff coefficient.

Merz and Parajka (2009) confirmed the relationship between the antecedent soil moisture conditions and the runoff coefficient using 64,000 flood events in 495 Austrian catchments with drainage areas ranging from 5 to 10,000 km^2. They indicated that soil moisture derived from soil moisture accounting schemes has more predictive power for the temporal variability of runoff coefficients than antecedent rainfall.

In the development of the procedure, the basic concepts outlined in the literature review are incorporated into the model which will be described in the next section.

3. THE PROCEDURE

3.1 Basic Equations

From the literature review, what can be concluded is that, the annual maximum flood generated from a catchment is a function of the following variables:

1. Amount of rain fall and/or the total volume of snowmelt.
2. Watershed size.
3. Watershed antecedent soil moisture conditions.
4. Watershed characteristics, including the shape of the watershed, the main stream length and its slope. These factors can be combined into watershed time response parameters such as the time of concentration, time to peak or the basin's lag time

The objective of this paper is to find a simple but effective way to combine these factors into a model allowing hydrologists and engineers to determine the most likely flood generating mechanism that results in the determination of an inflow design flood for a dam site.

There have been many hydrological models ranging from very simple and conceptual to very complicated and physically based models. To meet the requirements of this procedure, the model must be simple to use and reflect all of the important factors outlined in the literature review. And the required parameters must be easy to obtain.

Using these criteria, the USDA Soil Conservation Service (SCS) (1954) is selected. The SCS method has been widely accepted in US and many other countries. The method is described in the National Engineering Handbook Section 4: Hydrology (NEH-4) (SCS 1985). The model is simple and the parameters used are easy to obtain from readily available information. All of the four most important factors appear in the basic equations and hence their influence on flood peak and volume can be evaluated.

The SCS method is also called the curve number (CN) method. The SCS method assigns curve numbers to soil with different infiltration capacities. If a soil has higher infiltration rate, a lower CN is assigned to this type of soil. If the CN number is high for a type of soil, the infiltration capacity of the soil is low. CN changes from 0 to 100. A CN number equal to zero means that there will be no runoff and all precipitation becomes infiltration. On the other extreme, if CN is equal to 100 (water surface for example), all precipitation becomes runoff. Although CN numbers vary from 0-100, actual values found in natural soil typically range from 40-98 (Ponce and Hawkins 1996).

The SCS covers a complex category consisting of three factors: land use, treatment or practice, and hydrological conditions. It is realized that different land use affects the soil infiltration rates differently. Urban areas will have a higher CN number, since urban areas have more paved areas where the infiltration rate is reduced significantly no matter what type of soil exists under the paved surface.

In developing the SCS rain-runoff relationship (SCS 1985), the total rainfall was separated into three components: direct runoff (Q), actual retention (F), and the initial abstraction (I_a). Their conceptual relationship can be expressed as:

$$\frac{F}{S} = \frac{Q}{P - I_a} \tag{1}$$

Where S is the potential maximum retention storage. The actual retention F is

$$F = (P - I_a) - Q \tag{2}$$

Combining (1) and (2), the following relationship exists:

$$\frac{(P - I_a) - Q}{S} = \frac{Q}{P - I_a} \tag{3}$$

Equation (3) can be rearranged to solve for Q as:

$$Q = \frac{(P - I_a)^2}{(P - I_a) + S} \tag{3}$$

The initial abstraction Ia is the amount of water at the beginning of the storm that is not available for runoff. Therefore (P-Ia) is the amount of rainfall that is available after the initial abstraction has been satisfied. S is the storage in soil available for holding rainfall. S is a function of land use, interception, infiltration, depression storage and antecedent moisture.

The relationships among these parameters can be illustrated in Figure 1.

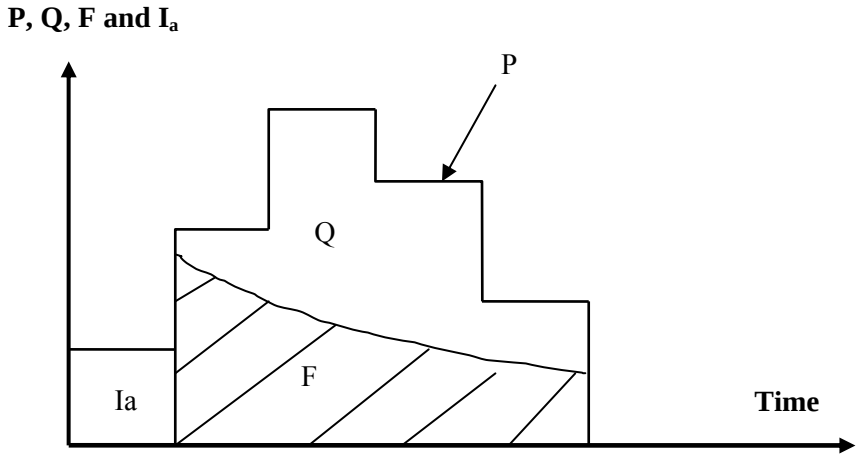

Figure 1 Separation of rainfall (P), runoff (Q), initial abstraction (I_a) and actual retention (F)

Empirical relationship indicates that initial abstraction Ia can be estimated as:

$$I_a = 0.2S \tag{4}$$

And hence

$$Q = \frac{(P - 0.2S)^2}{P + 0.8S} \tag{5}$$

Observation of equations (1) to (5) indicates that there is a missing link between these equations and CN values. The SCS runoff CN was linked with the water retention storage S:

$$S = \frac{25400}{CN} - 254 \quad (metric\ unit) \qquad or \quad S = \frac{1000}{CN} - 10 \quad (imperial\ unit) \tag{6}$$

When used in metric unit, S has a unit of millimetres (mm). When imperial unit is used, S is in inches (in). From equation (6), when CN approaches zero, the soil retention storage approaches infinity and all precipitation will be stored in the soil storage. The amount of runoff is zero. But when CN=100, the retention storage becomes zero, and all rainfall becomes runoff. These are the two extreme conditions. SCS investigated more than 4000 type of soils and assigned a CN to each of these soil types. The SCS CN method works for the mean soil moisture conditions which is also called AMC2 or CN2 condition. If the antecedent moisture conditions change, the runoff potential will deviate from the mean. When the antecedent moisture condition is dryer, the runoff potential will be lower. This is called AMC1 or CN1 condition. When the antecedent moisture condition is wetter, the runoff potential will be higher for the same type of soil. This is called AMC3 or CN3 condition.

To account for this variability, Hawkin et. al. (1985) developed two relationships that links AMC1 and AMC3 to AMC2 as follows:

$$CN_1 = \frac{CN_2}{2.281 - 0.01281 CN_2} \tag{7}$$

And

$$CN_3 = \frac{CN_2}{0.427 + 0.00573 CN_2} \tag{8}$$

Equations (1) to (8) are used to estimate the rainfall losses and runoff volumes from the watershed. The peak flood flows can then be related to the runoff volume and other watershed parameters. The main parameters are the drainage area and watershed response time characteristics.

$$q_p = \frac{f_p A Q}{T_p} \tag{9}$$

Where f_p is the peak rate factor, which normally equals 484 for imperial unit, A is the drainage area ($mile^2$ or Km^2), Q is the direct runoff rate (in or mm), T_p is time to peak (hour), and q_p is the peak flow rate (ft^3/s or m^3/s).

From equation (9), it is known that the peak flow will be higher if the drainage area is larger or the runoff volume is higher or the time to peak is shorter. This will form the basis of the procedure to identify the critical flood generation mechanism.

The time to peak parameter of a basin can be estimated by:

$$T_p = \frac{D}{2} + T_L \tag{10}$$

Where D is the duration of the rainfall block and T_L is the basin lag time defined as:

$$T_L = \frac{L^{0.8}(S+1)^{0.7}}{1900 Y^{0.5}} \tag{11}$$

Where L is the hydraulic length of the watershed in feet, S is the potential retention storage, and Y is the average basin slope in percent. The lag time is related to the time of concentration T_c as follows:

$$T_L = 0.6T_c \tag{12}$$

Equation (11) shows that the basin's lag time is a function of hydraulic length, potential retention storage and basin's average slope. The longer the hydraulic length or the larger the retention storage of the soil or the milder the slope, the longer the lag time will be for any watershed.

3.2 The Procedure

In order to determine the critical flood generation mechanism for dam safety studies, the following procedure can be followed. It should be noted that no matter which mechanism (storm flood or snowmelt flood) generate the critical flood for a watershed, the meteorological (amount of design storm or design snowmelt) and watershed parameters (watershed area, CN, lag time etc) will have to be estimated and hence the proposed method will not lead to any additional efforts. Once these parameters have been estimated, following the proposed procedure will help to determine the most critical flood generating mechanism and allow focusing on the simulation and evaluation of the most critical flood generation cases. This will eliminate the time to be spent on the flood generation conditions for which the most critical flood will not likely result and therefore will save significant time and budget for the dam safety project.

The procedure is described as follows:

1. Determine the design storm (ST) and design snowmelt volumes (SN),

2. Calculate the potential retention storage S for storm and snowmelt conditions. It should be noted that for the summer storm, the SCS CN_2 is normally used but the SCS CN_3 should be used for snowmelt conditions since at time of snowmelt flooding, the basin ground is normally saturated with higher runoff potential:

$$S_2 = \frac{25400}{CN_2} - 254$$

$$S_3 = \frac{25400}{CN_3} - 254$$

3. Using equation (3) to estimate the direct runoff Q_{ST} and Q_{SN} as follows:

$$Q_{ST} = \frac{(ST - 0.2S_2)^2}{ST + 0.8S_2}$$

$$Q_{SN} = \frac{(SN - 0.2S_3)^2}{SN + 0.8S_3}$$

4. Calculate the peak discharges as follows:

$$q_{pST} = \frac{f_p A Q_{ST}}{T_p}$$

$$q_{pSN} = \frac{f_p A Q_{SN}}{T_p}$$

5. From step 4, if $q_{pST} > q_{pSN}$ then it means that the peak flow generated by summer storm will be higher and hence the critical flood generating mechanism for this watershed is summer storm design event. If however, $q_{pST} < q_{pSN}$ then it means that the spring snowmelt event will generate higher flood peak and will be the critical flood generation mechanism for the watershed.

After step 5, one of the flood generating mechanisms will be eliminated from further investigation. From the procedure, it is seen that the important meteorological and basin parameters include: design storm and snowmelt volume, drainage area, basin's land use and soil conditions, initial abstraction and the basin length and slopes. All of these parameters play a certain role in flooding generation. The problem is a complicated issue and there is no one single parameter that dominates the flood generation mechanism.

4. SPECIAL CONDITIONS

It has been noticed the in Ontario that, some watersheds can have significantly different hydraulic responses for storm events and for rain on snowmelt events. During a storm event, the main parts of these watersheds are covered with heavy forest and grass. The retention storage is high and the retention time of these watersheds to storm water is normally long. The watershed response is slow.

During a rain on snowmelt event, however, the watershed is normally saturated or with frozen ground and hence the retention storage is at the minimum level. Due to the saturated conditions in the watershed, the response time of the watershed to rain on a snowmelt event can become extremely quicker than for a normal summer condition. The basin lag time could be reduced to hours from days. Due to the quick response, the peak rate will also become much higher than normal. Therefore, a small rain on a snowmelt event which may seem to be an insignificant event could result in a larger flooding imposing a significant risk to the downstream communities. Haga and Matsumoto (2005) reported similar watershed behaviour. They found that when a rainfall event occurs on saturated soil conditions, the basin response is much quicker than the response during a normal moisture state. They concluded that consideration of antecedent soil moisture conditions in the catchment as well as the rainfall amount and intensity are essential for understanding the watershed characteristics lag times.

This type of watershed behaviour could be evaluated by using the procedure developed in this paper. If historically there have been similar flood records in a study area, the IDF could be the result of rain on snowmelt event. To evaluate the potential impact, the hydrologist and engineers shall use shorter lag times for winter rain on snowmelt event assessments. If the resulting flood leads to more critical flood conditions, the IDF will be assessed for this type of event.

5. EXAMPLES

The procedure is used as an example for illustrating purpose. In 2001 to 2002, a dam safety assessment was undertaken for a typical Ontario dam that had been previously studied by Hatch in 1992. The dam has a drainage area of 499.5 km^2. Using the NRCC (1989) description, it can not be classified as large watershed. Therefore, it was difficult to determine if the summer design storm or spring snowmelt event would lead to a more critical flood condition. To quickly determine which event would lead to a critical flood, the procedure was applied.

In the hydrological assessment, the following meteorological and watershed parameters were obtained:
The drainage area = 499.5 km^2, the basin lag time was estimated to be 24 hours and the $CN_2 = 62$ the CN_3 can be estimated by equation (8) and the resulting value is $CN_3 = 79$. The CN_2 value will be used in the example for summer storm conditions and CN_3 value will be applied for spring snowmelt conditions.

The design storms and design snowmelt in the study region are presented in Table 1. From table 1, when the event duration is 24 hours, the total amount of rainfall (99 mm) is higher than snowmelt (62 mm). The resulting peak flow from the storm event (60 m^3/s) is slightly higher than the snowmelt event (59 m^3/s). This means that the amount of storm is more critical. For storm duration of 48 hours, the amount of design storm (119 mm) is still higher than snowmelt (110 mm). However, due to the higher runoff potential when the ground is saturated

during the spring snowmelt event, the total runoff volume of the snowmelt event is higher resulting in a higher peak flow for the snowmelt flooding. It is evident that the spring snowmelt events will lead to more critical flood conditions for three day duration events.

From the results, it can be seen that the amount of rainfall or snowmelt volume is an important factor in determining the peak flows but it is not the only factor.

The antecedent moisture conditions play a significant role in the flood generating processes and sometimes this may be more important than the amount of rainfall. This is consistent with the findings obtained by Merz and Blöschl, 2009. They concluded that the catchment antecedent moisture state is the dominate control on event runoff coefficient for their analyzed watersheds.

Table 1 Peak Flows Corresponding to Design Storms and Design Snowmelt Volumes

Duration (hour)	Summer Storm				Spring Snowmelt			
	Time to Peak (hour)	Rainfall (mm)	Runoff (mm)	Peak Flow (m^3/s)	Time to Peak (hour)	Rainfall (mm)	Runoff (mm)	Peak Flow (m^3/s)
24 hours	36	99	21	60	36	62	20	59
48 hours	48	119	32	69	48	110	57	123
72 hours	60	130	38	67	60	194	132	229

Table 1 results indicate that snowmelt flooding will lead to the IDF conditions for this dam site since the time to peak of the watershed is 24 hours, hence the selected IDF should last longer than 24 hours.

In the example used, it can be seen, for the summer storm conditions, that the intensity of the storm also plays an important role. For example, the three day total storm volume (130 mm) is higher than two day storm volume (119 mm). But the resulting peak flow is actually lower (67 m^3/s vs. 69 m^3/s) due to the difference in storm intensity. The average storm intensity of the three day event is 1.8 mm/hour but the two day average storm intensity is 2.5 mm/hour.

The conclusion obtained from this simplified procedure is consistent with the detailed HEC-1 model results. This confirmed the validity of the simplified method. In real world assessment, a watershed will likely be divided into more sub-watersheds and the results of flood estimates will also be different due to the uniform sub-watershed dividing.

6. CONCLUSIONS

A Dam safety assessment requires accurate determination of inflow design flood but the modelling of hydrological process can be very time consuming. As well, determination of the IDF normally lies on the critical path of the study as it is a pre-requisite prior to the performance of other assessments such as structure stability analyses. Therefore, reducing the time required for IDF estimation will contribute to the overall success of the dam safety analysis. In the past, there was no widely used methodology for the quick identification of the control flood generating mechanism. Therefore, hydrologists had to complete hydrological modelling for both summer floods and for spring snowmelt floods. From the results of these assessments, the critical flood conditions were then identified leading to increased costs and lost time. The method proposed in this paper combines important parameters in flood generating processes for the evaluation of critical flood generating mechanism based on widely applied hydrological principles.

It was found that the drainage area of a watershed is not the only parameter determining which flood generating mechanism will govern the inflow design flood. Other parameters such as meteorological input to a watershed, the characteristics of the study watershed including antecedent soil moisture conditions, soil type, basin hydraulic length and the average slope of the basin control the flood generation as well. Ignoring these factors will lead to incorrectly identified IDF conditions.

It is concluded that the method developed can provide an effective way for rapid identification of the critical flood generating mechanism. It should be noted that the above example used one sub-watershed in the assessment. For real projects, watershed delineation and reservoir routing might be needed for more complicated watershed configurations.

From the example, it is evident that the antecedent moisture conditions is one of the most important parameters affecting the flood flow estimation and the peak flow estimates are very sensitive to the antecedent soil moisture conditions. Therefore, accurately estimating the CN number is one of the most important factors affecting the accuracy of the results. In real world problem, the basin response time varies with seasons. During summer, the response time is affected by the surface vegetation cover conditions. During spring runoff period, the basin's response time may be affected by snow cover conditions. This factor should be evaluated carefully.

7. REFERENCES

BlÖschl, G., and Sivapalan, M., 1997, Process controls on regional flood frequency: Coefficient of variation and basin scale, Water Resources Research, Vol. 33, No. 12, 2967-2980.

Haga, H., Matsumoto, Y., et' al., 2005, Flow paths, rainfall properties, and antecedent soil moisture controlling logs to peak discharge in a granitic unchanneled catchment, Water Resources Research, Vol. 41, W12410, doi:10.1029/2005WR004236, 2005.

Hawkins, R. H., Hjelmfelt, A. T. and Zevenberger, A. W., 1985, Runoff probability, storm depth, and curve numbers, Journal of Irrigation and Drainage Engineering, ASCE 111(4), 330-340.

Merz, R. and BlÖschl, G., 2003, A process typology of regional floods, Water Resources Research, Vol. 39, No. 12, 1340, doi:10.1029/2002WR001952, 2003.

Metz, R. and BlÖschl, G., 2006, Spatio-temporal variability of event runoff coefficients, Journal of Hydrology, 331, 991-604.

Metz, R. and BlÖschl, G., 2009, A regional analysis of event runoff coefficient with respect to climate and catchment characteristics in Austria, Water Resources Research, Vol. 45, W10405, doi:10.1029 /2008WR007163, 2009.

National Research Council Canada, 1989, Hydrology of Floods in Canada, A Guide to planning and design, Publication Sales and Distribution Office National Research Council of Canada, Ottawa, Ontario.

Ponce, V. M. and Hawkins, R. H., 1996, Runoff curve number: has it reached maturity? Journal of Hydrological Engineering, Vol. 1, No. 1, 1996, 11-18.

Robinson, J. and Sivapalan, M., 1997,Temporal scales and hydrological regimes: Implications for flood frequency scaling, Water Resources Research, Vol. 33, No. 12, 2981-2999.

SCS National Engineering Handbook, (1985), "Section 4: Hydrology", Soil Conservation Service, USDA. Washington, D.C.

Stoddart, R. B. I. and Watt, W. E., 1970, Flood frequency prediction for intermediate drainage basins in Southern Ontario. Civil Engineering Research Report No. 66, Queen's University, Kingston.

US Department of Agriculture, Soil Conservation Service, 1954, Hydrology guide for use in watershed planning, Soil Conservation Service, USDA, Washington D.C.

REHAUSSEMENT ET CONSOLIDATION DES OUVRAGES AU POURTOUR DU RÉSERVOIR KÉNOGAMI, RÉGION DU SAGUENAY-LAC-ST-JEAN

Hélène Tremblay, Direction des barrages publics, Centre d'expertise hydrique du Québec, Canada
Julie Lafleur, Direction des barrages publics, Centre d'expertise hydrique du Québec, Canada
Jean-François Bellemare, Direction des barrages publics, Centre d'expertise hydrique du Québec, Canada

RÉSUMÉ:
En juillet 1996, les pluies abondantes qui se sont abattues sur le bassin versant du réservoir Kénogami ont provoqué un rehaussement du niveau d'eau jamais atteint par le passé. Ce rehaussement a entraîné un débordement de plusieurs ouvrages et des dommages considérables en aval. Il fut établi que cette crue exceptionnelle se situait à une période de retour supérieure à 10 000 ans. Cet évènement a amené le gouvernement du Québec à réviser la gestion des crues et à examiner la sécurité de ses installations afin d'assurer la sécurité des ouvrages.

Ainsi, des études ont été réalisées afin de proposer des solutions pour améliorer la régularisation des débits en aval et la gestion des crues. Ces études ont mené à la préparation d'un projet global qui a fait l'objet d'audiences publiques en 2003. Ce projet comptait différents volets dont le rehaussement et la consolidation des douze ouvrages, la modernisation des évacuateurs de crue et la mise en place d'un système de gestion prévisionnelle amélioré. La modernisation des évacuateurs et l'amélioration du système de gestion des crues ont déjà été réalisés et le gouvernement a autorisé les travaux de rehaussement et de consolidation des ouvrages en mars 2008.

Le présent document présente les travaux qui sont réalisés pour répondre à la composante du projet qui concerne le rehaussement et la consolidation la mise aux normes de l'ensemble des ouvrages qui compte trois barrages munis d'évacuateurs et neuf digues, ainsi que la modernisation de plusieurs évacuateurs du barrage Portage-des-Roches. De plus, afin d'assurer la fermeture du plan d'eau au passage de la nouvelle crue de sécurité, quatre nouvelles digues de fermetures devront être construites. La fin des travaux est prévue pour 2013.

ABSTRACT:
In July 1996, heavy rain fell on the Saguenay region, causing an important increase of the Kenogami reservoir water level. In fact, the water level reached a never previously seen value. This high water level provoked an overflow on many dams and huge damages in the Chicoutimi and Aux Sables rivers downstream of the Kenogami reservoir. This exceptional inflow was evaluated to have a 10 000 years recurrence interval. Following this event, Québec authorities decided to evaluate and improve the reservoir management and ensure the security of facilities.

Thus, technical studies have been conducted to bring solutions improving the high flow management on the Kenogami watershed. Those studies led to a global project presented to public hearings in 2003.

The following paper presents one of the components of this project, which includes the raising of the crests to ensure adequate freeboard, spillways mechanical equipment update and modernization, and structural improvements of the 12 dams and closure dykes of the Kenogami reservoir system. Furthermore, to ensure the complete closure of the reservoir up to the new security flood, 4 new closure dykes must be built. The end of the project is planned to be in 2013.

1. INTRODUCTION

En juillet 1996, les pluies abondantes qui se sont abattues sur le bassin versant du réservoir Kénogami ont provoqué un rehaussement du niveau d'eau jamais atteint par le passé. Ce rehaussement a entraîné un débordement de plusieurs ouvrages et des dommages considérables en aval. Il fut établi que cette crue exceptionnelle se situait à une période de retour légèrement supérieure à 10 000 ans (une vue d'ensemble du site est montrée à la figure 1).

Cet évènement a amené le gouvernement du Québec à examiner et améliorer la gestion des crues et à examiner la sécurité de ses installations afin d'assurer la sécurité des barrages. En 1999, un rapport avait été soumis au gouvernement par un comité d'experts (Comité d'experts, 1999) qui s'était alors penché sur les crues exceptionnelles du réservoir Kénogami, rapport dans lequel les membres formulaient des recommandations quant aux moyens à prendre pour atténuer les conséquences de semblables phénomènes à l'avenir.

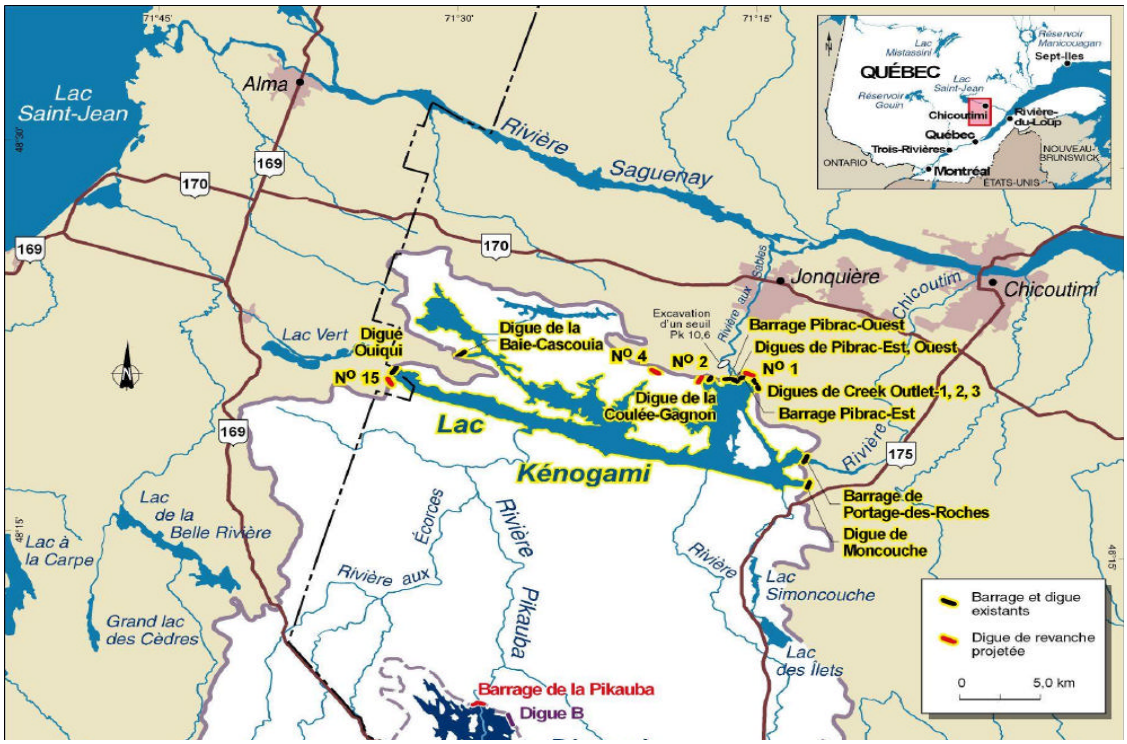

Figure 1. Localisation des ouvrages sur le lac-réservoir Kénogami

En juin 2000, le ministère des Ressources naturelles du Québec (MRN) a confié à Hydro-Québec le mandat de proposer des solutions pour améliorer la régularisation des débits en aval et la gestion des crues. Ainsi, Hydro-Québec déposa au Bureau d'audiences publiques sur l'environnement un projet permettant de sécuriser les ouvrages au pourtour du réservoir Kénogami (Hydro-Québec, 2002b). Ce projet prévoyait 1) la construction d'un réservoir amont sur la rivière Pikauba, 2) la consolidation et la mise aux normes des douze ouvrages de retenue au pourtour du réservoir, 3) l'aménagement d'un seuil sur le cours supérieur de la rivière aux Sables, 4) la modernisation d'évacuateurs, et 5) la mise en place d'un système de gestion prévisionnelle amélioré. La deuxième composante de ce projet prévoyait, entre autres, le rehaussement des ouvrages.

En avril 2006, l'évaluation de la sécurité des douze ouvrages du réservoir Kénogami a été mise à jour par le Centre d'expertise hydrique du Québec (CEHQ), en précisant l'état actuel des ouvrages et les différents travaux à réaliser (CEHQ, 2006b).

Le présent article résume l'ensemble des travaux qui sont présentement en cours sous la responsabilité de la Direction des barrages publics au Centre d'expertise hydrique du Québec (CEHQ). Il précise l'envergure des travaux correcteurs qui assureront l'intégrité des structures lors des événements extrêmes, l'évaluation des coûts et le calendrier de réalisation des travaux.

2 CRUE DE SÉCURITÉ ET LAMINAGE

2.1 Évaluations de la crue maximale probable (CMP)

À la suite de la crue de juillet 1996, le Ministère de l'Environnement et de la Faune (MEF) et Hydro-Québec ont réalisé conjointement une étude portant sur les crues du bassin du réservoir Kénogami (MEF et Hydro-Québec 1998). Celle-ci avait pour but de vérifier si les récents évènements allaient modifier les crues de conception des ouvrages. Ainsi, l'étude a permis d'évaluer des apports de différentes récurrences en effectuant une analyse fréquentielle des apports maximaux journaliers reconstitués du réservoir Kénogami. Les CMP d'été-automne et de printemps entrant au réservoir Kénogami ont été analysées en considérant trois scénarios. Ces scénarios sont les suivants :

- Combinaison de l'accumulation maximale probable de neige (AMPN) et de la pluie centennale;
- Combinaison de la pluie maximale probable (PMP) et de l'accumulation de neige centennale (AN100);
- PMP.

Différents scénarios de PMP ont été analysés et le plus critique a été retenu, soit celui où la pluie est centrée sur tout le bassin versant du Kénogami. Trois modèles hydrologiques (CEQUEAU, HSAMI et SSARR) ont été utilisés pour simuler les CMP et ont conduit à des débits maximaux journaliers comparables. La CMP la plus critique d'entre toutes est celle printanière combinant une AN100 avec une PMP.

Par la suite, vint en 2001 le projet de régularisation des crues du réservoir Kénogami et Hydro-Québec choisi de réviser la CMP en utilisant le modèle SSARR au pas de temps horaire (Hydro-Québec, 2001, 2002a, 2002b). Les résultats de cette analyse démontrent que les débits de pointe du modèle horaire dépassent substantiellement ceux du modèle journalier. Toutefois, les volumes demeurent sensiblement les mêmes que ceux évalués avec le modèle journalier.

Enfin, en 2004, Hydro-Québec a procédé à certains ajustements mineurs aux modèles SSARR basés sur l'usage d'un pas de temps horaire. Conséquemment, les valeurs des débits de pointe ont été influencées légèrement, mais les volumes des crues furent conservés. Les débits de pointe qui sont utilisés dans la présente étude proviennent de ces fichiers et sont précisés au tableau 1. Un autre modèle (HYDROTEL) avec un pas de temps de 3 heures (CEHQ, 2006a) a aussi été utilise pour valider l'intensité des CMP printanières déjà modélisées.

Tableau 1 : Débits de crues entrant au réservoir Kénogami

Récurrence (année)	Printemps		Été/automne	
	Débits journaliers (m^3/s)	Débits horaires (m^3/s)	Débits journaliers (m^3/s)	Débits horaires (m^3/s)
20	861	985	610	718
100	986	1124	887	1159
1000	1734	2089	1366	1806
10 000	1964	2365	1959	2611
CMP	5408	7046	5485	7241
Crue juillet 96			1993	2779

Le tableau 1 met en évidence l'intensité d'une éventuelle CMP en comparaison avec la crue exceptionnelle de juillet 1996. Ainsi, la crue de sécurité considérée pour les travaux actuellement en cour correspond à un peu moins de trois fois le débit de la crue de juillet 1996.

2.2 Capacité d'évacuation des ouvrages

Les appareils d,évacuation du barrage de Portage-des-Roches permettent l'évacuation des eaux vers la rivière Chicoutimi, tandis que ceux des barrages Pibrac-Est et Pibrac-Ouest, permettent l'évacuation des eaux vers la rivière aux Sables.

Le barrage de Portage-des-Roches comporte :

- 18 vannes verticales déversantes dont chaque vanne consiste en un regroupement de poutrelles en bois ceinturées de sangles en acier et dont l'opération est assurée par un appareil de levage se déplaçant d'un pertuis à l'autre (pertuis 1 à 18);
- 2 vannes verticales déversantes comportant chacune un mécanisme de levage indépendant (pertuis 19 et 20);
- deux passes à billes ne possédant pas de mécanisme de levage (pertuis 21 et 22).
- 11 vannes verticales de fond avec appareil de levage individuel (pertuis 23 à 33);

Quant au barrage Pibrac-Est, son évacuateur est constitué de :
- 7 vannes verticales déversantes avec appareil de levage individuel;
- 6 vannes verticales de fond avec appareil de levage individuel.

Le barrage Pibrac-Ouest comporte pour sa part :
- 6 vannes verticales déversantes avec appareil de levage individuel;
- 1 vanne verticale de fond avec appareil de levage individuel.

Les vannes des trois barrages peuvent être opérées sur place ou à partir de l'un des deux centres de service, à l'exception des 18 vannes verticales déversantes qui s'opèrent manuellement et des deux passes à billes du barrage Portage-des-Roches qui sont actuellmeent inopérantes.

2.3 Problématique et besoins

Les différentes études réalisées sur les ouvrages du réservoir Kénogami, mettent en évidence que, lors d'une hypothétique CMP, il y aurait déversement par-dessus certains ouvrages s'ils ne sont pas rehaussés (CEHQ, 2006b et 2007). Bien que certains ouvrages en béton puissent accepter un certain déversement, il n'en est pas de même pour toutes les structures. Pour les ouvrages en remblai, susceptibles d'érosion, un tel débordement par dessus les crêtes n'est pas souhaitable. Ainsi, afin d'assurer le contrôle des débits au passage d'une CMP, il a été décidé de rehausser tous les ouvrages au-dessus des niveaux atteints en CMP et d'inclure une revanche de sécurité.

En plus d'un rehaussement, différentes options ont été examinées dans le but d'améliorer la marge de manœuvre du gestionnaire lors de crues extrêmes et d'assurer l'exploitation sécuritaire des ouvrages. Ces options combinent le rehaussement des structures d'une part et, d'autre part, la réalisation de différents travaux pour améliorer l'efficacité et la fiabilité des évacuateurs de crues, tels que :

- La modernisation d'environ la moitié des 18 vannes déversantes du barrage Portage-des-Roches.
- La remise en service des passes à billes du barrage Portage-des-Roches.

Le laminage des CMP printanières et d'été-automne dans le réservoir Kénogami pour la solution recommandée a été simulé avec le modèle KENO97. Les hydrogrammes des CMP de printemps et d'été/automne ont été laminés afin d'évaluer pour chaque cas, le niveau atteint au réservoir Kénogami et le débit sortant par les rivières Chicoutimi et aux Sables.

Une analyse de sensibilité a été réalisée dans laquelle on considère la non disponibilité de 10 % ou 30 % de la capacité totale d'évacuation. Cette analyse de sensibilité permet de constater qu'une réduction de la capacité d'évacuation se traduit par un rehaussement non négligeable du plan d'eau. Selon les résultats obtenus, une réduction de 10 % de la capacité d'évacuation entraîne un rehaussement de 31 cm, rehaussement qui atteint 1,07 m si 30 % des évacuateurs sont non disponibles. Le tableau 2 présente les résultats du laminage des CMP de printemps et d'été/automne. Ces résultats démontrent l'importance d'augmenter la fiabilité des évacuateurs afin d'offrir au gestionnaire une plus grande marge de manœuvre.

Tableau 2 : Résultat du laminage de la CMP

Fiabilité des évacuateurs	CMP printanière		CMP été/automne	
	Niveau max (m)	Débit max (m^3/s)	Niveau max (m)	Débit max (m^3/s)
100% de la capacité d'évacuation	166,76	3764	166,56	3685
90% de la capacité d'évacuation	167,07	3531	166,85	3428

3 CRITÈRES CONSIDÉRÉS

3.1 Niveaux d'eau

La stabilité des ouvrages en crue extrême a été examinée en considérant une hypothèse de niveau d'eau amont conservatrice de 167,20 mètres. Ce niveau d'eau est légèrement supérieur aux niveaux de CMP établis, en incluant 10 % de capacité d'évacuation non disponible lors de l'événement.

Le niveau d'eau amont en condition normale est le niveau d'exploitation normal d'été, soit 163,70 mètres.

3.2 Crêtes des ouvrages rehaussées

Dans le cadre des travaux prévus, tous les ouvrages seront rehaussés afin d'empêcher les débordements au passage d'une crue extrême, tout en maintenant une revanche de sécurité minimale. Ainsi, l'élévation en crête des barrages en béton (Pibrac et Portage) a été fixée à 167,20 mètres et offrira une revanche de 44 cm (le niveau du plan d'eau au passage de la CMP étant de 166,76 mètres). Cette élévation assure qu'aucun débordement ne puisse survenir en considérant 10 % de vannes non fonctionnelles.

La digue Creek Outlet-1 et les deux digues Pibrac ne requièrent aussi qu'une revanche minimale. Ces structures sont d'anciens barrages de béton qui furent remblayés dans les années 90. Les crêtes de ces structures seront rehaussées à la cote 167,20 mètres. Il en est de même pour les digues Creek Outlet-2 et 3 qui sont des barrages poids en béton, sans remblai. Elles seront rehaussées à la cote 167,20 mètres et remblayées dans le cadre des travaux projetés.

Pour les digues susceptibles d'érosion, les rehaussements résultent de l'analyse de leur vulnérabilité à l'action des vagues (H-Q, 2002c). Ainsi, les digues Cascouia, Coulée-Gagnon seront rehaussés à la cote 167,76 mètres, soit 1,0 mètre au-dessus de la CMP. Les digues Moncouche et Ouiqui seront rehaussées davantage, car les analyses de remontée des vagues indiquent des rehaussements significatifs dans ces baies. Ainsi, la digue Moncouche sera rehaussée à la cote 168,76 mètres, soit 2,0 mètres au-dessus de la CMP et la digue Ouiqui seront rehaussés à la cote 168,26 mètres, soit 1,5 mètre au-dessus de la CMP.

Les rehaussements ont pour conséquence d'augmenter la longueur de chaque ouvrage afin d'assurer la fermeture jusqu'aux nouvelles cotes établies. Le tableau 3 résume l'ensemble des caractéristiques des ouvrages actuels et rehaussés. Les rehaussements pour chaque ouvrage sont discutés dans les paragraphes suivants.

Tableau 3 : Caractéristiques des ouvrages actuels et rehaussés

NOM	Caractéristiques actuelles (m)				hauteur	Caractéristiques après rehaussement (m)			
	longueur	hauteur	élévation noyau	élévation crête	vagues (m)	longueur	hauteur	élévation noyau	élévation crête
Moncouche	181	7.6	165.38	166.95	1.63	185.6	9.6	167.2	168.76
Portage-des-Roches	460.8	15.2	n/a	165.96	n/a	480	16.31	n/a	167.20
Coulée-Gagnon	153	7.9	164.77	166.61	0.9	190	9.49	167.2	167.76
Creek-Outlet 1	158.5	11	165.72	165.72	1.42	211.1	12.48	167.2	167.20
Creek-Outlet 2	36.6	3.5	165.67	165.67	1.42	55.2	5.03	167.2	167.20
Creek-Outlet 3	144.8	3.6	165.67	165.67	1.42	165	5.13	167.2	167.20
Pibrac-Est (digue)	117	7.6	165.8	165.8	0.92	160	9.0	167.2	167.20
Pibrac-Est (barrage)	173.7	13.7	n/a	165.72	n/a	176	15.05	n/a	167.20
Pibrac-Ouest (digue)	142.5	10.3	165.7	165.7	n/a	216	11.80	167.2	167.20
Pibrac-Ouest (barrage)	143.1	12.8	n/a	165.94	n/a	165	13.93	n/a	167.20
Cascouia	81	14.9	166.35	167	0.74	79	16.10	167.2	167.76
Ouiqui	360	12.4	n/a	166.9	1.43	456	14.2	n/a	168.26

3.3 Noyaux étanches

Les noyaux étanches de tous les ouvrages qui en possèdent seront rehaussés à la cote 167,20 mètres, soit les digues Moncouche, Coulée-Gagnon, Cascouia, Pibrac-Est, Pibrac-Ouest, Creek-Outlet-1, Creek Outlet-2 et Creek Outlet-3 (voir tableau 3).

4 RÉSUMÉ DES TRAVAUX

Les travaux recommandés prévoient le rehaussement des ouvrages, la remise en service des passes à billes du barrage Portage-des-Roches et la modernisation d'environ la moitié des pertuis des vannes déversantes du barrage Portage-des-Roches. Le rehaussement des ouvrages consiste à rehausser les crêtes et les écrans d'étanchéité des douze ouvrages et à construire 4 nouvelles digues de fermeture (points bas #1, 2, 15 et 18) afin d'éviter tout débordement au passage d'une CMP tout en considérant l'incertitude hydrologique et l'action des vagues dans le cas des digues érodables.

4.1 Digue Moncouche

La digue Moncouche (figure 2) est un ouvrage en terre possédant un écran étanche en béton prolongé par un mur écran de palplanches. L'imperméabilisation n'est pas complète jusqu'au roc.

Les travaux sur cette digue ont été réalisés entre février et mai 2009. Ils consistaient à excaver la crête pour rehausser le mur écran à la cote 167,20 mètres. Ensuite, la digue a été rehaussée pour obtenir une crête de 5,0 mètres de largeur à la cote 168,76 mètres (rehaussement de 1,81 m). La berme aval a été reprofilée aux élévations 164,50 mètres pour le palier supérieur et 163,00 mètres pour le palier inférieur.

Une des problématiques majeures à la digue Moncouche était l'écoulement important d'eau sous le mur écran provoquant des surpressions importantes au pied aval, dues à la présence d'une couche relativement imperméable. Afin de diminuer et de contrôler les pressions interstitielles au pied aval de la digue et ainsi éviter d'éventuels phénomènes d'érosion interne, une série de 15 puits de décharge ont été installés. Ces puits interceptent les eaux d'écoulement avant qu'elles atteignent la zone du pied de la berme et l'eau est acheminée par un drain dans le lac Moncouche.

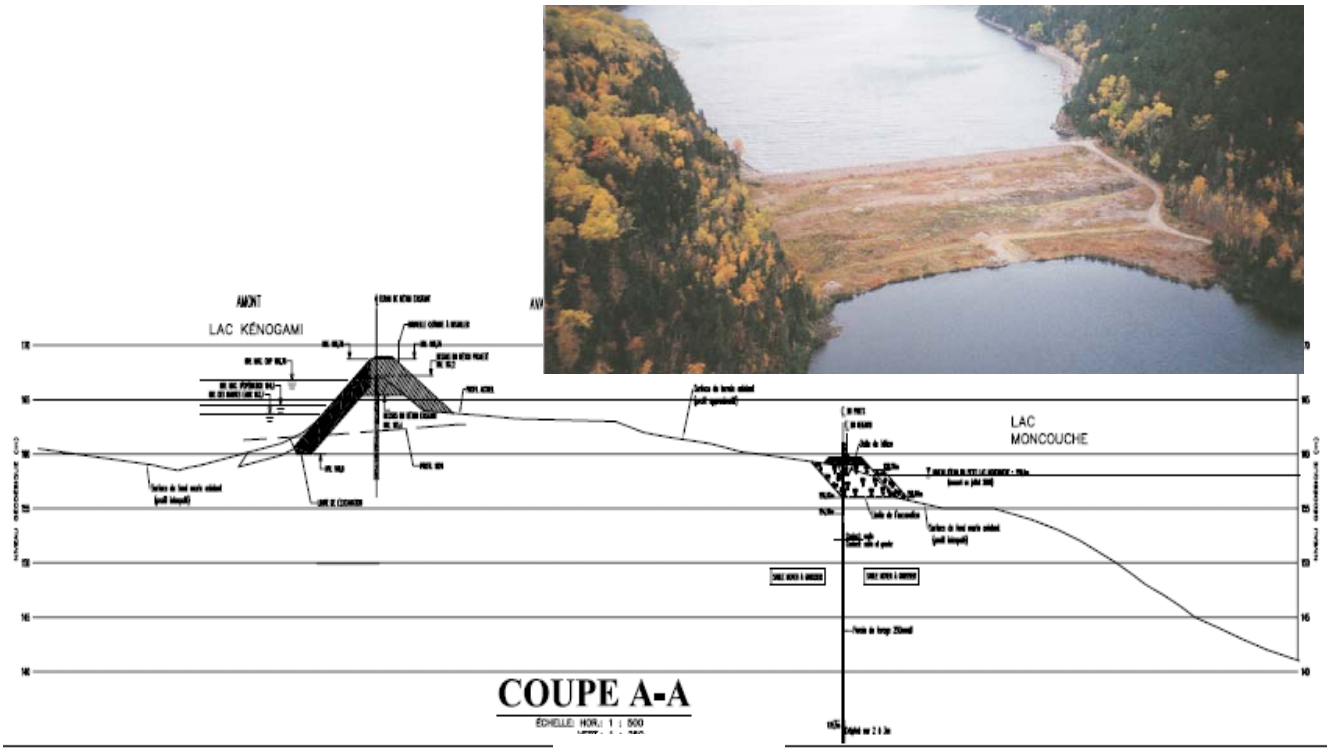

Figure 2. Digue Moncouche et coupe des travaux prévus pour la digue Moncouche

4.2 Barrage Portage-des-Roches

Le barrage Portage-des-Roches est un barrage de type poids en béton muni de 33 pertuis d'évacuation (figures 3 et 4). Ils permettent de contrôler les débits sortant dans la rivière Chicoutimi.

Pour cet ouvrage, plusieurs modifications au barrage sont prévues et l'ingénierie est actuellement en cours.

Figure 3. Barrage Portage-des-Roches

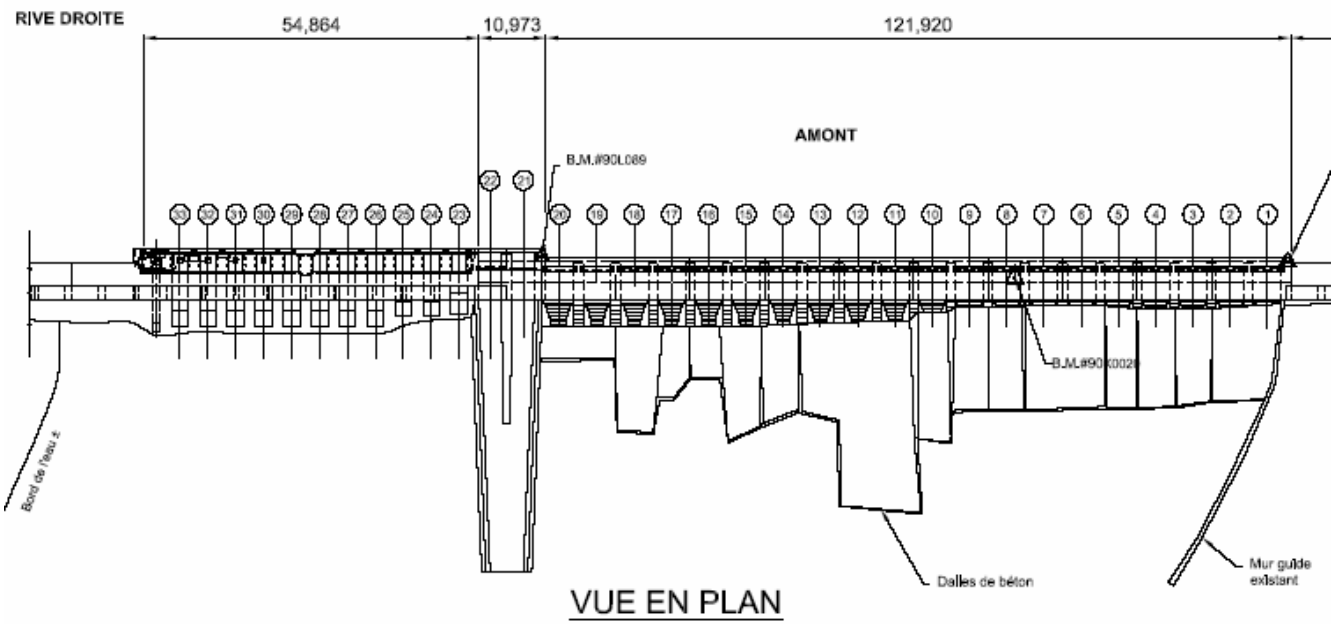

Figure 4. Vue en plan des évacuateurs au barrage Portage-des-Roches

4.2.1Remise en service des passes à billes (pertuis 21 et 22)

Cette portion des travaux consiste à remettre en service les pertuis des passes à billes du barrage Portage-des-Roches en y installant deux vannes individuelles indépendantes dans les pertuis actuels (figure 5). Ces travaux confèrent une souplesse et une sécurité améliorées en rendant disponible un équipement actuellement inopérant. Les deux vannes seront couplées à des systèmes de levage indépendants et seront munies d'un système de chauffage afin de pouvoir être utilisées par temps froid.

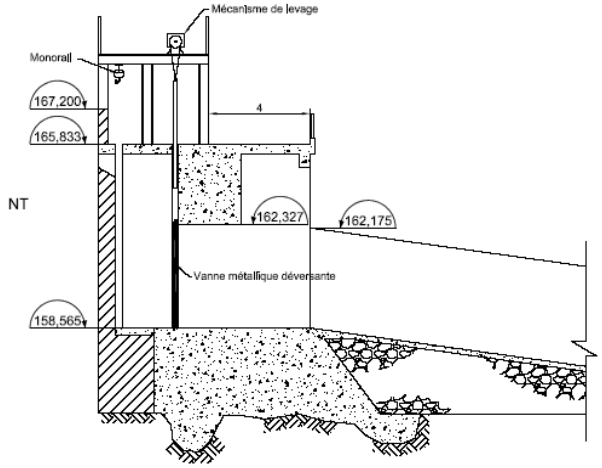

Figure 5. Modification des passes à billes

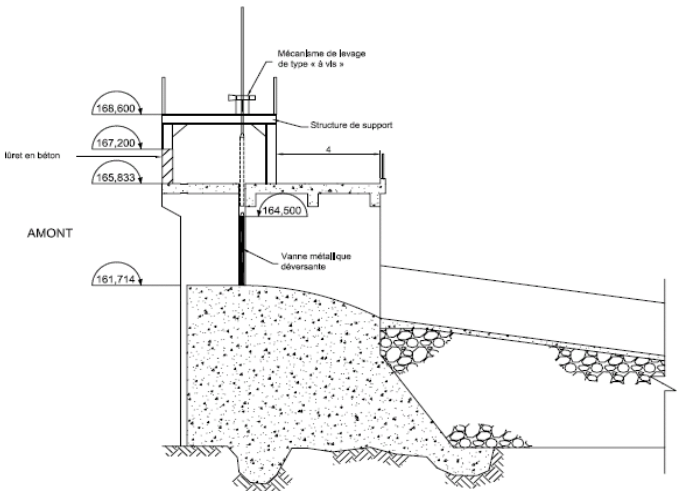

Figure 6. Modernisation des vannes déversantes

4.2.2 Modernisation des pertuis des vannes déversantes (pertuis 1 à 18)

Les vannes actuelles ont été fabriquées par l'assemblage de poutrelles et chaque vanne est opérée par l'utilisation d'un chariot treuil qui se déplace sur des rails. La modernisation consiste à remplacer certaines vannes actuelles construites en bois, par des vannes métalliques munies d'éléments chauffants à chaque extrémité, reliées à un

appareil de levage individuel. En ce moment, seulement deux vannes déversantes sont équipées de système de levage autonome (19 et 20). Dans le but d'augmenter la fiabilité des évacuateurs, la modernisation devrait se poursuivre sur 9 pertuis additionnel en les munissant de leur propre système de levage, ce qui accélèrerait les opérations lors des crues (figure 6).

4.2.3 Stabilisation de l'ouvrage, travaux de réfection et d'entretien

Des analyses de stabilité réalisées sur les différentes sections du barrage ont démontré que la stabilité de certaines sections de l'ouvrage devrait être augmentée en installant des ancrages actifs au roc. Aussi, certains travaux de réfection et d'entretien ont été identifiés par le CEHQ et seront réalisés dans le cadre de ce mandat, dont :

- le comblement d'une cavité sous le pertuis 25 amont;
- la réparation des piliers gauches N^{os} 26, 27 et 28.

4.3 Digue Coulée-Gagnon

La digue Coulée-Gagnon est une digue en terre possédant un noyau étanche en béton appuyé sur le roc. Le chemin St-Dominique passe en partie sur la crête de la digue (figure 7).

En 1996, lors du déluge du Saguenay, un débordement est survenu à la digue Coulée-Gagnon, endommageant la route qui constitue une portion de la digue. Cette digue doit donc être rehaussée tout comme les autres ouvrages. La difficulté de ce site est la présence de la rue St-Dominique sur la moitié est de la digue qui entre en conflit avec le rehaussement du noyau d'étanchéité et de la crête de la digue. Ainsi, pour ne pas devoir rehausser la route, il est recommandé de déplacer l'axe de la moitié est de la digue vers l'amont et de mettre en place un nouveau mur écran pour imperméabiliser cette portion de digue.

En résumé, les travaux consistent à rehaussement la digue et son prolongement de part et d'autre pour assurer la fermeture à la cote 167,76 mètres, à l'ajout d'enrochement dans la pente amont et d'une berme au pied aval, au rehaussement du stationnement adjacent à la digue, au rehaussement d'une portion des chemins situés aux deux extrémités de la digue et à la construction d'une nouvelle descente de bateaux.

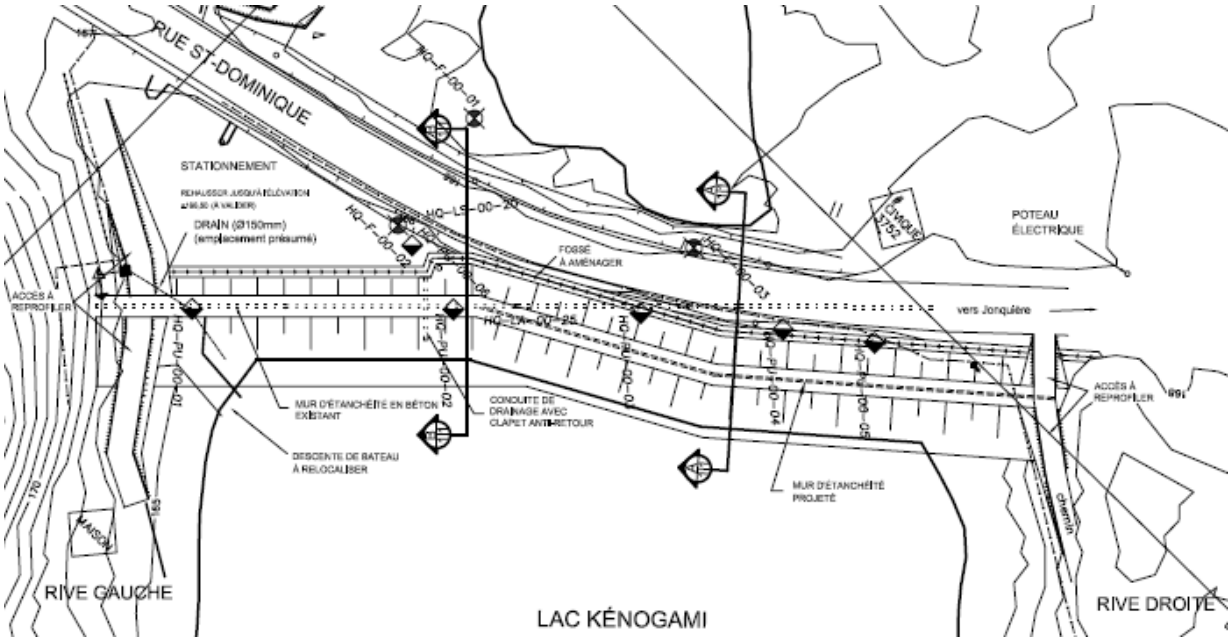

Figure 7. Travaux prévus à la digue Coulée-Gagnon

4.4 Digues Creek Outlet 1, 2 et 3

Les digues Creek Outlet sont des ouvrages de type barrage poids en béton. La digue Creek Outlet 1 est remblayées en amont et en aval avec de l'enrochement, alors que les deux autres sont uniquement constituées de la structure en béton (figure 8).

Figure 8. Digue Creek-Outlet 1

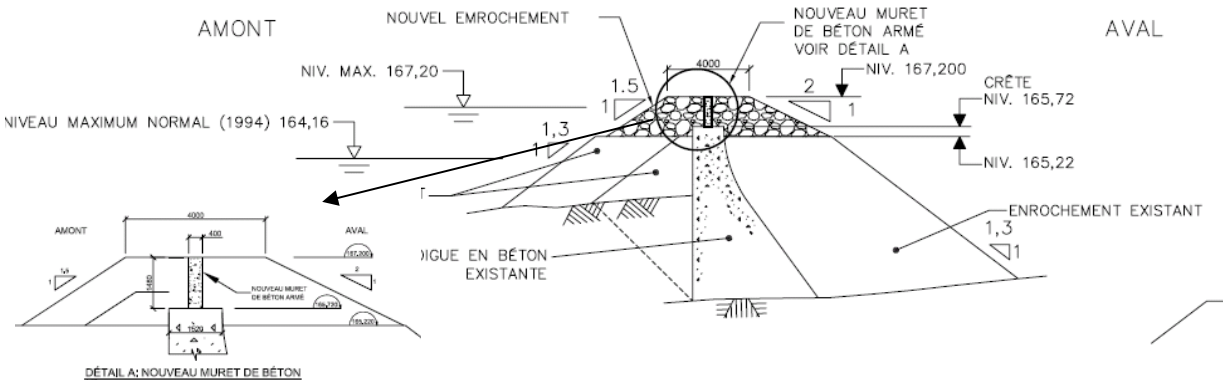

Figure 9. Travaux typiques projetés pour le rehaussement de la digue Creek Outlet-1

Les travaux projetés aux digues Creek Outlet (figure 9) se limitent à rehausser les structures en béton avec un muret de béton armé jusqu'à la cote 167,20 mètres, à prolonger le muret aux deux extrémités des structures en béton existantes pour assurer la fermeture des digues jusqu'à cette même cote, et à remblayer les structures de Creek Outlet 2 et 3 et les prolongements de Creek Outlet 1 avec de l'enrochement en amont et en aval.

4.5 Digues Pibrac-Est et Ouest

Les digues Pibrac-Est et Pibrac-Ouest sont constituées d'un mur poids en béton remblayé du côté aval seulement avec un tout venant granulaire (figure 10).

Les travaux consistent à rehausser les structures en béton avec un muret en béton armé jusqu'à la cote 167,20 mètres et à réparer le béton de surface des faces amont qui sont exposées aux intempéries (figure 11). Les travaux aux digues Pibrac-Est et Pibrac-Ouest ont été réalisés de septembre 2008 à mai 2009.

Figure 10. Digue Pibrac Ouest

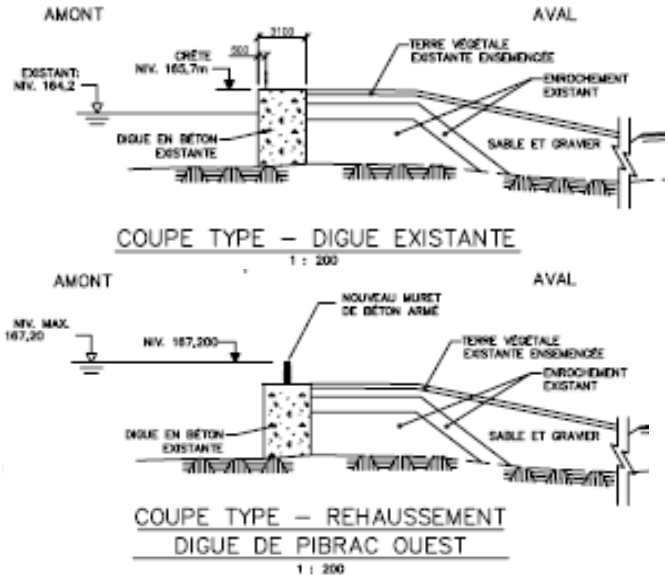

Figure 11. Coupe type digues Pibrac

4.6 Barrages Pibrac-Est et Ouest

Les deux barrages Pibrac-Est et Pibrac-Ouest sont des barrages de type poids en béton munis d'évacuateurs qui permettent de contrôler les débits sortants dans la rivière aux Sables (figures 12 et 13). Le barrage Pibrac-Est possède 6 vannes de fond et 7 vannes déversantes alors que le barrage Pibrac-Ouest possède 1 vanne de fond, 2 passes à billes et 4 vannes déversantes.

Les travaux consistent principalement à rehausser les deux ouvrages (figure 14). Les équipements d'évacuation des 2 barrages ont tous été modernisés en 2002. Toutefois, suite à la nouvelle crue de sécurité à considérer, certaines sections des deux barrages doivent être consolidées à l'aide d'ancrages actifs au roc, dont la section des vannes de fond au barrage Pibrac-Est et les sections des déversoirs, des passes à billes et de la vanne de fond au barrage Pibrac-Ouest.

De plus, quelques anomalies à corriger ont été identifiées dans la section de la vanne de fond au barrage Pibrac-Ouest où de l'infiltration importante est visible le long du pertuis. La source de ce problème d'infiltration et les travaux correcteurs seront précisés ultérieurement.

Figure 12. Barrage Pibrac Ouest

Figure 13. Barrage Pibrac Est

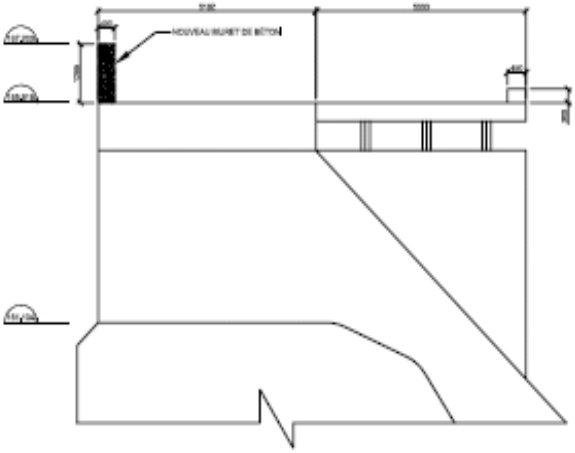

Figure 14. Coupe type du muret de béton pour le rehaussement du barrage Pibrac-Ouest

4.7 Digue Cascouia

La digue Cascouia est un ouvrage constitué d'un mur-poids en béton fondé sur le roc complètement remblayé avec un tout venant en sable et gravier (figure 15).

Les travaux projetés prévoient la réalisation d'un chemin d'accès, à excaver le sommet de la digue jusqu'à la structure de béton, à rehausser cette structure jusqu'à la cote 167,20 mètres avec un muret de béton armé, à prolonger la structure de béton aux deux extrémités afin d'assurer la fermeture à cette même cote, à rehausser la digue jusqu'à la cote 167,76 mètres à l'aide de tout venant granulaire, et enfin à protéger le parement amont avec de l'enrochement. Les travaux devraient débuter à l'automne 2009.

Figure 15. Digue Cascouia

Figure 16. Digue Ouiqui

4.8 Digue Ouiqui

La digue Ouiqui est un ouvrage en remblai dont la fondation et le remblai sont principalement constitués de matériaux granulaires perméables (figure 16). Certaines portions du remblai sont à l'état lâche et la digue ne possède pas de noyau étanche. Des phénomènes de boulance ont été observés par le passé dans le Lac à Louis situé au pied aval de la digue, de même que l'occurrence de 2 glissements, ce qui indiquerait la présence d'un écoulement souterrain important en provenance du lac Kénogami. Afin de rendre la digue Ouiqui conforme aux normes minimales de sécurité, la digue doit être stabilisée et la crête rehaussée en fonction de la CMP (figure 17). L'ingénierie détaillée est actuellement en cours et les travaux devraient débuter à l'été 2010.

4.8.1 Rehaussement de la digue Ouiqui

Cette digue sera rehaussée jusqu'à la cote 168,26 mètres à l'aide d'un remblai perméable en matériaux granulaires. Les faces amont et aval seront protégées par de l'enrochement.

4.8.2 Consolidation de la digue Ouiqui

La solution recommandée pour diminuer les risques de liquéfaction de la pente amont de la digue Ouiqui, est de densifier la couche lâche par une méthode qui sera précisée dans la phase d'ingénierie détaillée (i.e. vibro-flottation en profondeur et/ou compaction dynamique en surface).

Étant donné la faible compacité du remblai de la digue Ouiqui, il est recommandé d'adoucir la pente amont, afin d'augmenter sa stabilité. La raison principale est que la densification ne se fera pas sur l'ensemble de la digue, mais seulement sur une bande de remblai le long de la pente amont.

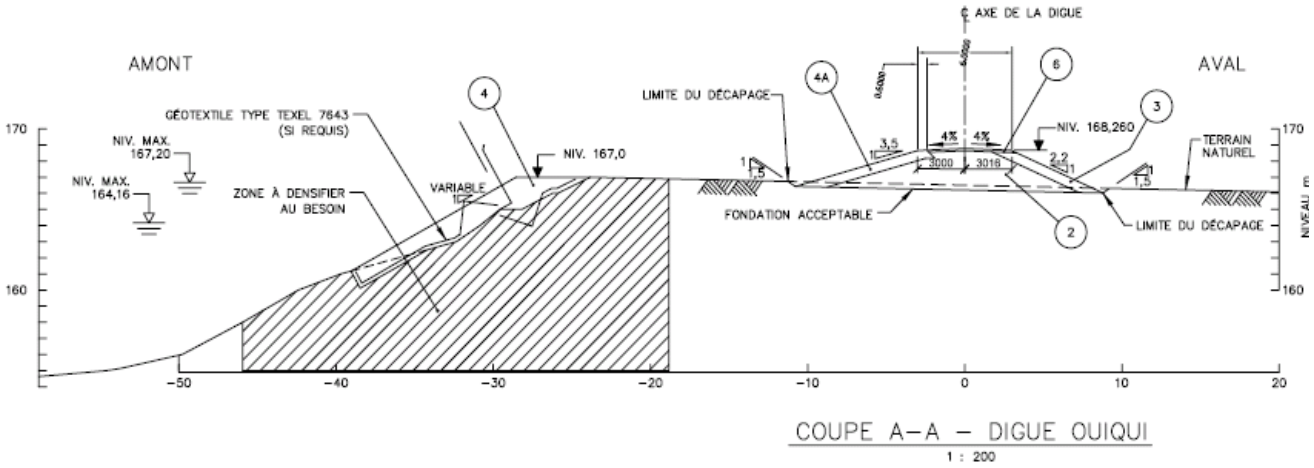

Figure 17. Travaux proposés par Hydro-Québec (Hydro-Québec, 2002) pour la digue Ouiqui

4.8.3 Drainage du pied aval de la digue Ouiqui (talus du lac à Louis)

Des travaux correctifs sont recommandés pour éviter l'amorce de nouveaux glissements de terrain dans le talus nord du lac à Louis, suite aux phénomènes de résurgences et suintement. Ces résurgences sont généralement causées par de fortes infiltrations, à travers la fondation de la digue. Ces débits d'infiltration peuvent être interceptés par une série de puits de décharge et dissiper ainsi les pressions interstitielles élevées induites par ce mouvement d'eau dans la fondation. Ainsi, l'installation d'une série de puits de décharge est envisagée dans le but de réduire les pressions interstitielles dans ce secteur.

4.9 Points bas # 1, # 2, # 15 et # 18

Suite à la remontée possible du plan d'eau au passage d'une CMP, 4 points bas ayant une élévation inférieure à la CMP, soit la cote 167,76 mètres, ont été identifiés. Ainsi, 4 nouvelles structures doivent être construites pour assurer la fermeture du réservoir.

Les travaux projetés aux points bas consistent à décaper la surface du sol sous l'emprise de la nouvelle digue et de construire un massif avec noyau imperméable reposant sur le terrain naturel (fondation imperméable ou roc) jusqu'à l'élévation 167,76 mètres, de les remblayer complètement avec un tout venant et de les protéger avec un parement amont et aval en enrochement (figure 18).

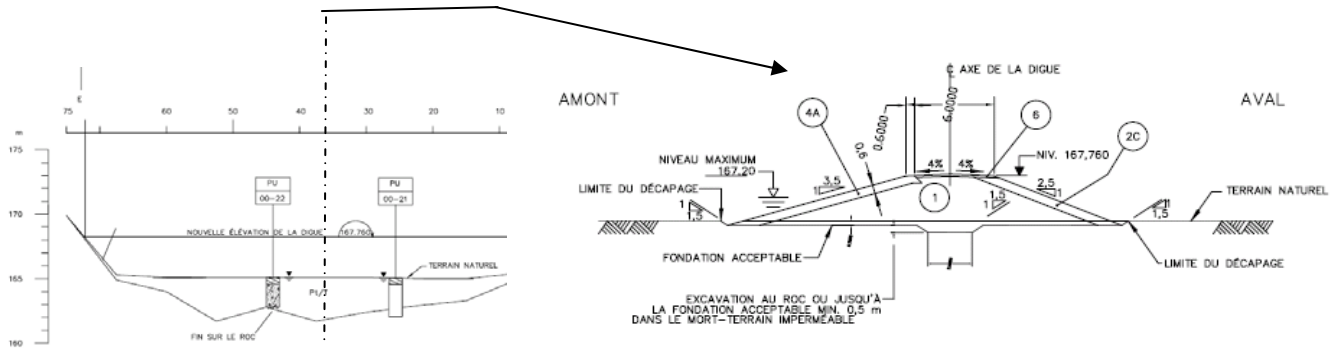

Figure 18. Exemple de travaux de construction aux points bas (Hydro-Québec, 2002)

5 ESTIMATION DES COÛTS

Les travaux recommandés consistent au rehaussement de tous les ouvrages afin de contrôler les débordements au passage d'une crue extrême, à se doter d'une souplesse supplémentaire dans la gestion des crues extrêmes en rendant disponibles les passes à billes du barrage Portage-des-Roches, et à améliorer la fiabilité des évacuateurs en équipant 9 des 18 pertuis qui n'ont pas encore été modernisés au barrage Portage-des-Roches de systèmes de levage individuels. Le coût global estimé pour réaliser l'ensemble de ces travaux est de 30 M$.

6 APPROBATIONS GOUVERNEMENTALES ET AUTORISATIONS

Les travaux recommandés dans ce document ont fait l'objet d'une étude d'impact sur l'environnement qui a été réalisée par Hydro-Québec en 2002 (Hydro-Québec, 2002b). Ainsi, un décret gouvernemental autorisant l'ensemble des travaux a été délivré pour lequel le CEHQ a été identifié comme promoteur et maître d'œuvre. Indépendamment, les travaux à réaliser sur chacun des ouvrages devra faire l'objet de demandes de certificats d'autorisation en vertu de la Loi sur la sécurité des barrages et de la Loi sur la qualité de l'environnement, de même que des demandes en vertu de la Loi sur la conservation et la mise en valeur de la faune.

7 CALENDRIER DE RÉALISATION DES TRAVAUX

Le projet a officiellement débuté en mars 2008 suite à la délivrance du décret gouvernemental autorisant les travaux. La première année a été consacrée à la préparation des plans et devis et à la réalisation d'appel d'offres. Jusqu'à présent, les travaux de chantier prévus sur 3 des 12 ouvrages ont déjà été réalisés, soit les digues Pibrac-Est, Pibrac-Ouest et Moncouche. L'ingénierie détaillée de 4 ouvrages est actuellement réalisée par le CEHQ, soit pour les digues Cascouia et les digues Creek Outlet 1, 2 et 3. Les chantiers sur ces ouvrages sont prévus pour l'automne 2009 ou l'hiver 2010. Aussi, 2 contrats de services d'ingénierie sont présentement en cours, un pour la digue Ouiqui et un autre pour le barrage Portage-des-Roches. Les travaux de chantier pour ces deux ouvrages sont prévus débuter au printemps ou à l'été 2010.

Les travaux aux barrages Pibrac-Est et Ouest, à la digue Coulée-Gagnon et pour les points bas sont prévus débuter en 2011.

La réalisation de l'ensemble des travaux est prévue être complétée pour 2013.

8 REMERCIEMENTS

Les auteurs tiennent à remercier tous ceux et celles qui ont participé au développement de ce projet, en particulier M. Alain Nadeau, ingénieur à la Direction des barrages au CEHQ pour son implication dans les concepts préliminaires et à l'évaluation des coûts, ainsi que de plusieurs spécialistes de Hydro-Québec qui ont préparé l'avant-projet pour le rehaussement et la consolidation des ouvrages au pourtour du réservoir Kénogami.

9 RÉFÉRENCES

CEHQ, 2006a, Division de l'hydrométéorologie « Analyse des CMP simulées au bassin versant du Lac-Kénogami depuis 1997 »

CEHQ, 2006b, « Étude d'évaluation de la sécurité – Réservoir Kénogami », 12 volumes

CEHQ, 2007, « Énoncé d'envergure des travaux de mise aux normes – Lac-réservoir Kénogami »

Comité d'experts, 1999, « Rapport du comité d'experts sur les crues exceptionnelles du lac-réservoir Kénogami »

Hydro-Québec, 2001, « Gestion des crues extrêmes du Lac-Réservoir Kénogami : étude de modélisation et laminage de la CMP »

Hydro-Québec, 2002a, « Gestion en conditions normales et en crues extrêmes du réservoir Pikauba et du lac-réservoir Kénogami – Rapport sectoriel d'avant projet – Hydrologie »

Hydro-Québec, 2002b, « Régularisation des crues du lac Kénogami : Étude d'impact sur l'environnement, volume 3. Sécurisation du pourtour du lac Kénogami »
Hydro-Québec, 2002c, « IAC, Kénogami : Étude de faisabilité, régine du vent et vagues caractéristiques. »
Ministère de l'Environnement et de la Faune (MEF) et Hydro-Québec, 1998, « Études des crues du bassin du réservoir du Lac-Kénogami », Volume 1 – Principal
Ministère de l'Environnement et de la Faune (MEF) et Hydro-Québec, 1998, « Études des crues du bassin du réservoir du Lac-Kénogami », Volume 2 – Les annexes.

HYDRAULIC DESIGN OF THE LOWER SPILLWAY FLUME AT BUNTZEN LAKE

Ken Christison, P.Eng., Northwest Hydraulic Consultants Ltd, North Vancouver, BC, Canada
Graham Lang, P.Eng, BC Hydro, Burnaby, BC, Canada
Osmar Penner, E.I.T., BC Hydro, Burnaby, BC, Canada
William Daley Clohan, E.I.T., Northwest Hydraulic Consultants Ltd., North Vancouver, BC, Canada

ABSTRACT:
The existing spillway at BC Hydro's Buntzen Lake reservoir consists of an upper inlet weir and concrete apron, a riprap-lined channel leading to an access road bridge, a steep natural canyon and a lower spillway flume which discharges to Indian Arm. The access road to the Lake Buntzen 1 (LB1) Power House runs on top of the lower spillway flume and below the LB1 penstock. While the upper inlet weir allows for about 46 m^3/s capacity without overtopping the dam, the lower spillway capacity is limited to approximately 25 m^3/s without overtopping onto the access road decking on the flume as well as the adjacent slopes. This limitation is due to the geometry of the lower spillway entrance.

As part of a project to upgrade the lower spillway flume, a hydraulic design was undertaken to increase the conveyance of the lower spillway while maintaining the unique access requirements associated with this project. The design effort concentrated on the geometry of the flume approach channel, the size and profile of the flume, and a method for dissipating energy and protecting the structure at the outlet to Indian Arm. The design effort was supplemented with a 1:16 scale physical model of a section of the approach channel, the partially covered spillway flume, a flip bucket, and part of Indian Arm. The physical model test results helped identify entrance capacity, design pressures in the flip bucket, minimum discharge required for initiation of flip action and the effects on performance of varying tailwater conditions.

RÉSUMÉ:
L'évacuateur de crues du réservoir du lac Buntzen de BC Hydro comprend un déversoir, deux chenaux (enrochement et état naturel) suivit d'un coursier qui déverse dans le cours d'eau Indian Arm, immédiatement à l'est de la centrale LB1. Bien que la capacité d'évacuation de la partie supérieure de l'évacuateur soit d'environ 46 m^3/s, sans débordement par-dessus le couronnement du barrage, la capacité du coursier est limitée à environ 25 m^3/s. Ce sont les conditions d'approche du coursier qui restreignent la capacité de l'évacuateur de crues.

Jusqu'à récemment, l'évacuateur de crues du lac Buntzen n'était utilisé que rarement car l'opération de deux centrales assurait de la redondance au niveau de la capacité. La capacité hydraulique de l'évacuateur fut excédée à seulement quelques reprises au cours des 100 premières années de fonctionnement. Cependant, en 1999, une des centrales fut désactivée et l'autre n'est pas toujours fiable. Par conséquent, l'évacuateur fut utilisé en 2001, octobre 2003, novembre 2006, janvier 2007, et occasionnellement depuis octobre 2007.

Une initiative de conception fut entreprise afin d'optimiser la capacité hydraulique du coursier de l'évacuateur de crues tout en respectant les limites imposés par l'accès requis sous le coursier. Un modèle physique réalisé à l'échelle de 1:60 comprend le coursier dans son ensemble depuis la zone d'approche jusqu'à la zone de dissipation d'énergie dans le bief d'aval (Indian Arm). Les résultats de l'étude avec modèle physique ont permis d'optimiser le comportement hydraulique du coursier et saut de ski aussi bien en situation normale qu'en conditions extrêmes.

1. INTRODUCTION

The proposed spillway flume will replace an existing flume located adjacent to BC Hydro's Buntzen Lake LB1 Power House located on the eastern shore of Indian Arm, BC (see Figure 1). The spillway flume conveys natural runoff and Buntzen Dam spills from a steep natural rock channel, under an overhead penstock, and into receiving salt waters of Indian Arm.

Figure 1. General Project Location

Physical modeling has been used to assist in the design and optimization of the main hydraulic aspects of the project. The use of the physical model allowed the design engineers to quickly determine capacity, visualize flow conditions, and evaluate potential design modifications. The model was fabricated with the intent to evaluate entrance conditions, flume hydraulics, and alternative flip bucket designs. The physical model tests would reduce construction risk and provide BC Hydro with a higher level of confidence in the design.

2. PROJECT BACKGROUND

Inflows to Buntzen Lake reservoir are from the local catchment area as well as from a 40 m^3/s capacity tunnel from Coquitlam Lake reservoir. The maximum flow through the LB1 powerplant is 55 m^3/s.

The existing spillway at BC Hydro's Buntzen Lake reservoir consists of an upper inlet weir and concrete apron, a riprap lined channel leading to the access road bridge, a central 'canyon' and a lower spillway flume which discharges to the Indian Arm immediately to the east of the LB1 Power House.

While the upper inlet weir allows for about 46 m^3/s capacity without overtopping the dam, the lower spillway capacity is limited to approximately 25 m^3/s without overtopping onto the adjacent access road. This limitation is due primarily to the geometry of the entrance to the lower spillway as presented in Figure 2; previous studies have estimated that the capacity of the flume portion of the spillway is greater than 40 m^3/s.

Figure 2: View looking upstream of the existing flume entrance

Figure 3: View of the existing outfall

Until recently, the spillway at Buntzen was used seldomly because there was redundancy and capacity in having two operating powerhouses LB1 and LB2. There were only a few spill events in the first 100 years of operation. In 1999, the LB2 plant was permanently taken offline and there have been reliability issues with the single unit LB1 plant. In consideration of the site constraints, the consequences of overtopping the flume, and flood frequencies, a design flow of 86 m^3/s was established for the lower spillway flume.

3. LAYOUT OPTIONS

A variety of options for separating the access road to LB1 powerhouse and the spillway alignment were investigated by BC Hydro. Due to the costs and implementation issues, the option chosen was to continue to have the access road on top of the spillway flume. Therefore, layout options for the spillway flume were constrained by the need to provide traffic passage over the flume and under the penstock.

3.1 Flume Layout

The initial concepts investigated for the spillway flume were based on the use of single and double concrete box culverts. However, these options were eliminated due to the size of the culvert sections required and issues with constructability and stability under the design hydraulic forces.

The option chosen was a cast-in-place section of dimension 3.6m wide by 3.0m high. This section enabled cover with pre-cast panels for road decking as well as fitting within site constraints on width.

3.2 Entrance Layout

A critical part of the design work was to shape the entrance to the flume so that the design flow would accelerate from the natural canyon outlet and into the flume layout cross section while rounding a bend of approximately 20 degrees.

Channels with a variety of geometries were investigated first with both 1-D and 2-D numerical models and then with a simple physical model. It was found that a gradually tapered entrance would require a very long approach distance to accelerate the flow suitably.

A more effective approach was found to include a more abrupt contraction followed with a transition section of at least 6 m length with the same width as the flume but with higher side walls. A layout with a symmetrical bell shaped entrance that aligned with the canyon rock contours was selected for further testing.

3.3 Terminus structure

A scour hole has undermined the current flume outlet which discharges at high tide level without provision for energy dissipation. High velocities and return currents along the left bank downstream from the outlet have also caused severe erosion of the adjacent parking area.

Therefore, a key component of the flume replacement options assessment was to protect the structure from being undermined as well as to minimize further erosion of the adjacent parking lot area. Protection of a seagrass area along the Indian Arm foreshore to the right of the flume outlet also had to be considered, as well as an objective to minimize construction activities below high tide. The range of tide heights and therefore tailwater levels for the structure is more than 5m, which makes for challenging hydraulic design for discharging flows with outlet velocities as high as 15 m/s.

Options assessed included flip buckets and stilling basins as well as straight riprap flumes down to low low water levels. The option that minimized foreshore construction and cost the least was a flip bucket.

4. PH MODELLING

4.1 Model Layout

The physical hydraulic model of the favoured layout was constructed in Northwest Hydraulic Consultants' North Vancouver laboratory. The model, as shown in Figures 4 and 5, was built to a scale of 1:16 and reproduced approximately 150 m of the approach channel, flume entrance transition, flume, and tailrace in the Indian Arm. The overall elevation difference represented in the model between the upstream channel and the downstream bathymetry is approximately 20 m.

Figure 4: Overall Model Layout from above the tailrace

Figure 5: Images from above the flume entrance and flip bucket

The model basin was mounted on a raised wooden deck framed with dimensional lumber to permit visualization of the flow patterns from above along the entire length of the model. The wetted perimeter along the model flume was fabricated using acrylic sheets to ensure that the prototype channel roughness was well represented in the model. The tailrace was installed as per the bathymetric survey information with placed 50 mm to 100 mm model (800 mm to 1600 mm prototype) rock.

Flow to the upstream approach channel was circulated through the model using a centrifugal laboratory pump. The total inflow was supplied to a head box, fitted with a butterfly valve and orifice plate for flow control and measurement. Flow leaving the tailbox was discharged directly into the laboratory sump.

4.2 Model Instrumentation

Flow to the model was circulated with a centrifugal pump, regulated with valves, and measured with an orifice plate before entering the two model head boxes. The orifice plates were sized appropriately and installed in accordance with American Society of Mechanical Engineers (ASME) standards. Experience with this discharge measurement system has indicated an accuracy of better than ±2 percent.

A water surface profile was recorded along the walls of the channels extending from the terminal flip structure to upstream of the flume. Water surface elevations were recorded to identify the locations of the transverse waves down the flume and determine maximum pressures at both the spillway entrance and with the flume. Due to turbulence water surface measurements are accurate to the nearest 0.25 inch model (4 inches prototype).

4.3 Test Program

A series of laboratory workshops were conducted to observe the effectiveness of various entrance and flip bucket geometries under a variety of flows ranging between 2 m^3/s to 86 m^3/s. Observations included:

- capacity of the flume entrance;
- water surface elevation and hydraulic grade line data throughout the model;
- hydraulic jump characteristics upstream of the flip bucket during low flow events, and
- flow conditions downstream of the flip bucket.

From the workshops a proposed design was developed and incorporated into the model design. Final design documentation tests were then conducted to confirm that the proposed design could satisfy the study objectives over a range of expected operating conditions.

4.4 Test Results

4.4.1 Entrance Conditions

Flows of up to 86 m^3/s were modeled to confirm capacity of the flume entrance. Under all modelled conditions transverse waves formed upstream of the flume. The waves, Figure 6, continued through the transition and into the curved flume entrance. Within the curve, super-elevated flow conditions along the left wall dominated the transverse waves. Recorded water surface elevations indicate that the flume entrance easily conveyed flows of 46 m^3/s and below.

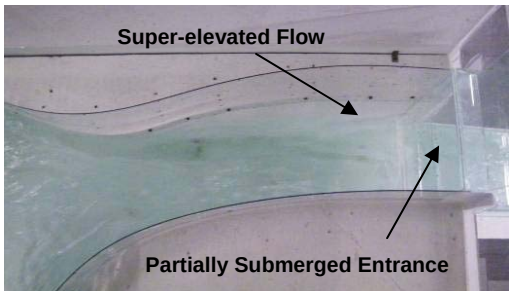

Figure 6: Flow conditions upstream of the flume

At the entrance to the covered flume, at the design flow of 86 m^3/s, super-elevation is expected to generate water surface elevations up to 0.9 m above the underside of the flume deck along the left wall while lowering the water surface to 0.9 m below the underside of the flume deck along the right wall. The rounded entrance geometry allows the elevated flow to pass into the covered flume while maintaining free surface flow conditions along the right side of the flume. Typical conditions at the flume entrance during design flow events are presented in Figure 7.

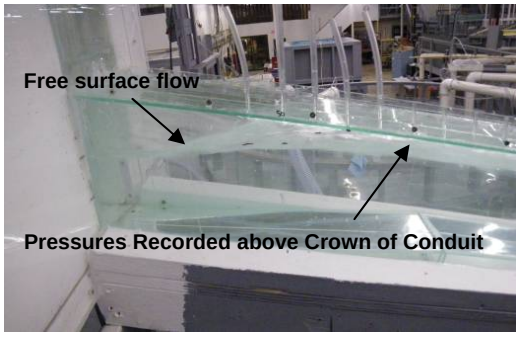

Figure 7: Flow conditions downstream of the flume entrance

4.4.2 Flume Hydraulics

The transverse wave generated by the super-elevation upstream of the flume entrance propagates down the entire length of the spillway. Immediately downstream of the entrance to the covered flume, the wave reflects to the right side of the flume, generating uplift pressures of up to 1.5 m. The left side of the channel remains open to allow the movement of air. It is expected that uplift pressures will be observed for the first 12 m of the covered flume. Below this point, the water surface does not re-attach to the top of the flume. Figure 7 presents flow conditions in the upstream section of the flume at 86 m^3/s.

The slope transition downstream of the penstock crossing generates additional pressures on the flume as flow transitions to the 2.5% slope. At this location, pressures reach 5.0 m while the water surface remains well below 3.0 m depth. Normal pressures are observed about two meters downstream of the transition. Figure 8 illustrates flow conditions in the vicinity of the slope transition.

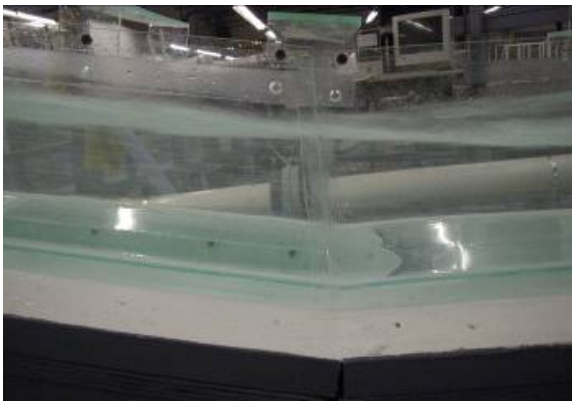
Figure 8: View of the slope transition. Discharge = 86 m^3/s


View of the slope transition. Discharge = 45 m^3/s

4.4.3 Terminus Structure – Flip Bucket

A number of downstream structure variations were considered during the development testing workshops. Considering that a primary objective of the design was to reduce potential scour along the bank supporting the flume, a flip type structure was quickly determined to be an effective alternative as the high velocity jet would flip away from the shore and out into Indian Arm. Various flip bucket designs were considered to:

- increase the cross-section area of the jet to help dissipate energy;
- minimize flow required to washout the hydraulic jump forming upstream of the flip, and
- eliminate standing water in the flume by allowing the channel to drain.

Configurations tested included the following:

(a) a flip defined by a constant curvature across the width of the flume, with the limits of the flip in plan tapered from the longest extension and highest flip angle in the center of the flume to a shorter extension and thus lower flip angle at the sides of the flume;

(b) the same curvature as configuration (a), but with the limits of the flip in plan tapered from the longest extension at the sides of the flume to a shorter extension and lower flip angle at the center;

(c) a full flip of constant curvature across the width of the flume; and,

(d) a central 'tooth' flip with a smaller radius of curvature, a step on either side of greater radius and lower flip angle, and a horizontal channel at either edge of the flume.

Variations in taper angles or step widths of the various configurations were tested. Option (a) generally produced the most effective spreading of the jet at higher discharges; however, the lateral extent of the spread approached too closely to a downstream bank on the left side. Extending the side walls downstream of the extent of the flip at the edges contained the lateral spread, but increased the threshold flow required to wash out the hydraulic jump. Option (b) was found to concentrate the flow towards a central jet, in particular at lower discharges. At high discharges, option (c) effectively maximized the distance from the flip bucket to the impact zone for the entire flow as an alternative to spreading the jet. It performed poorly under low flows, however, requiring a significantly higher threshold flow to wash out the hydraulic jump than the other configurations. Option (d) achieved a good compromise of the various performance criteria – effective spread of the impact zone of the jet, a low threshold flow to wash out the hydraulic jump, and free drainage for seepage and runoff accumulation.

Given that the spillway flow is not gate-regulated, low flows are expected to constitute a substantial portion of the spillway operation. In light of this factor and the other design considerations, option (d) was selected as the preferred flip bucket configuration.

The proposed design, Figure 9 on the following page, includes a stepped tooth centered at the end of flume. A 0.4 m channel on either side of the tooth allows lower flows to pass beside main flip while providing a drain for rainfall accumulation and seepage. The drain in elevation is set to El. 2.55 m, equivalent to both the lowest point in the approach channel and high tide levels. Side walls and a secondary step confine lower seepage and drainage flows within these channels.

Figure 9: View from downstream of the flip bucket

View from the right of the modelled flip bucket

The secondary step is located between the drains and the main flip helps pass lower flows. This secondary step is 0.4 m wide, extends up to El. 3.22 m, and is defined with a radius of 19 m. This step also promotes the spreading of the jet at higher flows decreasing the intensity of the plunging conditions.

The main flip is 2.0 m wide and extends to El. 3.89 m with a radius 10 m. It is designed to flip the majority of higher flows out into Indian Arm with a trajectory of 30 degrees.

The test results indicate that the flow is flipped up to 30 m away from the end of the flip structure at design flow conditions while the lower flows drain onto the riprap defining the shore. Flow conditions are also presented in Figure 10 to Figure 13.

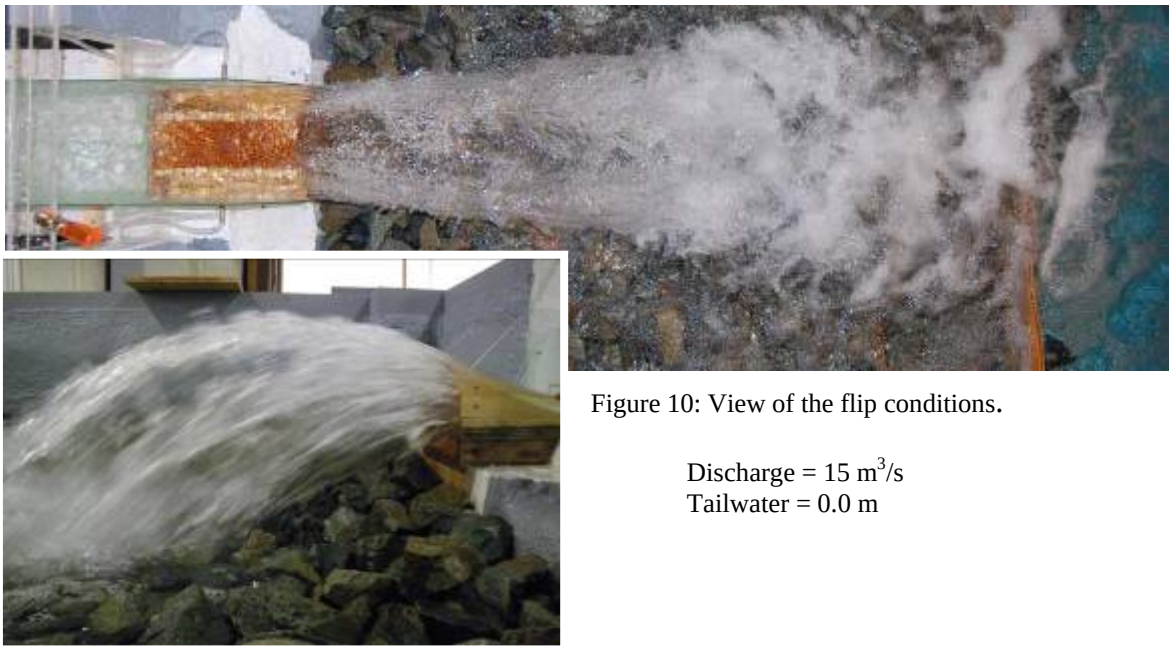

Figure 10: View of the flip conditions.

Discharge = 15 m^3/s
Tailwater = 0.0 m

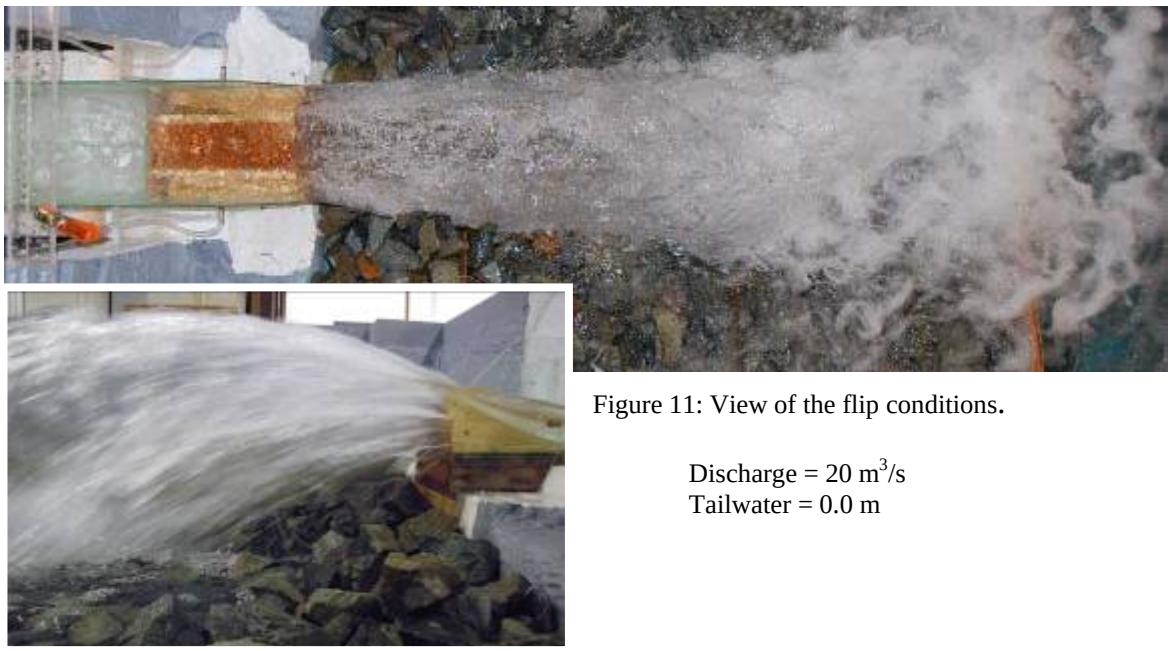

Figure 11: View of the flip conditions.

Discharge = 20 m^3/s
Tailwater = 0.0 m

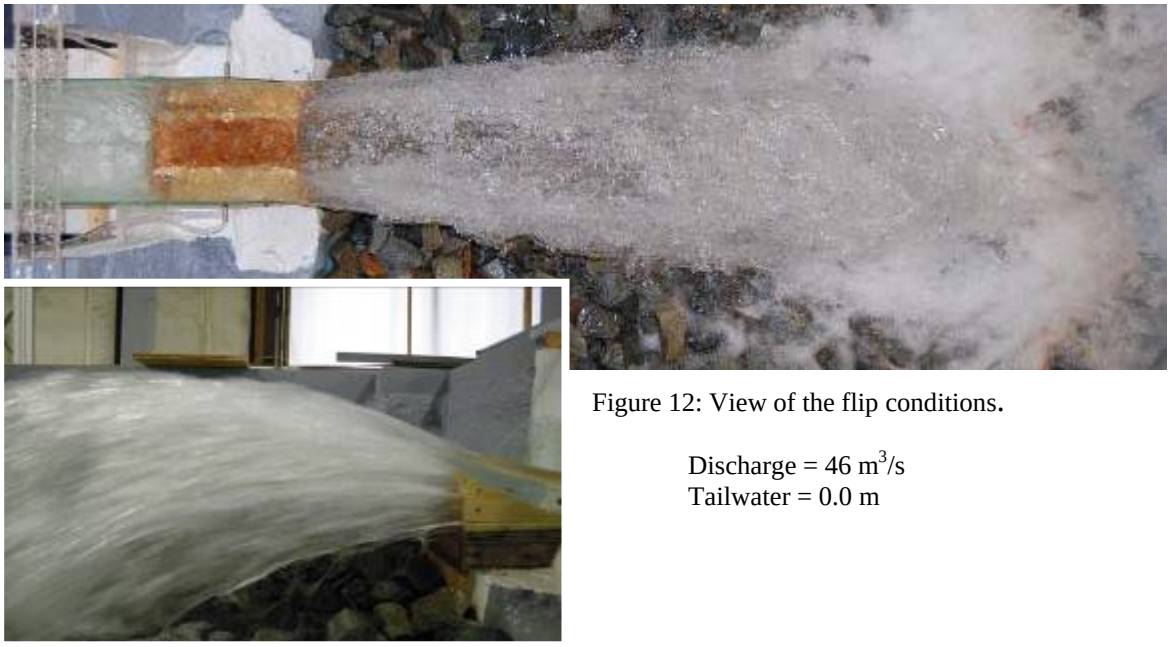

Figure 12: View of the flip conditions.

Discharge = 46 m^3/s
Tailwater = 0.0 m

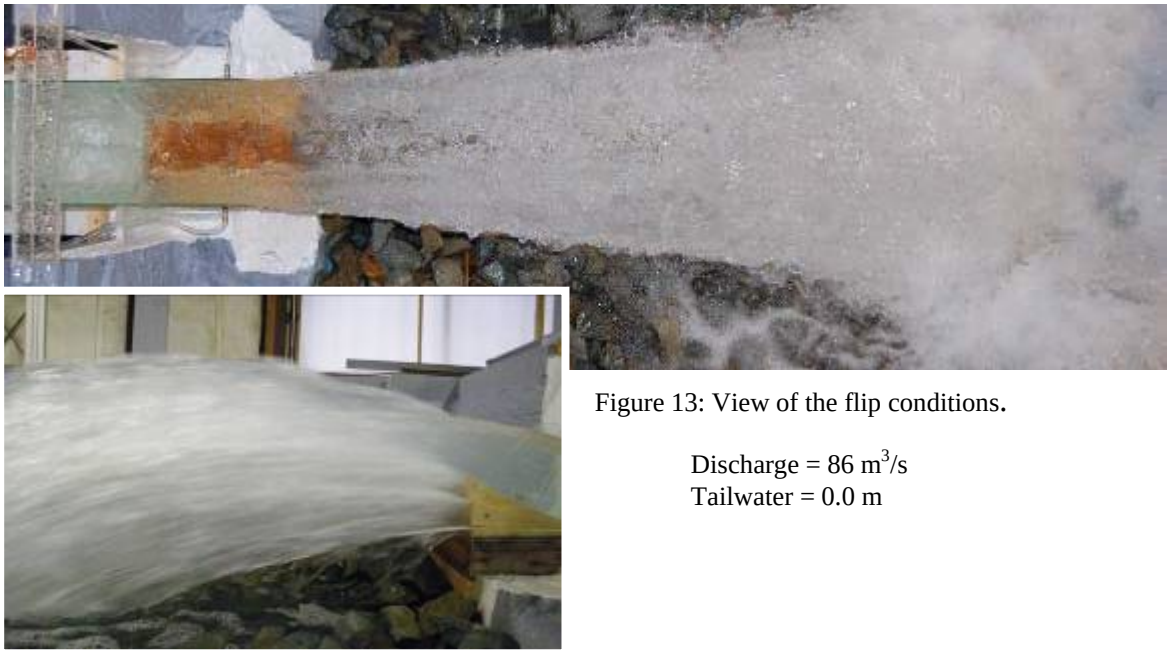

Figure 13: View of the flip conditions.

Discharge = 86 m^3/s
Tailwater = 0.0 m

Lower flows generate a hydraulic jump upstream of the flip and a discharge of 7 m^3/s is required to wash the jump out of the flume. Once the jump has been washed out of the flume a lower flow of approximately 2 m^3/s is required re-establish the jump. This by-stable flow phenomenon, hysteresis, is common with the formation of hydraulic jumps.

The maximum velocities recorded adjacent to the left bank reached 2.8 m/s during design flow events. This implies a D_{50} of 300 mm is sufficient to protect the bank from return flow velocities. However, additional scour immediately downstream from the flip bucket and away from the bank is expected.

4.4.4 Debris Testing

Additional tests were conducted to identify the impacts debris may have on the capacity of the flip structure. As stated above, at flows less than 7 m^3/s, a hydraulic jump can form within the downstream section of the flume.

The hydraulic jump forms a re-circulating flow that traps both floating (wood) and heavier (rocks) material upstream of the flip. When the discharge increases the debris is washed out of the channel.

The debris barrier upstream of the flume is designed to allow debris smaller than 0.7 m to pass through and into the flume. During the debris testing, rocks of approximately 0.5 m (prototype) were introduced upstream of the channel. Although infrequent, these rocks did become wedged within the 0.4 m wide slot between the intermediate step and the channel wall. However, the capacity of the flume was not impacted and the additional spray was not significant.

To reduce the potential of debris collecting one design modification that was considered was slightly adjusting the width of the slot between the flip bucket and the channel wall. The upstream slot width would be reduced and tapered to a greater width at the end of the flume. Although not considered as part of the model testing, this modification is not expected to significantly impact the operation of the flip bucket during design flow conditions.

5. SUMMARY AND CONCLUSIONS

A 1:16 scale physical hydraulic model was used to evaluate the hydraulic design of the proposed Buntzen Power Plant No.1 Lower Spillway. The model reproduced approximately 150 m including a section of the approach channel, the entire spillway flume, and the tailrace. Detailed design development workshops directed by BC Hydro resulted in a lower spillway design capable of passing the design flow of 86 m^3/s. The proposed design was then evaluated to confirm the hydraulic characteristics and performance.

Under all flow conditions transverse waves formed within the approach channel and continued through the transition and into curved flume entrance. Within the curve super-elevated flow conditions dominated the transverse waves. At 86 m^3/s the super-elevation forced the water surface above the crown of the entrance along the left wall while lowering the water surface along the right wall. The rounded entrance geometry allows the elevated flow to pass into the covered channel while maintaining free surface flow conditions along the right side of the channel.

The super-elevation upstream of the flume entrance generates a transverse wave that propagates down the entire length of the spillway. Immediately downstream of the entrance the wave reflects to the right side of the flume, creating uplift pressures of up to 1.5 m, while the left side of the channel remains open to allow the movement of air. Approximately 12 m downstream of the entrance the water surface remains detached from the top of the flume.

The slope transition generates additional pressure on the flume. At this location localized pressures reach 5.0 m while the water surface remains well below 3.0 m depth.

The proposed terminus structure design included a single stepped tooth centered at the end of flume. A channel on either side of the tooth allows lower flows to pass beside the main flip while providing a drain for rainfall accumulation and seepage. The secondary steps between the drains and the main flip help pass lower flows while promoting spreading of the jet at higher flows. The main flip is designed to flip the majority of higher flows out away from the shore and into Indian Arm.

A discharge of 7 m^3/s is required to wash the jump out of the flume. Once the jump has been washed out of the flume, a lower flow of approximately 2 m^3/s is required to re-establish the jump.

The maximum velocities recorded adjacent to the left bank reached 2.8 m/s during design flow events.

6. ACKNOWLEDGEMENTS

The authors wish to emphasize that the hydraulic design of the spillway is only one component of the spillway replacement project, and would like to acknowledge the contributions of Peter Buchanan, P. Geo., Simon Drexl, P.Eng., Sandra Wilson, R.P.Bio., as well as other project team members.

HIGH RESOLUTION 3D HYDRAULIC NUMERICAL MODELING FOR WEP ENVIRONMENTAL APPROVAL AND ENGINEERING

David B. Fissel, ASL Environmental Sciences Inc., Sidney, BC, Canada
Jianhua Jiang, ASL Environmental Sciences Inc., Sidney, BC, Canada

ABSTRACT:
The Waneta Expansion Project, a partnership of Columbia Power Corp. and Columbia Basin Trust, involves the construction of a second powerhouse at the Waneta Dam on the Pend d'Oreille River just upstream of its confluence with the Columbia River. During the WEP environmental review process, a key issue was the sub-population of white sturgeon in the confluence waters. Extensive biophysical analyses were carried out to examine potential effects, using a hydraulic 3-D numerical model developed specifically for this reach of the two rivers. The model had a very high resolution of 3 m by 3 m in the horizontal and 10 vertical layers for a total of 92,000 grid elements. It was calibrated and validated using data obtained from field surveys of river velocities, water levels and temperatures for a variety of flow conditions. Using the model, the pre- and post-project river velocities and temperatures were computed and compared, specifically regarding effects in the deepwater habitat of the Waneta Eddy, in the near-bottom velocities in the egg deposition areas and in the late summer water temperatures. These analyses, along with fisheries biological interpretations, were used in the comprehensive review by the BC Environmental Assessment Office and Federal Government Departments, particularly the Dept. of Fisheries and Oceans. The Project received its Environmental Approval Certificate in November 2007. The 3-D numerical model was also used for input to engineering issues on the water levels immediately downstream of the Waneta expansion plant and water velocities in the headpond with the plant in operation.

RÉSUMÉ:
Le Projet d'Expansion de la Waneta, un partenariat entre la Columbia Power Corp. et le Columbia Basin Trust, vise la construction d'une deuxième centrale électrique au barrage de Waneta sur la rivière Pend d' Oreille juste en amont de sa confluence avec la rivière Columbia. Le processus d'études environnementales (WEP) touche principalement la population d'esturgeon blanc dans les eaux du confluent. Des analyses biophysiques approfondis ont été effectuées pour examiner les effets possibles sur la dite population en utilisant un modèle hydraulique numérique à trios dimensions développé spécifiquement pour la région des deux rivières. Le modèle a une résolution fine de 3 m par 3 m en vue de plan et 10 couches horizontales en profondeur pour un total de 92 000 éléments pour l'ensemble de la grille. Le modèle a été calibré et validé en utilisant des données obtenues lors de mesures des champs de vitesse de l'eau, des niveaux d'eau et des températures pour une série de conditions de débit. En utilisant le modèle, les vitesses et les températures prise avant et après le projet ont été calculées et comparées; particulièrement, les effets sur l'habitat en eau profonde des eaux tournantes de cette région (Waneta Eddy), sur les vitesses du fond dans les secteurs de dépôt d'œufs et sur les températures de l'eau vers la fin de l'été ont été comparées.

En incluant des interprétations biologiques de pêche, ces analyses ont été employées dans la revue complète par le bureau d'évaluation environnementale du C.B. et les services gouvernementaux fédéraux, en particulier Pêches et Océans Canada. Le projet a reçu son certificat d'approbation environnementale en novembre 2007. Le modèle numérique à trois dimensions a également été employé lors de l'évaluation des contraintes hydrauliques immédiatement en avale du Projet et en qui concerne le champ de vitesse en amont de la prise d'eau de la nouvelle centrale durant son opération.

1. INTRODUCTION

The Waneta Expansion Project (WEP), a partnership of Columbia Power Corporation and Columbia Basin Trust, involves the construction of a second powerhouse at the Waneta Dam on the right bank of the Pend d'Oreille River just upstream of its confluence with the Columbia River (Figure 1). The expansion project may have potential effects on the flow and circulation patterns in the area of the confluence of the Columbia and Pend d'Oreille rivers. During the WEP environmental review process, a key issue was the sub-population of white sturgeon in the confluence waters. Previous studies revealed that this confluence area has some significant morphological and circulation features, which are important for white sturgeon such as the deepwater low-speed Waneta Eddy for sturgeon rearing and feeding and the jet-like, high-speed Pend d'Oreille River outflow for sturgeon spawning and egg deposition (Hildebrand and Fissel, 1997; Hildebrand, 2001).

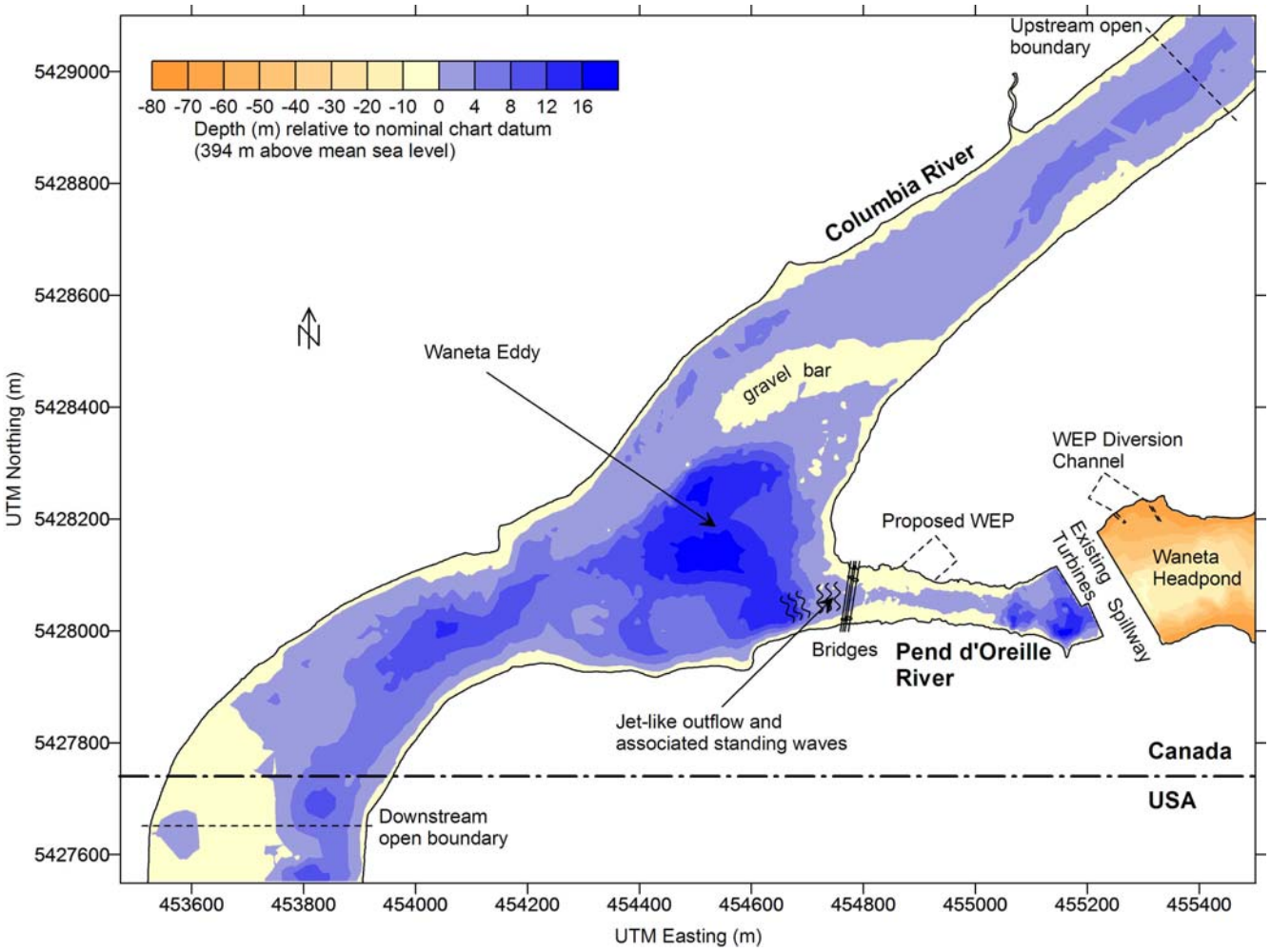

Figure 1: Study area showing geometry, model domain and boundaries.

The confluence of the Columbia and Pend d'Oreille rivers is located about 500 m north of the Canada and USA border (Figure 1), where flows from the upstream Columbia River and the Pend d'Oreille River join together before passing into the United States. The center of the confluence is a region of a large embayment with a water depth up to 18 m or more, much deeper than the surrounding areas. The flows in this area appear comparatively weak, typically less than 0.5 m/s, and usually rotate in counter-clockwise direction, known as the Waneta Eddy. On the northern side of the Waneta Eddy, the main channel of the Columbia River features large flows through typical water depths of 2 to 6 m relative to chart datum at 394 m above mean sea level (MSL). Just upstream of the confluence of the two rivers, a large gravel bar extends out from the eastern shore which confines the main flows of the Columbia River to a comparatively narrow channel along the western shore. Immediately to the south of the Eddy is the strong jet-like outflow from the Pend d'Oreille River into the Columbia River. The

flows under the road and rail bridges, where the Pend d'Oreille waters enter the Columbia River, are normally turbulent due to the shallow and narrow Pend d'Oreille passageway. This discharge zone is characterized by large standing waves indicative of a supercritical flow regime. The highly turbulent, standing wave area extends downstream as far as the southeast corner of the deep portion of the Waneta Eddy.

Extensive biophysical analyses were carried out to examine potential effects, using a hydraulic 3-D numerical model COCIRM developed specifically for this reach of the two rivers. The model had a very high resolution of 3 m by 3 m in the horizontal and 10 vertical layers for a total of 92,000 grid elements. It was calibrated and validated using data obtained from field surveys of river velocities, water levels and temperatures for a variety of flow conditions. Using the model, the pre- and post-project river velocities and temperatures were computed and compared, specifically regarding effects in the deepwater habitat of the Waneta Eddy, in the near-bottom velocities in the egg deposition areas and in the late summer water temperatures. These analyses, along with fisheries biological interpretations, were used in the comprehensive review by the BC Environmental Assessment Office and Federal Government Departments, particularly the Dept. of Fisheries and Oceans. The Project received its Environmental Approval Certificate in November 2007. The 3-D numerical model was also used for input to engineering issues on the water levels immediately downstream of the WEP plant and water velocities in the headpond with the plant in operation.

2. IMPLEMENT OF 3D COCIRM

2.1 Brief description of the 3D model

In this study, a high resolution 3D numerical model, COCIRM, is applied to simulate the flows in and around the confluence of the Columbia and Pend d'Oreille rivers as well as in the Waneta headpond. The "COCIRM" model, developed over the past several years, represents a computational fluid dynamics approach to the study of river, estuarine and coastal circulation regimes. The model explicitly simulates such natural forces as pressure heads, buoyancy or density differences, wind stress and drag arising from the shoreline and the river bottom. The model applies the fully three-dimensional basic equations of motion combined with a second order turbulence closure model, then solves for the time-dependent, three-dimensional velocities (u, v, w), turbulence kinetic energy (q), water surface elevation (ξ), water temperature (T) and salinity (s) (Jiang, 1999; Jiang et al, 2003; Fissel and Jiang, 2008). The model is capable of representing discharge outfalls and intakes in a realistic manner. A semi-implicit finite difference method was applied in the COCIRM model. This numerical solution method has the advantages of a minimal degree of implicitness, good stability and consistency, and high computational efficiency at a low computational cost. The horizontal grid element sizes are typically in the range of 5 to 100 m. The vertical sigma-grid or z-grid may be distributed unevenly, with typically 10 – 20 layers.

This COCIRM model operated on two separated domains, respectively the confluence model downstream of Waneta Dam and the headpond model upstream of Waneta Dam. The bathymetry data used in both model areas have the resolution of 3 m or better. The confluence model extends approximately 1260 m upstream from the Waneta Eddy and 1050 m downstream to an area just south of the Canada and US border. The model runs on a grid with 3 m by 3 m horizontal grid cell size and 10 equally-spaced sigma layers. The inflow discharges from the upstream boundaries at the upstream Columbia River, existing Waneta Dam and proposed WEP tailrace were given and represented in a realistic manner in the model (Jiang and Fissel, 2002). The boundary conditions for the downstream portion of the Columbia River were specified through a modified form of Sommerfeld radiation approach introduced in Orlanski (1976).

The headpond model includes the proposed WEP diversion channel and a portion of Waneta Dam headpond extending approximately 1.5 km upstream from the dam. The model runs on a horizontal grid of size 3 m by 3 m and 15 vertical sigma-layers with higher resolution near the bottom in order to appropriately represent near-bottom turbulence boundary layer and sediment processes. The outflow discharges from the spillway, existing Waneta Dam turbines, and proposed WEP turbines are represented in a realistic manner in the model. The open boundary conditions at the upstream end were specified by water levels (Jiang and Fissel, 2008).

2.2 Model calibration and validation

In the confluence area, the flow patterns and the outflow standing waves, etc., appear to be dynamic and vary considerably with different flow combinations of the Columbia and Pend d'Oreille rivers. To evaluate the model performance and validate it as a reliable tool for the environmental assessment, the flow combinations of the two rivers in all model calibration and validation cases must span a substantial range of discharges to represent various flow features for which the in situ observed current data are available. Since 1994, extensive field measurements of currents in this region, mostly in the confluence area, have been carried out by ASL Environmental Sciences Inc. and R.L. & L. Environmental Services Ltd., using ship-borne ADCP (Birch, 1994; Birch, 1996; Hildebrand and Fissel, 1997; Birch and Boubnov, 2001; Birch and English, 2001). These data allow for the extensive model calibration and validation cases realized in this study. In total, two calibration cases (C1 and C2) and seven validation cases (V1 – V7) were selected and carried out. These cases are believed to be sufficient for the model validation requirements (Table 1).

In the headpond model, one calibration case and one validation case (Table 1) were conducted to optimize the major hydrodynamic parameters to give the best fit between the modeled and in-situ observed velocity vertical profiles and flow patterns measured in the field survey by ADCP in 2008 (Fissel et al., 2008)

Table 1: Summary of model calibration and validation cases.

Model area	Model case		Discharge (m^3/s)				Temperature (°)		Observation taken
			Upper Columbia River	Pend d'Oreille River			Upper Columbia River	Pend d'Oreille River	
				Exsiting Power house	Spillway	Total			
Confluence	Cali.	C1	1,812	229		229	18.8	22.4	Aug. 31, 94
		C2	2,300	725	209	934	2.5	1.5	Feb. 08, 96
	Validation	V1	1,982	510		510	18.8	22.2	Aug. 30, 94
		V2	951	147		147			Jul. 15, 01
		V3	1,104	227		227			Oct. 20, 01
		V4	1,104	510		510			Oct. 20, 01
		V5	951	283		283			Jul. 15, 01
		V6	2,550	34		34			Oct. 06, 96
		V7	2,039	720	359	1,079	10.0	13.0	May 18, 94
Headpond	Calibration			775		775			Apr. 9, 08
	Validation			402		402			Apr. 8 – 9, 08

The model was initially tested and operated in calibration runs. Various physical parameters, mainly bottom drag coefficient and horizontal and vertical eddy diffusivity coefficients, were repetitively adjusted to achieve optimal agreement with the observations. The vertical diffusivity for the model, as derived from the second order turbulence closure model (Mellor and Yamada, 1982), was found to be robust. Some adjustments of the horizontal diffusivity were made through the user-specified calibration parameter in Smagorinsky's formula (Smagorinsky, 1963). The bottom drag coefficients were the most important parameter for the purpose of model calibration. Once reasonable agreement is attained in the calibration runs (as seen in Figure 2 for the C1 model case), the model was next operated in validations runs using the previously optimized physical parameters and compared with different observation data sets. The agreement between the model outputs and the observations is used to assess the capabilities of the model. Following the methods of Murphy and Winkler (1987), the results of the validation model runs were compiled and analysed in detail. The resulting modelling validation report (Fissel and Jiang, 2002) was the basis for a favourable peer review of the model conducted anonymously a DFO numerical modelling scientist.

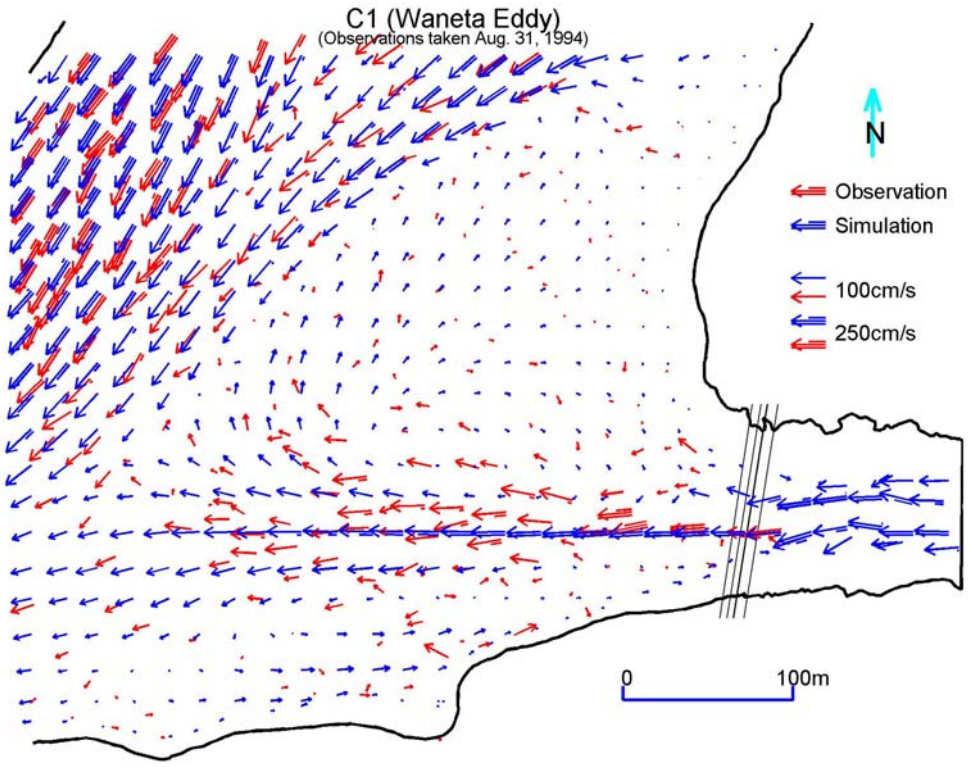

Close-up of the Waneta Eddy with Simulated flows at a depth of 2.2 m

Columbia River flow: 1812 m^3/s, Pend d'Oreille River flow: 229 m^3/s

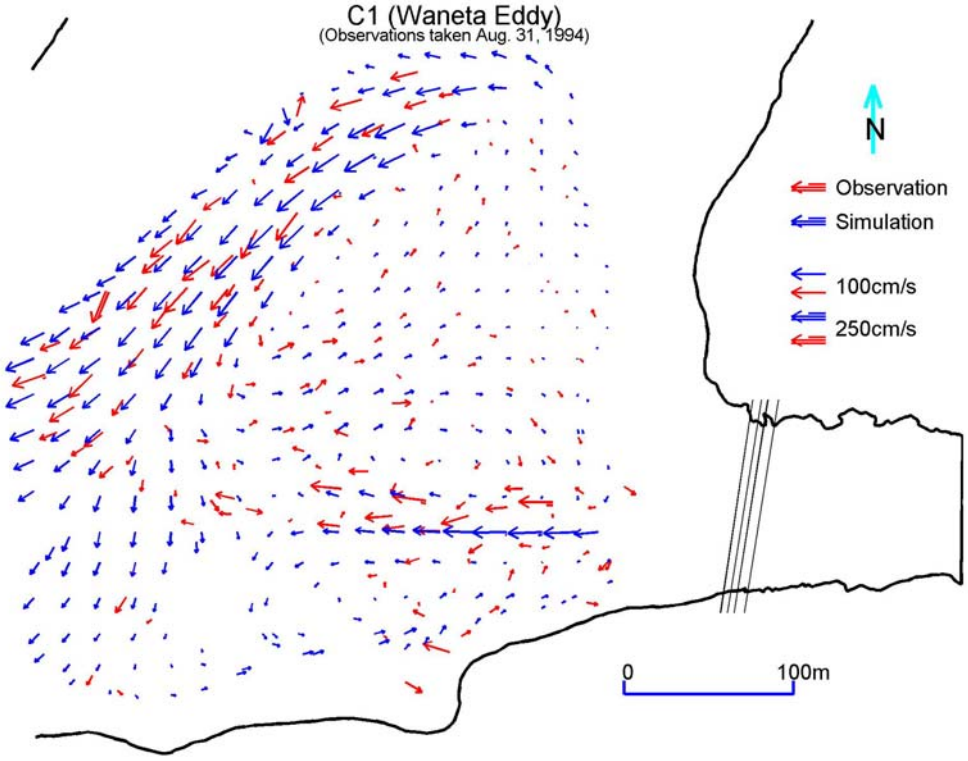

Close-up of the Waneta Eddy with Simulated flows at a depth of 8.2 m

Columbia River flow: 1812 m^3/s, Pend d'Oreille River flow: 229 m^3/s

Figure 2: C1 model results for the Waneta Eddy area at 2.2 m (upper panel) and 8.2 m (lower panel) water depths, with comparisons to observations from Aug. 31, 1994.

2.3 Dynamic Confluence Circulation Patterns

The confluence circulation patterns vary dynamically with the variations of discharges from upper Columbia River and Pend d'Oreille River. At extremely low Pend d'Oreille River flow, such as the "speed-no-load flow" of 34 m^3/s in the validation case V6, the entire embayment area from the gravel bar to the southern shore is occupied by a large counter-clockwise eddy (labeled as C in Figure 3), driven by the shears of the main Columbia River flow. The weak Pend d'Oreille River flow joins the eddy along the eastern bank. As the Pend d'Oreille River discharge increases, the outflow gains more and more momentum to break through the big eddy. In these cases, the actual circulation patterns are dependent not only on the Pend d'Oreille River flow, Q_{pdr}, but also on the Columbia River discharge level, Q_{col}. For moderate to high levels of Q_{col} (≥ 1,300 m^3/s), the outflow gradually shifts southward towards to southern shore as the Q_{pdr} increases. At the same time, the clockwise eddy (labeled as P inFigure 3, which is driven by the shear of the Pend d'Oreille outflow, gradually shrinks and the counter-clockwise eddy C becomes dominant. During this process, a third eddy appears near the southern shore, namely south shore eddy (labeled as S in Figure 3), driven by the shears from both Columbia main flow and the Pend d'Oreille outflow, and disappears at high level of Q_{pdr}. For the low flow level (Q_{col} < 1,300 m^3/s), the gravel bar acts as a weir or dam with little or no water passing over it. As a result, the deep water area is dominated by the clockwise eddy P if the Pend d'Oreille River discharges are at low to modereate levels (100 – 500 m^3/s). At the high flow level (Q_{pdr} > 500 m^3/s), the water elevation at the confluence increases and the gravel bar is submerged with a considerable amount of water passing over it. Consequently, the counter-clockwise eddy C becomes dominant again.

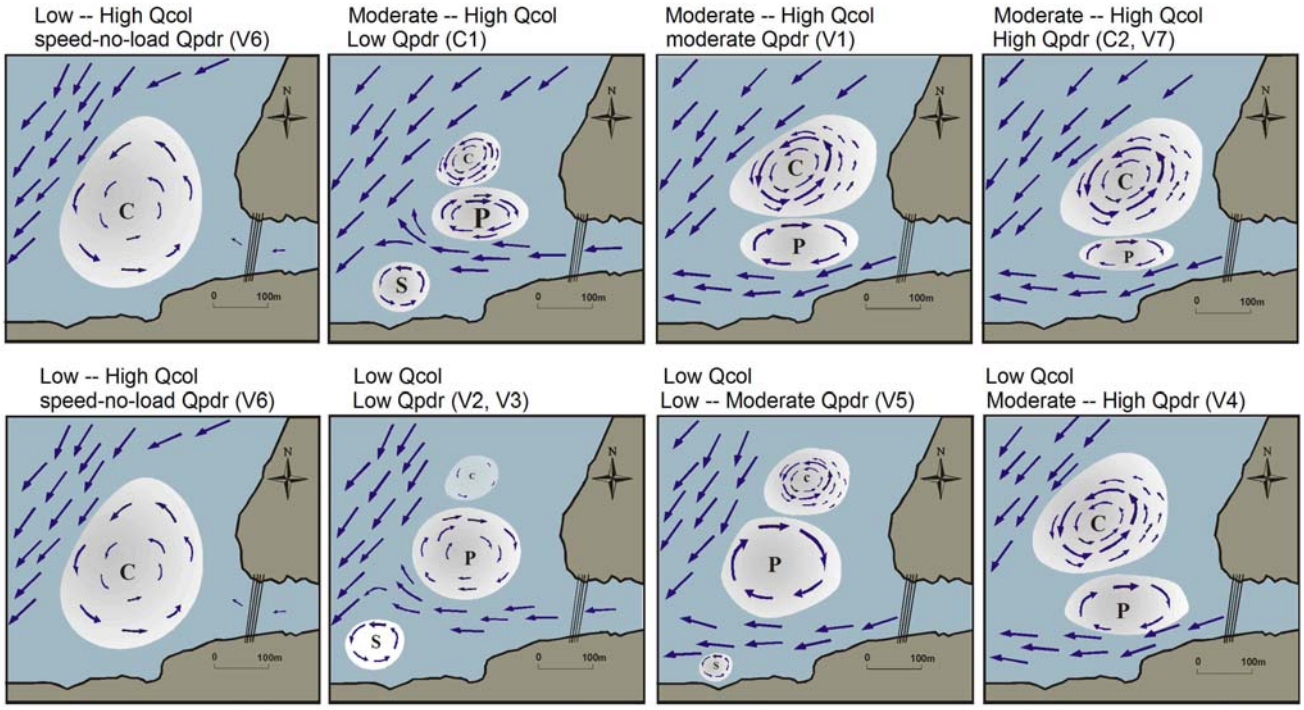

Figure 3: Schematic diagram of the circulation patterns in the confluence area.

3. MODEL RESULTS SUPPORTING WEP ENVIRONMENTAL APPROVAL

3.1 Productive Habitat Area

Following completion of WEP, the Canadian Pend d'Oreille hydroelectric system daily flows will be reshaped to maximize electricity generation values. This will result in post-project operations increasing daily variations in water levels below Waneta Dam, and consequently, potential loss of fish habitat in the confluence area

downstream of Waneta. As a key parameter for the WEP environmental approval, the productive habitat area within the varial zone was estimated based on the 3-D model results. The varial zone is the area that lies between the upper and lower annual water levels that occurs in each reach. The productive capacity of the littoral zone associated with the confluence area was modelled over time with the assumption that wetted area had a benthic recovery time of 20 days. In the modelling effort, this was simulated by assuming no habitat value for the first 10 days after being re-wetted, followed by immediate full recovery after day 10. This value was selected based on literature reviews of periphyton and benthic macro-invertebrate recovery times of de-watered habitat.

To examine the changes in productive habitat below Waneta Dam between pre- and post-project conditions, an empirical model was developed to compute habitat availability of the littoral zone in the river reference area. Because of the complexity in flow patterns, the model was separated into four sub-regions in order to facilitate the derivation of appropriate relationships. These four sub-regions are respectively Columbia downstream of confluence, center of confluence, Columbia upstream of confluence, and Pend d'Oreille River. The river reference area in the first sub-regions is primarily dependent on the Columbia River discharge, and the river reference area in the last sub-regions is primarily dependent on the Pend d'Oreille River discharges. In the other two sub-regions, the river reference areas are dependent on both Columbia and Pend d'Oreille river discharges.

The empirical model is derived as a least square fit of the 3-D numerical model derived wetted area (A), applied separately to each of the four sub-regions, as a function of the Columbia and Pend d'Oreille river discharge values (Q_{col} and Q_{pdr})

$$A = \alpha Q_{pdr} + \beta Q_{col} + \chi \left(\frac{1}{Q_{pdr} + Q_{col}} \right)^{\delta} + \varepsilon \qquad (1)$$

Where α, β, γ, δ and ε are the coefficients derived from the least square fit.

The empirical model wetted area values are in very good agreement with the wetted area reference data, as obtained from the 3-D numerical model for over 40 combinations of river flows. Correlation coefficients exceeding 0.995 were attained for all four sub-regions.

The changes in daily productive habitat area downstream of the Waneta Dam, resulting from the operation of WEP, was computed by individual years from 1991 to 1999, inclusive, and for the average values for the 1991 – 1999 period (as seen in Figure 4). The computations were with the present enhancement version (WSFAP-1998) and the Post-Project Enhancement version (WSFAP-PPE) of the White Sturgeon Flow Augmentation Program, which has been accepted by the appropriate regulatory agencies. In summary, the daily average reduction in productive habitat area relative to Pre-Project conditions as computed over the full year based on the nine year average values is 0.37 hectares for Post-Project with WSFAP-PPE as compared to 0.34 hectares for Post-Project with WSFAP-1998. The difference between 0.37 and 0.34 is very small being well within the normal daily variability of productive habitat area.

3.2 Low Velocity Habitat Area

The low velocity area affected by the Waneta Eddy relevant flows represents another important white sturgeon habitat in the Pend d'Oreille/Columbia confluence, as per the WEP environmental approval requirement. The 3-D model results provide detailed insight into the potential impact of the WEP regarding this habitat issue. A total of five representative flow discharge combinations were carefully selected for modelling, based on the simulation of the Pend d'Oreille discharges for the average 1991 to 1999 conditions at different times of the year, along with the average Columbia River discharges for the same dates. Well-established environmental habitat flow parameters specified by the project's fisheries consultant were computed and mapped for the selected cases.

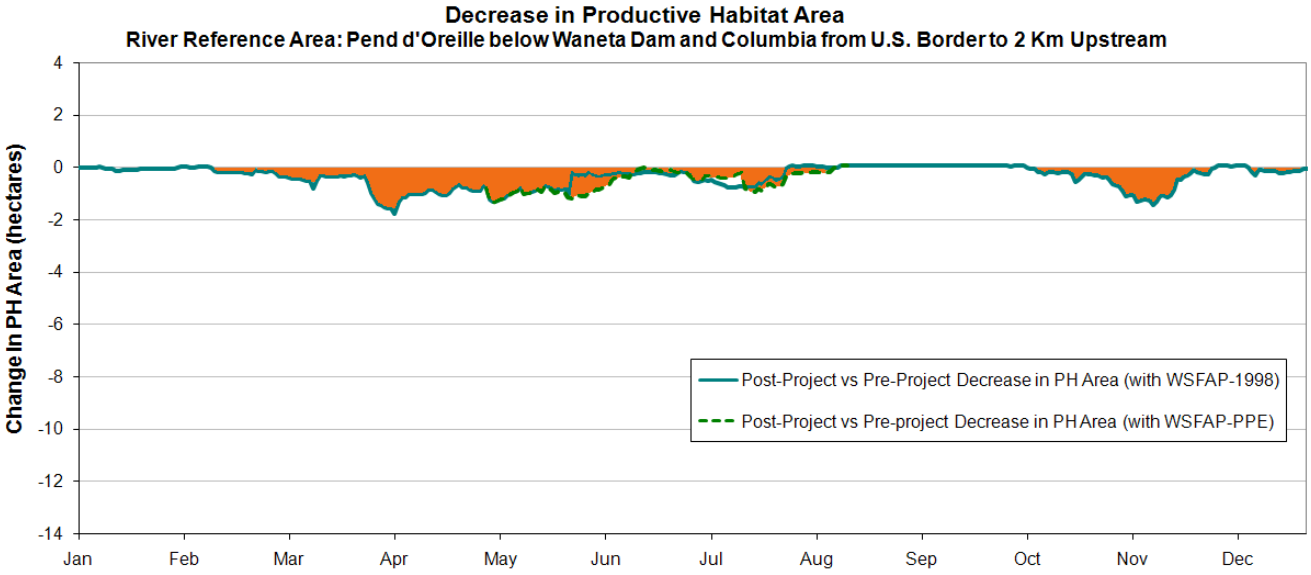

Figure 4: Average decreases in productive habitat area resulting from the operation of WEP for the 1991 – 1999 period.

The model results (as seen in Figure 5 for Case 1) show that changes in the low velocity areas affected by the Eddy relevant flows at various times throughout the year can be either positive or negative. In all but one case (not shown), these area changes are very small. The low velocity habitat area change in the one exception (Case 5), which shows a reduction of 28% in low velocity area during light load hours on one average day in early November, is well within the range of low flow area reductions that occur at other times under pre-project conditions. In all five cases considered, the physical effect of the project on Eddy near-bottom temperature changes are found to be much smaller than 1.5 °C, generally considered by fisheries biologists as a threshold level for discernible biological effects.

3.3 Near-Bottom Velocities at Different Locations of Egg Mats

Extensive historical surveys have shown that the strong flow areas along the south shore of the Columbia/Pend d'Oreille confluence are important white sturgeon spawning and incubation habitat in the June to July spawning period. As one of the key issues for the WEP environmental approval, the 3-D model results were used to estimate the potential effect of WEP operations on the near-bottom velocities at a total of nine locations of egg mats, which were identified from recorded data of incubating eggs in the spawning area (Figure 6). An empirical model was developed to examine the changes in the near-bottom velocities at these locations between pre- and post-project conditions. The empirical model is derived as a least square fit of the 3-D numerical model derived near-bottom velocity (V_b), applied separately to each of the nine locations of egg mats, as a function of the Columbia and Pend d'Oreille river discharge values

$$V_b = \alpha' Q_{pdr}{}^{\beta'} + \chi' Q_{col}{}^{\delta'} + \varepsilon' \left(\frac{1}{Q_{pdr} + Q_{col}} \right)^{\phi'} + \varphi' \left(\frac{Q_{pdr}}{Q_{pdr} + Q_{col}} \right)^{\gamma'} + \eta' \left(\frac{Q_{col}}{Q_{pdr} + Q_{col}} \right)^{\lambda'} + \mu' \qquad (2)$$

Where $\alpha', \beta', \chi', \delta', \varepsilon', \phi', \varphi', \gamma', \eta', \lambda'$ and μ' are the coefficients derived from the least square fit.

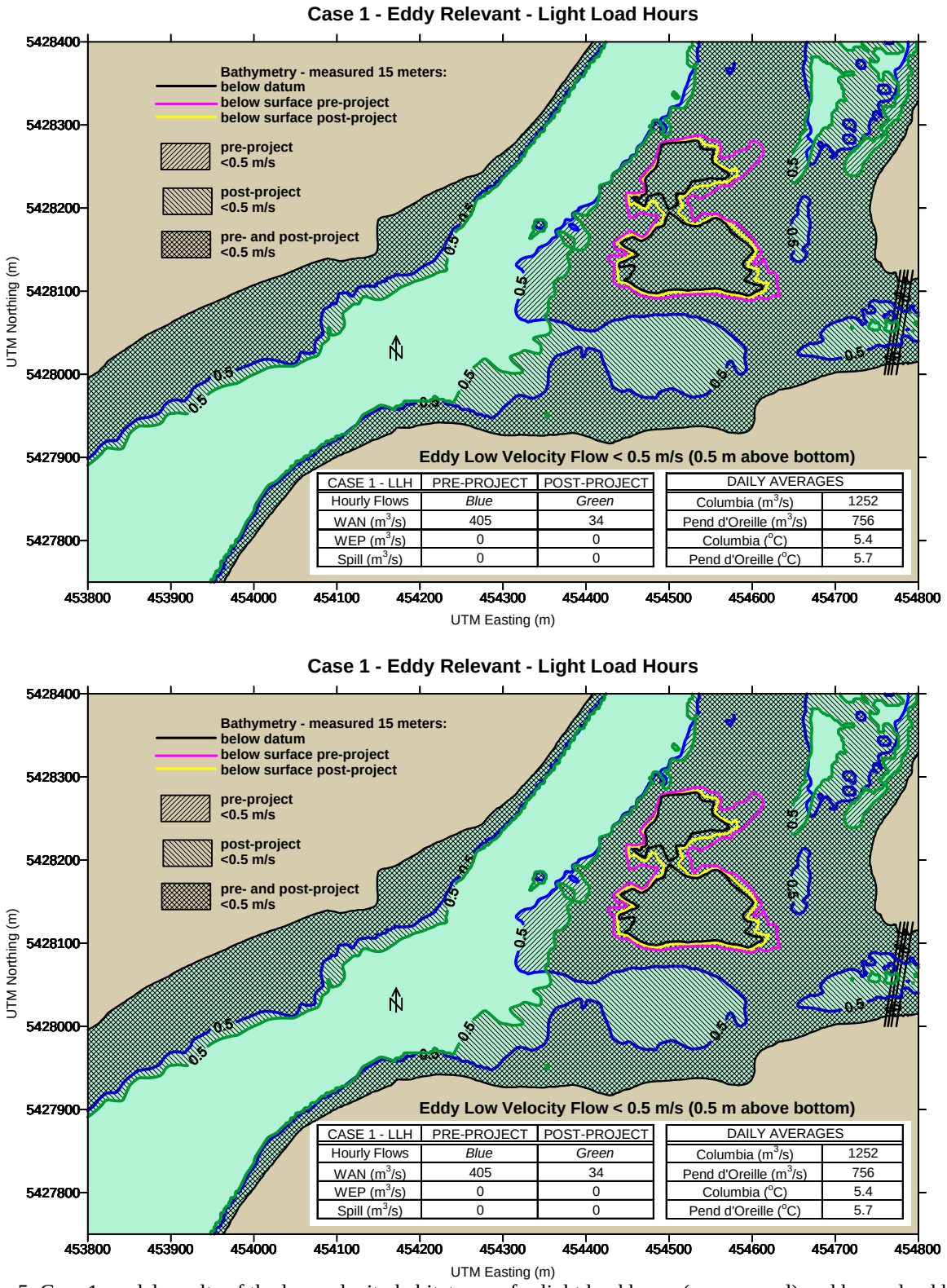

Figure 5: Case 1 model results of the low velocity habitat areas for light load hours (upper panel) and heavy load hours (lower panel).

The empirical model near-bottom velocity values are in very good agreement with the near-bottom velocity data, as obtained from the 3-D numerical model for over 40 combinations of river flows. Correlation coefficients exceeding 0.95 were attained for all nine locations.

The changes in the near-bottom velocities at the selected nine sites, resulting from the operation of WEP, were computed for a total of eight years, respectively 1996, 1998 and 2000 – 2005, when the white sturgeon incubations were monitored. Reduced flow velocities can result in increased egg predation reducing recruitment of white sturgeon. The flow histograms (not shown) indicate that the near-bottom velocities are generally 1.0 to > 2.4 m/s at most of the egg mat sites (sites C4, D1, E1 E1.5 and M1; locations shown in Figure 6) for seven of the eight years. In 2001, a year having the lowest discharges in past 40 years, the velocities are generally less than 1.0 m/s. The near-bottom velocities at site C1, and to a lesser degree at site C3, are noticeably reduced by comparison to the mat locations in the mainstem of the Columbia River flows. At site C1, the velocities are generally about 0.6 – 1.0 m/s in June and 0.2 – 0.6 m/s in July. The egg mat velocities were also modelled using hourly flows for the Pend d'Oreille River which would occur under post project conditions indicating only small differences from pre-project conditions. These modelling data supports the conclusion of no significant negative effects of past Pend d'Oreille flows or future project related flow changes on white sturgeon egg spawning/incubation.

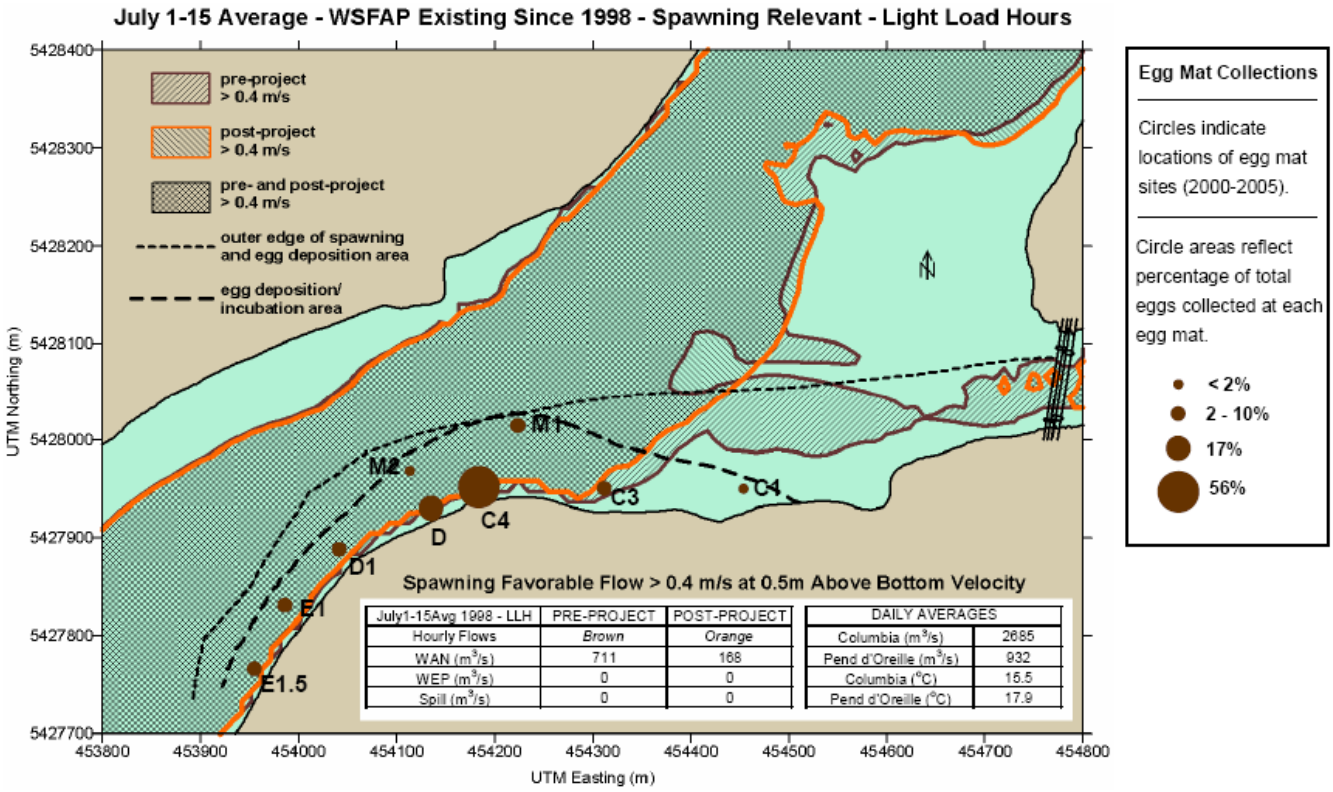

Figure 6: Map showing white sturgeon egg mat locations.

4. MODEL RESULTS SUPPORTING WEP ENGINEERING

4.1 Water Levels Downstream of Waneta Dam

After successful WEP Environmental Certificate application, the developed 3-D model was used to support the WEP engineering. One of the WEP engineering issues is the water elevations in Pend d'Oreille River. The model was applied to derive water elevations in Pend d'Oreille River downstream of Waneta Dam for various combinations of the flow rates from the Columbia river, existing Waneta Dam and WEP turbines as well as for several flow conditions under the effect of WEP rock fill workpad. These model results (not shown) provided detailed information of the water elevations at the WEP and existing Waneta Dam tailraces and the water level profiles along the Pend d'Oreille River outflow for WEP engineering design.

Before the applications, the model water elevations were calibrated and validated using the measured water elevations along left and right river banks at the Pend d'Oreille outflow region in 2007. Figure 7 shows the comparisons between modeled and observed water elevations for three flow conditions. It is seen that the model results are in good agreement with the observations in terms of the shapes of the water surface profiles and the big water drop under the bridges. Some discrepancies between the model results and data exist. The model water elevations are lower than the observations by around 0.15 m downstream of the bridges and by around 0.3 m upstream of the bridges. It is believed that these discrepancies are mainly caused by insufficient/inaccurate bathymetry input. It is also suggested that further refinement of the model parameters, especially bottom drag coefficient, is necessary to further improve the model performance.

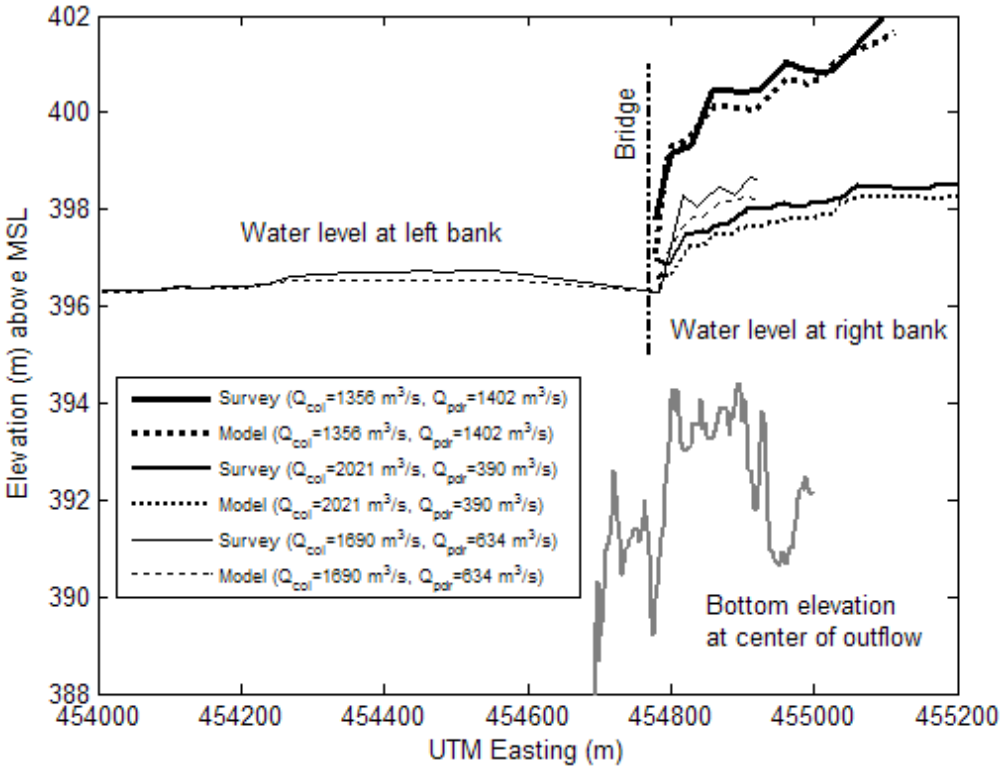

Figure 7: Modeled and observed water surface elevations in the outflow area.

4.2 Flows in Waneta Headpond

Another WEP engineering issue is the potential effect of WEP diversion channel (Figure 1) on the ambient near-bottom currents and consequently on the resuspension of the bottom sediments in the Waneta headpond area. These changes may lead to either positive or negative impact on contaminants releasing in the bottom sediments to downstream of Waneta Dam, which may have accumulated over many years in the past from deposition of Pend d'Oreille River sediments as they entered the comparatively large depths of the headpond where the velocities are reduced and sediments settle out of the water column onto the riverbed. To examine any possible changes to the near-bottom velocities, caused by the WEP operations, the 3-D model was applied to the headpond area with a horizontal resolution of 3 m by 3 m and 15 vertical sigma-layers having higher resolution near the bottom (Jiang and Fissel, 2008).

The model, at first, was calibrated and validated using the ADCP surveys of water velocities in the headpond area conducted in 2008 (Table 1). Figure 8 shows velocity vertical profile comparisons at three sites A – C (see Figure 9) for the calibration case. It is observed that the model velocity profiles at sites A and B are in good agreement with the observations. At site C, the model under-predicted the flow speed by about 3 cm/s compared to the observations.

The modeled headpond flow patterns were compared with observations at three vertical levels, respectively 2.5 m, 7.5 m and 12.5 m depths from the surface. Figure 9 shows the comparisons at 12.5 m depth respectively for the calibration and validation cases. Overall, the modeled headpond flow patterns are in good agreement with the observations. From these results, it is found that the flow patterns in the headpond are very analogous to those induced by basins with restricted outlets, such as sinks. In general, the flows appear to gradually converge and meanwhile become stronger towards the turbine intakes. At the southern corner upstream of the spillway, a well-developed, counter-clockwise eddy appears both in the model and observations with a size of around 100 m in diameter. In the proposed WEP diversion channel approach area, the velocities appear to follow shoreline and gradually turn from WNW to WSW before converging into the intakes. The typical flow speeds in this region range from 0.1 m/s to 0.3 m/s with weaker velocities near the shore.

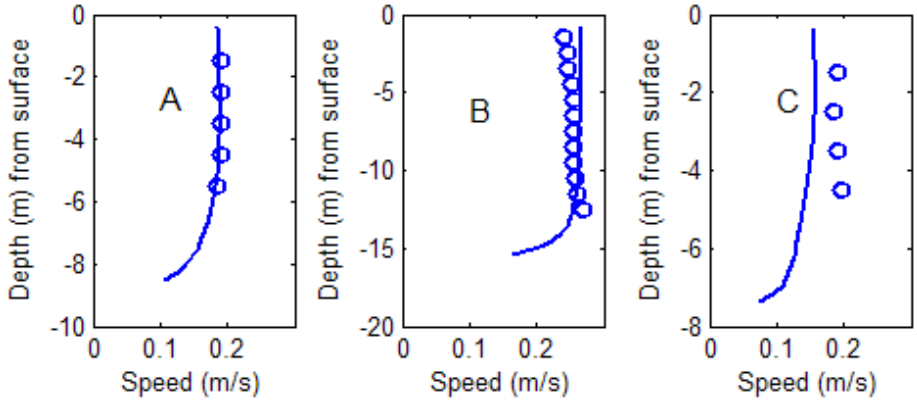

Figure 8: Calibration case modeled (solid lines) and in-situ observed (open circles) velocity vertical profiles at sites A – C.

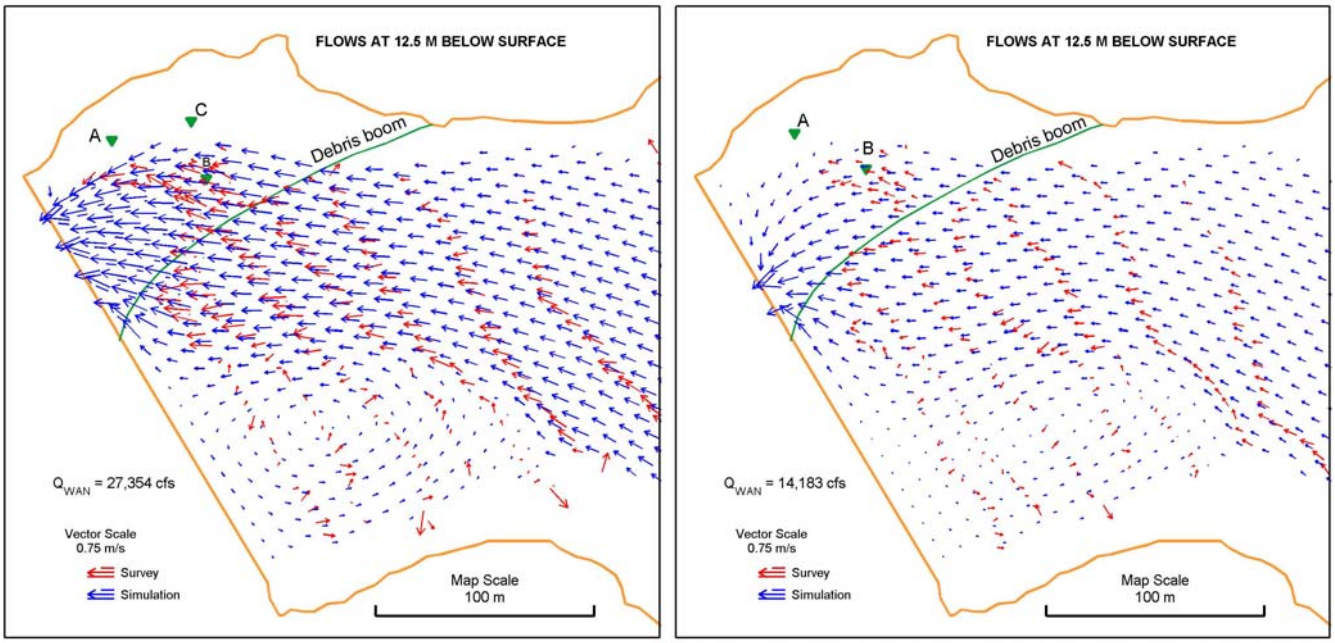

Figure 9: Modeled and observed results of the headpond velocities at 12.5 m depth for the calibration case (left panel) and the validation case (right panel).

After validation, the model was then applied to simulate the velocities in the headpond area for various combinations of discharges rates through the existing Waneta and WEP turbines, and the spillway. Figure 10 shows the model headpond velocities at 1 m above bottom for a case with an existing Waneta turbine discharge of 852 m^3/s and a WEP turbine discharge of 620 m^3/s. From these model results, it is found that that when WEP is in operation, the near-bottom velocities within the diversion channel attain speeds of up to 1.4 m/s or greater. At the entrance to the diversion channel approach within the existing headpond, where excavation will be required in building the approach to the WEP intake, the near-bottom flow speeds are of particular interest. The

near-bottom velocities in this area (bounded by 5,428,170 and 5,428,193 UTM North coordinates and by 455,260 and 455,330 UTM East coordinates) range from 0.06 to 1.01 m/s, with median values of 0.20 m/s – 0.50 m/s.

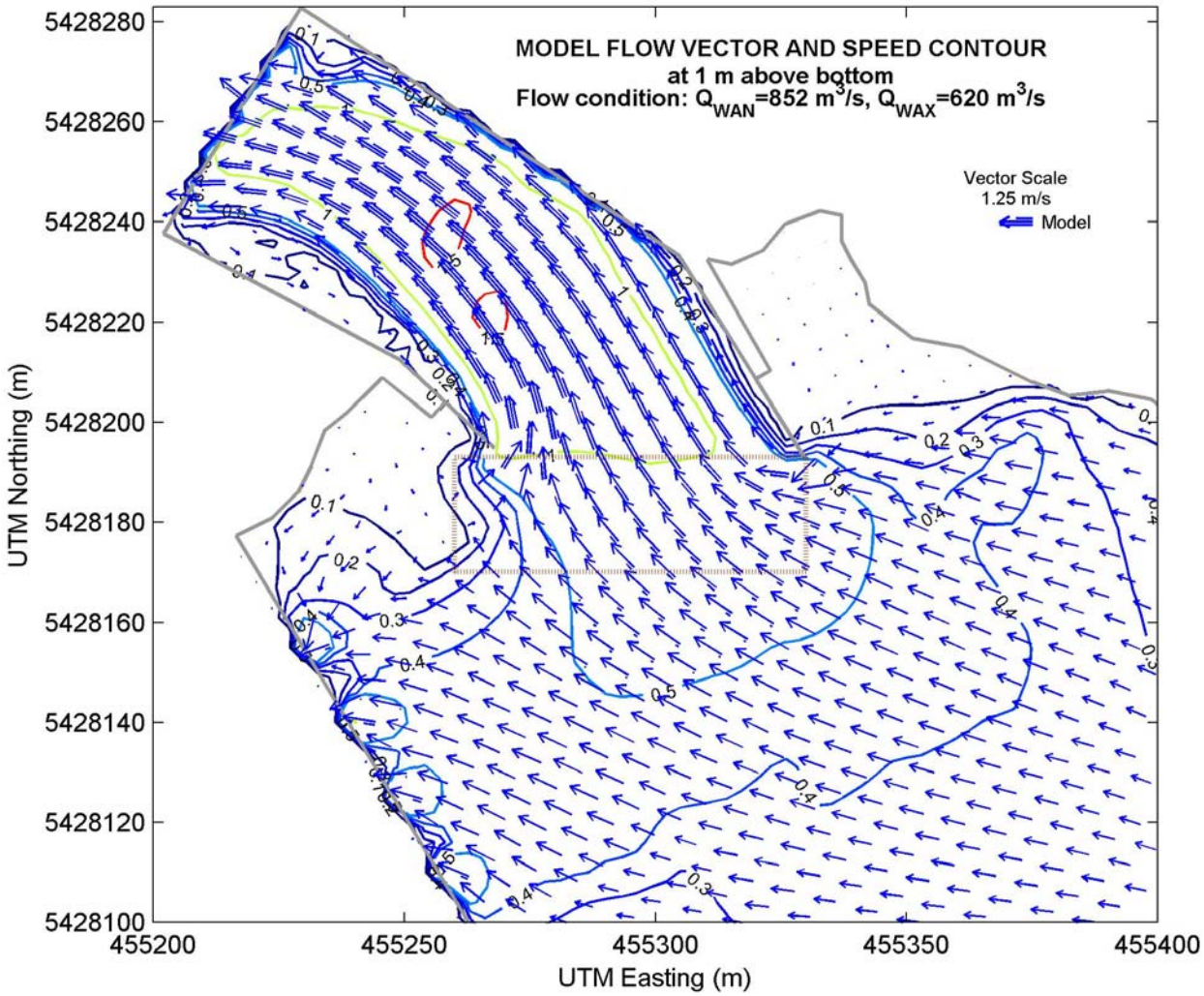

Figure 10: Model results of the headpond velocities at 1 m above bottom for a case with an existing Waneta turbine discharge of 852 m^3/s and a WEP turbine discharge of 620 m^3/s.

5. SUMMARY AND CONCLUSIONS

The high resolution, 3-D coastal circulation numerical model COCIRM was successfully adapted and optimized through extensive calibration and validation processes in supporting the WEP environmental approval and engineering. A key issue of the WEP environmental assessments is the potential effects of the WEP operations on the flows in the confluence area of the Columbia and Pend d'Oreille rivers, which provide important habitats for white sturgeon, such as the deep water, low-speed Waneta Eddy for sturgeon rearing and feeding and the jet-like high-speed Pend d'Oreille River outflow for sturgeon spawning and egg deposition. In 2003, the 3-D model COCIRM was accepted as an acceptable basis for the WEP environmental assessment purposes by the Canadian regulatory agencies and First Nation groups based on a favourable peer review of the model by an anonymous numerical modeller of the Department of Fisheries and Oceans, Canada. The potential impacts of the WEP on the flows in the confluence area were examined using extensive model predictions with numerous flow combinations from the Columbia River, the existing Waneta Dam and the WEP. These predicted results show either positive or minor negative impacts of the WEP operations on the fishery habitats in the confluence area. Based in part on these numerical model studies, environmental approval for the WEP was granted in 2007.

In supporting the WEP engineering, the developed 3-D model was used to simulate the water elevations in Pend d'Oreille River and the near-bottom velocities in the Waneta headpond area under the impact of the WEP operations. The model was validated for both applications using the field survey data. It is found that the 3-D model is a useful tool for the WEP engineering issues in terms of good agreements between modeled and observed water elevations in Pend d'Oreille outflow, and velocities in the headpond area. In Pend d'Oreille River, the model results provide detailed information of water elevations at the existing and WEP tailraces as well as water surface profiles in the outflow area, which are essential for appropriate WEP tailrace design and construction. In the headpond area, the model provides detailed predictions of the changes in the near-bottom velocities resulting from the WEP operations. These predictions serve as a useful guide for the WEP diversion channel design, excavation, and necessary measures to prevent the bottom sediment contaminants from being resuspended during the construction of the WEP diversion channel and at the new flow conditions when the WEP is in operation.

6. ACKNOWLEDGEMENTS

We wish to express our appreciation to the Columbia Power Corporation for the opportunity to undertake this study, especially Bill Freeman, Victor Jameff, Elroy Switlishoff, Robert Teichroew, Wally Penner, Wally Malkinson and Theodora Borissov. We would also like to thank John Nunnm Radmila Krzman and Robin Fitzgerald of Klohn Crippen Berger Ltd. for providing the model inputs and overall direction, and Larry Hildebrand of Golder Associates Ltd. (formerly R.L. & L. Environmental Services Ltd.) for insights and advise related to the fisheries and biological issues. Thanks also extend to our colleagues Rick Birch, Dave Billenness, Vincent Lee, Dave English, Keath Borg, Rob Bowen and Bernadette Fissel for providing detailed field data, and graphic, mapping and administrative assistance.

7. REFERENCES

Birch, R., 1996. Current Velocity and Temperature Structure of the Waneta Eddy February 8-10, 1996. *March 1996 Report for Cominco Ltd.*, ASL Environmental Sciences Inc., Sidney B.C. Canada. 33 p. + appendices.

Birch, R., 1994. Current Velocity and Temperature Structure of the Waneta Eddy, Junction of the Columbia and Pend d'Oreille Rivers, B.C. May 18-19 & Aug 30-31, 1994. *March 1995 Report for B.C. Hydro*, by ASL Environmental Sciences, Sidney, B.C., Canada, Sidney, B.C., Canada, 22 p. + appendices.

Birch, R. and P. Boubnov, 2001. Current Velocity Structure of the Waneta Eddy, July 14-15, 2001. *August 2001 Report for Cominco Ltd. and Columbia Power Corporation,* by ASL Environmental Sciences Inc., Sidney, B.C., Canada, 28 p. + appendices.

Birch, R. and D. English, 2001. Data Report: Current Measurements in the Pend d'Oreille River. *October 2001 Report for Columbia Power Corporation and Cominco Ltd.* , by ASL Environmental Sciences Inc., Sidney, B.C., Canada, 29 p.

Casulli, V. and R.T. Cheng, 1992. Semi-implicit finite-difference method for three-dimensional shallow water flow. *International Journal for Numerical Methods in Fluids*, 15, 629-648.

Fissel, D.B. and J. Jiang, 2002. 3-D Numerical modeling of flows at the confluence of the Columbia and Pend d'Oreille Rivers: examination and evaluation of performance. *Report for Columbia Power Corporation* by ASL Environmental Sciences Inc., Sidney BC, Canada, xi + 78 p. + Appendices.

Fissel, D.B., J. Jiang, D. Billenness, K. Borg and J. Lawrence, 2008. 3D Numerical Modeling of Flows and Sediment Transport in the Waneta Dam Headpond: Model Development and Field Survey. *Unpublished Report for Columbia Power Corporation, Castlegar B.C.*, by ASL Environmental Sciences Inc., Sidney, B.C., Canada, vii + 43 p.

Fissel, D.B. and J. Jiang, 2008. 3D Numerical modeling of flows at the confluence of the Columbia and Pend d'Oreille rivers. In: *Estuarine and Coastal Modeling: proceedings of the eighth international conference*, ed. M.L. Spaulding. American Society of Civil Engineers, 928-941.

Hildebrand, L. 2001. White Sturgeon Spawning at Waneta – 2001 Investigations and Historical Data Summary. *Report for Columbia Power Corporation* by R.L. & L. Environmental Services Ltd., Castlegar, B.C., Canada.

Hildebrand, L. and D.B. Fissel, 1997. Measurement of Low Velocity Habitat in Waneta Eddy (Columbia River). *Report for Cominco Ltd.* by R.L. & L. Environmental Services Ltd., Castlegar, B.C., Canada.

Jiang, J., 1999. An Examination of Estuarine Lutocline Dynamics. *Ph. D. Thesis*, University of Florida, Gainesville, Florida, 226 p.

Jiang J. and D.B. Fissel, 2002. Numerical modeling of flows at the confluence of the Columbia and Pend d'Oreille Rivers: Phase 2 report for the proposed Waneta Expansion Project. *Report for Columbia Power Corporation* by ASL Environmental Sciences Inc., Sidney BC, Canada, xviii + 249 p. + unnumbered Appendices (on CD).

Jiang, J. and D. Fissel, 2008. 3D Numerical Modeling of Velocities in the Waneta Dam Headpond. *Unpublished Report for Columbia Power Corporation*, Castlegar B.C., by ASL Environmental Sciences Inc., Sidney, B.C., Canada, 40p.

Jiang, J., Fissel, D.B. and Topham, D. 2003. 3D numerical modeling of circulations associated with a submerged buoyant jet in a shallow coastal environment. *Estuarine, Coastal and Shelf Science*, 58, 475-486.

Mellor, G.L. and T. Yamada, 1982. Development of a turbulence closure model for geographical fluid problems. *Review of Geophysics*, 20(4), 851-875.

Millero, F.J. and A. Poisson, 1980. Density of seawater and the new International Equation of State of Seawater. *IMS Newsletter*, Number 30, g. Wright, ed., Special Issue 1981-1982, UNESCO, Paris, France, page 3.

Murphy, A. H. and R. L. Winkler, 1987. A general framework for forecast validation. *Monthly Waether Review*, 115, 1330-1338.

Orlanski, I.A. 1976. A simple boundary condition for unbounded hyperbolic flows. *Journal of Computational Physics*, 21, 251-269.

Smagorinsky, J. 1963. General circulation experiments with the primitive equations: I. the basic experiment. *Monthly Weather Review*, 91, 99-164.

AN INTEGRATED COMPUTATIONAL FLUID DYNAMICS AND FISH HABITAT SUITABILITY MODEL FOR THE POINTE DU BOIS GENERATING STATION

David S. Brown, M.Eng., P. Eng., KGS Acres, Winnipeg, Manitoba, Canada
Don MacDonell, M.N.R.M., North/South Consultants, Winnipeg, Manitoba, Canada
Kevin Sydor, M.Sc., P. Eng., Manitoba Hydro, Winnipeg, Manitoba, Canada
Nicholas Barnes, M.Sc., Manitoba Hydro, Winnipeg, Manitoba, Canada

ABSTRACT:
The Pointe du Bois Generating Station, originally constructed in 1911, is located on the Winnipeg River northeast of Winnipeg, and is currently the oldest hydroelectric generating station still in operation in Manitoba. Due to the age of this plant, the current facility needs major repair or replacement. In addition, the facility does not meet the standards defined by the current CDA Guidelines. As such, Manitoba Hydro is currently developing a cost-effective modernization solution that addresses the safety concerns while being sensitive to environmental and regulatory issues.

The Winnipeg River is one of the most productive lake sturgeon (Acipenser fulvescens) fisheries in southern Manitoba. In addition, lake sturgeon has been designated by the Committee on the Status of Endangered Wildlife in Canada as 'endangered' in the Winnipeg River and is being considered for listing under the Species at Risk Act by the federal government. The area immediately downstream of the Pointe du Bois G.S. exhibits a range of physical characteristics and flow conditions that appear to create conditions that results in important spawning habitat for lake sturgeon.

This paper describes innovative techniques involving the use of state of the art computational fluid dynamics (CFD) models in parallel with a habitat suitability index (HSI) model based on site-specific knowledge of lake sturgeon spawning behaviour to develop a integrated CFD/HSI model, which will be used to develop creative and practical physical solutions to maximize lake sturgeon spawning habitat downstream for any modernization work in the future at Pointe du Bois.

RÉSUMÉ:
La Centrale de Pointe du Bois, située sur la rivière Winnipeg au Nord-Est de Winnipeg, fut initialement mise en service en 1911. Elle est présentement la plus ancienne centrale hydroélectrique encore en service au Manitoba. Du fait de son âge, l'installation actuelle nécessite des réparations majeurs ou un remplacement. De plus, cette installation ne satisfait pas aux standards des Directives pour la sécurité des barrages de l'ACB. Par conséquent, Manitoba Hydro développe présentement une solution de modernisation rentable, qui vise à régler les préoccupations liées à la sécurité tout en considérant les enjeux environnementaux et réglementaires.

La rivière Winnipeg est l'hôte de l'une des plus productives populations d'esturgeon jaune (Acipenser fulvescens) du Sud du Manitoba. L'esturgeon jaune a récemment été désigné comme espèce "en péril" dans la rivière Winnipeg par le Comité de la Situation des Espèces en Péril au Canada, et est considéré pour être inscrit sur la liste des espèces en péril par le gouvernement fédéral. Le secteur immédiatement à l'aval de la Centrale de Pointe du Bois présente une importante diversité de caractéristiques physiques et de variété d'écoulement qui semblent créer des conditions bénéfiques aux habitats de fraie de l'esturgeon jaune.

Cet article présente des techniques innovatrices impliquant l'utilisation de modèles numériques hydrodynamiques combinés à un modèle d'indice de qualité d'habitat (IQH) développé sur la base de connaissances locales spécifiques sur le comportement de fraie de l'esturgeon, afin de générer un modèle intégré, qui aidera au développement de solutions pratiques et créatives, maximisant les habitats favorables à la fraie de l'esturgeon jaune à l'aval de futurs travaux de réaménagement à Pointe du Bois.

1 INTRODUCTION

1.1 History of Pointe du Bois and the Winnipeg River

The Pointe du Bois Generating Station (G.S.) is located on the Winnipeg River approximately 8.5 km upstream of the Slave Falls G.S., 170 km by road northeast of Winnipeg, 43 km east of Lac du Bonnet and 80 km southeast of Pine Falls as shown in Figure 1. The site is located entirely within Whiteshell Provincial Park. The Winnipeg River generally flows from southeast to northwest with its headwaters in Lake of the Woods in Northwestern Ontario and Minnesota and empties into Lake Winnipeg in Manitoba. The drainage area that contributes to the total Winnipeg River flow at Pointe du Bois is approximately 126,000 km^2.

There are 14 hydroelectric generating stations within the Winnipeg River drainage basin. Eight are located in Ontario upstream of Pointe du Bois on the Winnipeg, English and Rainy rivers and are owned and operated by Ontario Power Generation (OPG) and Abitibi Consolidated Inc. Manitoba Hydro owns and operates six generating stations along the Winnipeg River, including Pointe du Bois, Slave Falls, Seven Sisters, McArthur, Great Falls, and Pine Falls. Flows at Pointe du Bois are regulated mainly by dams at the outlets of Lake of the Woods and Lac Seul, located upstream of Pointe du Bois. The Lake of the Woods Control Board (LWCB) directs the management of the waters of these lakes and the Winnipeg and English rivers that contribute to inflows at Pointe du Bois. The LWCB was formed in 1919 and operates under Canadian and provincial legislation and a Canada-US treaty.

The existing Pointe du Bois generating station and associated water control structures, shown in Figure 2, were constructed between 1909 and 1926. The powerhouse was constructed in two phases, with the first phase commissioned in 1911 (Units 1 to 4 and 7) and the next eleven units phased in by 1926 to the present capacity of 72MW. The site also has ninety-two spillways and five sluiceways, in which all but six of the spillways are manually operated and take significant time and effort to open and close. Despite extensive ongoing maintenance and upgrades over the years, the existing facilities require major repair or replacement to maintain current dam safety standards, provide a safer working environment for staff, and ensure reliability of power production.

The Pointe du Bois G.S. is a run of the river station that has a maximum rated flow capacity through the turbines of approximately 710 m^3/s, although this flow is rarely ever realized through the powerhouse due to the deterioration of the plant. During periods when the flow exceeds the plant capacity, excess water is passed through the spillway and flows over the spillway rapids to the river downstream of the G.S. The estimated average daily flow for the Winnipeg River at Pointe du Bois is approximately 880 m^3/s. As such, it is quite a common occurrence to have flow pass over the spillway rapids.

Although well constructed, the Pointe du Bois G.S. suffered considerable deterioration through the first 40 years of operation, mainly related to durability and performance of early concrete mixes. In 1954 a study to determine the station's condition and alternatives for redevelopment was undertaken by the City of Winnipeg, which owned the asset at the time. The most feasible alternative was to extend the facility's reliable lifespan by 20 years through rehabilitation, and defer redevelopment until a later date nearer the existing facilities end of life. Issues of plant condition, efficiency and capacity were again re-evaluated in the mid-1970s during the operation licence renewal. Studies undertaken in 1971 and 1977 concluded again that the existing facility had considerable useful life remaining and continued operation, maintenance and rehabilitation were favourable versus redevelopment.

Given the increased deterioration and age of the plant by the 1990s, Manitoba Hydro increased the intensity of studies to evaluate modernization alternatives and a decision will be made later this year. These studies are focusing on developing a modernization alternative that meets the following key objectives: 1) minimizes the environmental effects, 2) provides an economical project, 3) minimizes negative socio-economic effects, and 4) eliminates the current dam safety concerns. Of particular concern from an environmental perspective is the potential impact of the modernization project on lake sturgeon (*Acipenser fulvescens*) spawning habitat downstream of the Pointe du Bois G.S. This paper focuses on the technical aspects of a tool that is being

developed for use in the environmental assessment and design process to minimize potential effects of the project on the suitability of aquatic habitat for lake sturgeon spawning.

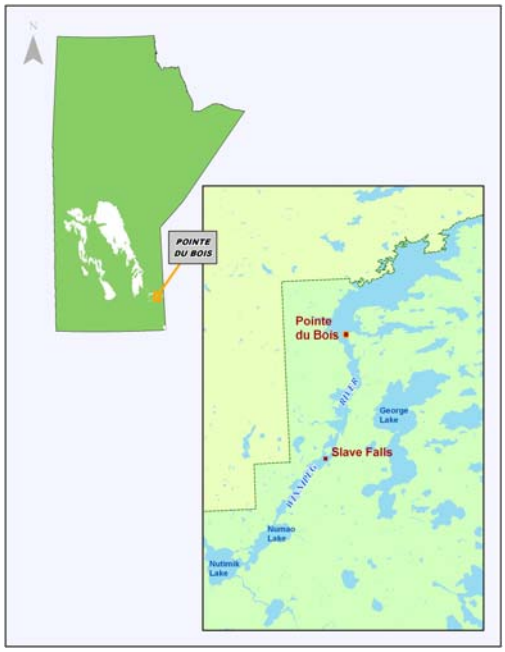

Figure 1: Location of Pointe du Bois

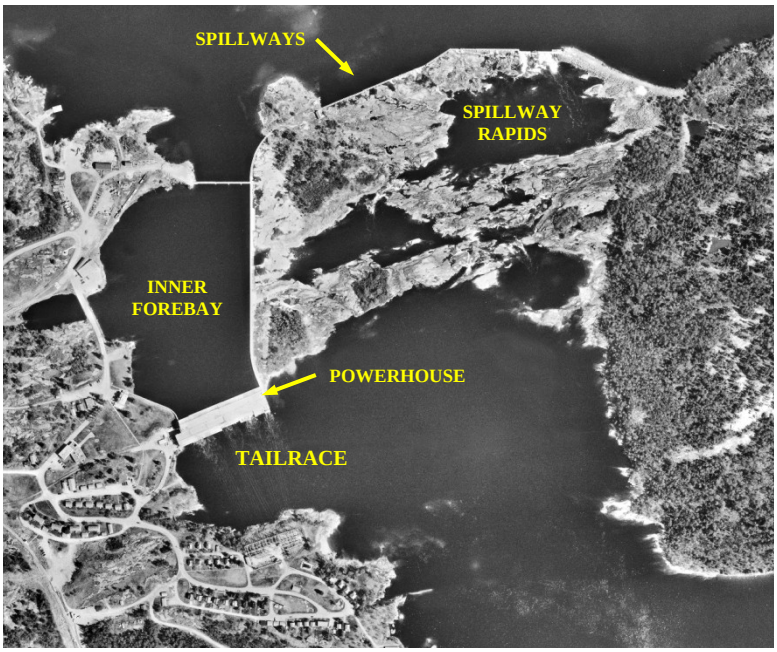

Figure 2: Pointe du Bois Structures and Site Plan

1.2 Importance of Winnipeg River as Lake Sturgeon Habitat

The lake sturgeon is the largest strictly freshwater fish in Canada, reaching lengths of up to two metres and weights in excess of 140 kilograms. In addition to their size, lake sturgeon possess a number of other biological traits that distinguish them from other freshwater fish including longevity (>100 years), old age at maturity (up to 20 years), and extended spawning periodicity (up to five years between spawning). Lake sturgeon spawn in spring and typically migrate up rivers to turbulent rapids or falls to deposit eggs. Spawning can take place in depths of less than one metre to thirty metres over gravel, cobble, boulders, and jagged bedrock substrates that provide sufficient interstitial spaces for egg incubation and oxygenation. Spawning generally takes place at water temperatures of 9 to 14^{o}C and the eggs require approximately eight days to hatch. The larvae will remain in the substrate until the yolk sac is absorbed (approximately 16 days) and then drift downstream where they will seek out suitable habitat for foraging

Lake sturgeon was once an abundant species across the Lake Winnipeg drainage basin. Commercial exploitation of stocks beginning in the late 1800s and habitat changes have resulted in severely depleted populations. Although lake sturgeon remain abundant in certain portions of the Winnipeg River, the population has been designated as “endangered” by the Committee on the Status of Endangered Wildlife in Canada (COSEWIC) and is currently being considered for listing under Species at Risk Act (SARA) by the federal government.

The lake sturgeon population between Pointe du Bois G.S. and Slave Falls G.S. is one of the populations within the Winnipeg River that appears to be thriving. This reach of the river is currently thought to provide optimal habitat for all life stages of the species. The area immediately downstream of the Pointe du Bois G.S. and spillway provides the only spawning habitat in the reach. As such, it will be important to maintain this habitat when modernization of the existing facility at Pointe du Bois is undertaken.

2 INTEGRATED CFD & HSI MODEL

As noted above, the reach of the Winnipeg River downstream of Pointe du Bois contains one of the most abundant populations of lake sturgeon in Manitoba. Any changes to the flow regime downstream of Pointe du Bois associated with the modernization could affect the population of lake sturgeon. However, the structural condition and safety concerns associated with the existing generating station means that changes would have to occur. Therefore, Manitoba Hydro considered it essential to carefully consider the environmental effects of any proposed modernization alternative on lake sturgeon habitat. One of the primary tools in this evaluation was the use of an integrated Computational Fluid Dynamics (CFD) and Habitat Suitability Index (HSI) model. An HSI model is used to assess how well a given body of water can support a particular fish life stage and species or to evaluate impacts on fish habitat resulting from water regime changes. As such, an HSI model can be used as a design tool for any modernization alternative to determine potential effects of construction and operation on lake sturgeon spawning areas, as well as, to incorporate mitigation measures that could improve the areas around the structures for lake sturgeon spawning.

Due to the complex nature of the hydraulics at the Pointe du Bois site to estimate the hydraulic conditions within the lake sturgeon spawning areas it was determined that a detailed three-dimensional CFD model would be required. The complex hydraulics of the spillway flow as it discharges off of the spillway rapids into the spawning habitat cannot be captured accurately with a model of less sophistication than a three-dimensional model. The CFD model has the capability to estimate the flow patterns and velocity conditions for a range of river flows immediately downstream of the spillway rapids in sufficient detail to be incorporated into the HSI model.

The HSI model is being developed using the detailed hydraulic outputs from the CFD model, along with site-specific characteristics of the river related to lake sturgeon. There is ample literature regarding lake sturgeon spawning habitats that both supports and contradicts the presence of the successful lake sturgeon spawning in the Winnipeg River both downstream of the Pointe du Bois G.S. and downstream of the Slave Falls G.S. As such, significant effort has been spent by Manitoba Hydro to research and understand the spawning characteristics of lake sturgeon at the two generating stations. The incorporation of this site-specific information to the HSI model is considered to be crucial to the successful application of the model in replicating the existing conditions and predicting spawning conditions under a range of flow conditions.

At the subsequent phases of the Pointe du Bois Modernization Project, the integrated CFD/HSI model will be used in the process for assessment and selection of the general arrangement for the project, and in developing compensation designs that sustain high quality lake sturgeon spawning habitat.

3 AQUATIC STUDIES AT POINTE DU BOIS

Manitoba Hydro has been active in monitoring the spawning and other life stages of the lake sturgeon downstream of Pointe du Bois from 2006 to 2009. The aquatic activities have focused on gaining an understanding of the size and condition of the population, the habitat utilization near the structures at Pointe du Bois, identification of the important habitats including the physical attributes of those habitats, as well as the extent of lake sturgeon movements in the vicinity of Pointe du Bois.

These studies have included carrying out detailed substrate typing that using a number of methods that include a Quester Tangent vertical echo-sounder to discriminate acoustic classes, Ponar studies to validate the substrate classifications, underwater videography, and scuba surveys.

Specific activities that were carried out to understand the behaviour and spawning preferences of lake sturgeon included carrying out an egg deposition study, by placing egg collection mats in all potential spawning areas, carrying out larval drift studies, and monitoring the presence of mature/spawning sturgeon with large-mesh gill nets.

In addition to the substrate and aquatic studies described above, Manitoba Hydro carried out a number of detailed velocity measurements during the spawning seasons using an Acoustic Doppler Current Profiling (ADCP) instrument to determine both depth averaged velocities and velocities immediately above the riverbed in the locations of known spawning grounds. The ADCP data proved to be important, not only in the calibration/verification of the CFD model, but also for the validation of how the depth-averaged velocities from the CFD model related to the near bottom velocities. Water levels were also recorded at several locations during spawning.

The aquatic studies markedly improved the understanding of the behaviour and spawning preferences of lake sturgeon and are contributing to the development of an integrated CFD/HSI model to represent the suitable lake sturgeon spawning areas at Pointe du Bois.

4 HYDRAULIC CHARACTERISTICS OF POINTE DU BOIS

4.1 CFD Model

The computational fluid dynamics (CFD) model component of the HSI model that was adopted for the study was the FLOW-3D numerical model developed and supported by Flow Science, Inc. of Santa Fe, New Mexico, USA. FLOW-3D is a well-tested commercial software used in CFD modelling. Using numerical techniques, FLOW-3D solves the equations of fluid motion to obtain transient, three-dimensional solutions to multi-scale, multi-phase flow problems. FLOW-3D has been utilized numerous times in the past for assessing complex hydraulic problems by Manitoba Hydro in the design future generating stations such as Wuskwatim, Keeyask, Conawapa, as well as assessing existing concerns such as those that exist at the Kelsey G.S. powerhouse intake (Groeneveld, et al. 2001).

To complete the numerical analyses, FLOW-3D uses a rectangular grid of variably sized cells, termed a computational mesh, to define the flow region. The geometry of the fluid region is defined within the rectangular grid by computing the volumes of each grid cell that is either blocked by solid object or open to fluid. For each cell, fluid flow quantities such as velocity, pressure, and density are retained and finite-difference approximations to the equations of motion are then used to calculate the temporal and spatial distribution of these values. The finite-difference method is designed to solve the CFD governing equations for a fluid flow (i.e. the continuity equation and Navier-Stokes equations).

4.2 Model Development

Computational Domain

The FLOW-3D model developed for Pointe du Bois consists of a reach of the Winnipeg River that extends both upstream and downstream of the existing generating station. It should be noted, however, that the focus of the HSI model is primarily on the downstream side of the station.

The river bathymetry and topography that define the Winnipeg River from Eight Foot Falls (1.4 km downstream of the Pointe du Bois G.S.) to approximately 400 m upstream of the existing spillways was used to define the elevation data input to the FLOW-3D model. The elevation data was input into FLOW-3D as X, Y, and Z coordinates at a 5 m by 5 m resolution in the X and Y directions. For the model to correctly represent the flow patterns downstream of the Pointe du Bois G.S., the downstream model extent was situated just upstream of Eight Foot Falls.

The sizing of the computational mesh adopted for the model was selected so as to balance computation performance against accuracy of model results during the model development stage. In order to capture more detail near the powerhouse, a detailed mesh with a sizing of 1.25m x 1.25m x 0.5m in X, Y and Z directions was used in the powerhouse intake area for the upstream model and in the tailrace for the downstream model. For areas further from the powerhouse, a coarser mesh (5m x 5m x 1m) was used. This mesh size was judged to be

the optimum size to adequately define the hydraulic characteristics of the river, while at the same time minimizing the computational time.

Boundary Conditions

The upstream boundary of the model (i.e. the outer Forebay) was defined in the model as a water level equivalent to the forebay Full Supply level (FSL) of 299.10 m.

The downstream boundary of the model (i.e. Winnipeg River just upstream of Eight Foot Falls) was also defined as a water level. The downstream water levels, or tailwater levels, were based on the tailwater rating curves for the river downstream of the Pointe du Bois G.S developed in previous studies by KGS Group and Manitoba Hydro. It should be noted that, although, the tailwater rating curve represents the water levels at the powerhouse, it was considered to be acceptable, since the water levels between the location of the model boundary and the powerhouse do not differ significantly for the relatively low flows being considered for this assessment. The water levels in this reach are governed by the control at the Slave Falls G.S., the narrows just upstream of Slave Falls G.S., and Eight Foot Falls. There begins to be a noticeable difference in water levels between the G.S. and Eight Foot Falls for flood flows in excess of about 2,000 m^3/s.

To improve the simulation efficiency, the CFD model was divided into two parts along the axis of structures. Therefore, inflows and outflows corresponding to the flow capacities of the spillway and powerhouse were utilized to represent the flow that passes through the structures. For the model simulations of the existing environment, the spillway discharge for the downstream part of the model was defined by locating the inflow source in the bottom of the upper most pool on the spillway shelf rather than along the spillway axis. This was done to simplify the numerical simulations, since the flow immediately downstream of the spillway is very turbulent. As well, the geometry in this area is also very complicated.

Analysis of Model Results

Due to the complex hydraulic nature of the spillway rapids in combination with the large sized computational domain, the time for the model simulations to reach nearly steady-state conditions was quite significant, ranging from four to seven days of computational time for each model simulation. Near steady-state conditions were achieved by comparing the computed flow rates from the model to the input flow rates defined at the model boundaries until they were near equivalent. To assess the steady state hydraulics, several time steps were selected from the output dataset and using a customized post-processor. Hydraulic characteristics such as, water surface elevation, flow depth, depth-averaged velocities, as well as velocity and turbulent kinetic energy at 1 m above the riverbed were extracted from the FLOW-3D model output for post-processing. These hydraulic characteristics were converted into a 5m x 5m ArcGIS grid file that could be transferred as input to the HSI model.

4.3 Model Calibration

The FLOW-3D model was calibrated for the May 19, 2007 flow conditions at Pointe du Bois, which coincided with the timing of the lake sturgeon spawning in 2007. During the spawning monitoring program that was being carried out at the time, Manitoba Hydro completed a number of hydrometric surveys to complement the fisheries data. Vertical velocities within the river downstream of the G.S. were recorded with the use of an Acoustic Doppler Current Profiling (ADCP) instrument, which estimates the horizontal and vertical velocity components as a function of depth.

The flow conditions that occurred in May of 2007 represent a relatively low flow condition with all of the flow being conveyed though the powerhouse and not the spillway. In contrast, during May of 2006, flows were relatively high and the spillways were used to spill excess flow, however, there was no ADCP data recorded that year. Therefore, the model calibration could only be carried out for flow conditions that are representative of powerhouse flow. As well, ADCP velocity profiles were only obtained in the tailrace of Pointe du Bois and not in the forebay; therefore, this data could only be used to calibrate the downstream part of the model. As a result,

the upstream part of the model could not calibrated to recorded velocity data; however, any adjustments that were required to the downstream part of the model based on the calibration was also made to the upstream part.

The flow conditions at Pointe du Bois for May 19, 2007 were defined using both the daily hydraulic records from the powerhouse, as well as, the flows recorded from the ADCP measurements. There was a minor discrepancy between the ADCP discharge estimates and those listed in the daily hydraulic report. Therefore, to ensure that the model was simulating the hydraulic conditions for the same flow as for the ADCP recorded velocities, the powerhouse flow was defined as the flow that was recorded by the ADCP. The flow and operating conditions adopted for the May 19, 2007 model calibration simulation are:

- Total River Flow = 473 m^3/s
- Forebay Water Level = 299.06 m
- Tailrace Water Level = 284.69 m
- Powerhouse Flow = 470 m^3/s (Turbines #1, 2, 5, 8, 9, 12, 15, 16, Service Unit #1)
- Spillway Gate Leakage Flow = 3 m^3/s

A comparison of the recorded velocities along one of the ADCP transects and the estimated velocities are shown in Figure 3. The ADCP profiles show a significant deviation, or noise, in the velocity magnitude across the transect. This is due to the fact that the ADCP instrument was used to record velocities across a transect in fairly turbulent flow conditions. ADCP instruments are better suited to recording the velocities over time in a fixed position. That being said, the ADCP data provided a good verification of the model velocities and flow patterns and demonstrated that the model produced a good representation of these hydraulic parameters.

In addition to the hydraulic data that was used to calibrate the FLOW-3D model, a series of hydraulic characteristics were provided for both the assessment of the aquatic data collected during the 2007 spawning monitoring program and the development and calibration of the HSI model. This data included the flow depth, the depth-averaged velocity, the velocity 1 m above the riverbed, and the turbulent kinetic energy (or turbulence) 1 m above riverbed for flow conditions observed on May 19, 2007. Figure 4 shows the model results for some of the parameters provided as input to the HSI model.

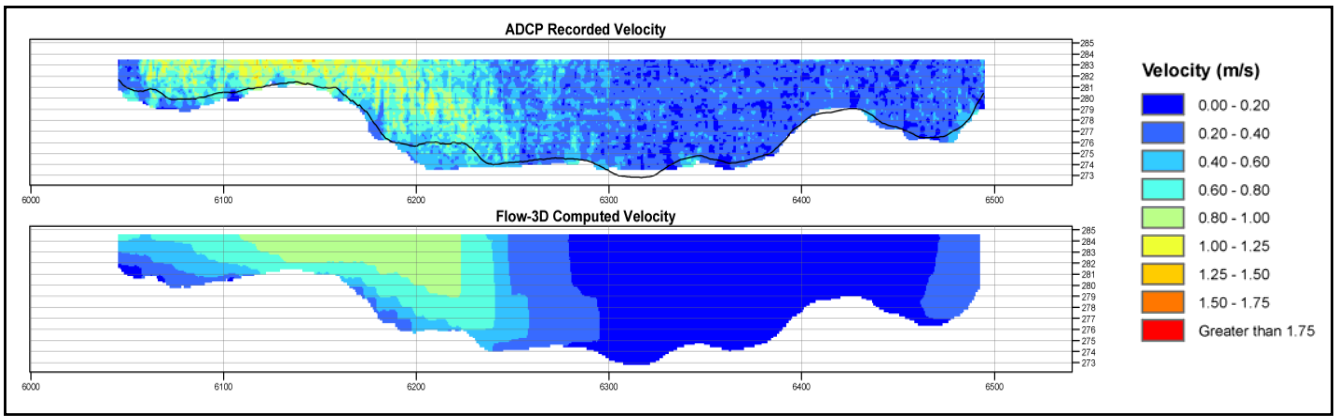

Figure 3: Comparison of Recorded and Estimated Velocities

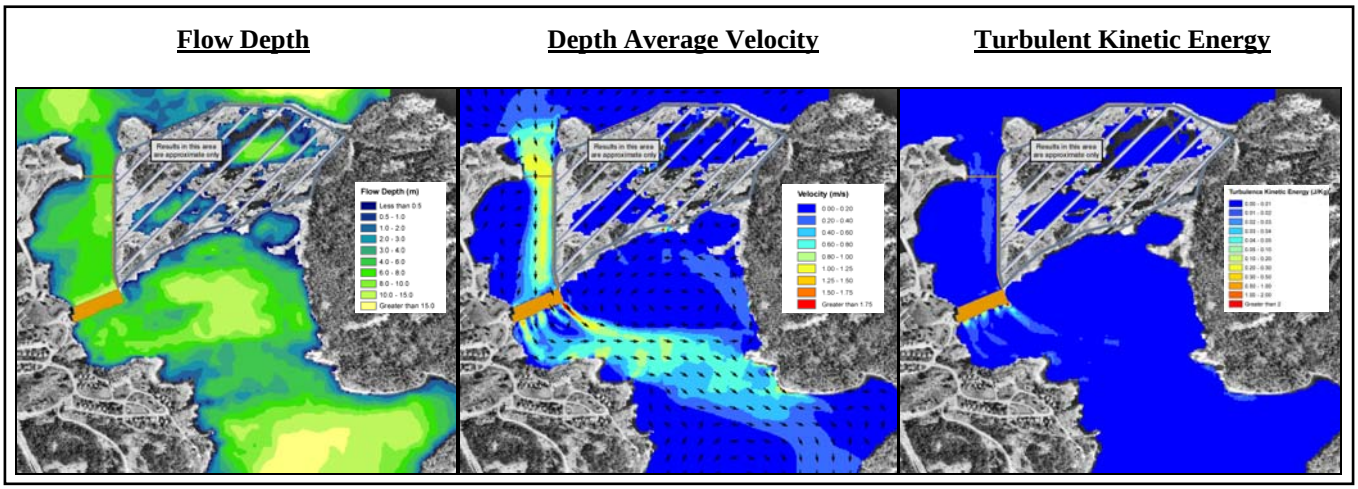

Figure 4: Estimated Hydraulic Conditions for May 19, 2007

4.4 Replication of Existing Flow Conditions

In addition to using the CFD model to replicate the hydraulic conditions on May 19, 2007, the model was used to estimate the conditions that occurred during other lake sturgeon spawning monitoring programs carried out on May 14, 2006 and May 29, 2008. These hydraulic conditions were utilized, in combination with the results from the May 17, 2007 simulation to validate the HSI model for the existing environment. Incorporation of the flow conditions in both 2006 and 2008 into the HSI model was important as in each of these years the spillway was passing flow during the lake sturgeon spawning season. These CFD model results provided important hydraulic information for the HSI model for the area immediately downstream of the spillway rapids. The flow conditions for the flood events of both 2006 and 2008 were very similar and are outlined below. Figure 5 shows the replicated depth average velocities for the flow conditions that occurred on May 14, 2006.

May 14, 2006

- Total River Flow = 1,318 m^3/s
- Forebay Water Level = 299.06 m
- Tailrace Water Level = 285.23 m
- Powerhouse Flow = 636 m^3/s
- Spillway Flow = 682 m^3/s

May 29, 2008

- Total River Flow = 1,261 m^3/s
- Forebay Water Level = 299.08 m
- Tailrace Water Level = 285.25 m
- Powerhouse Flow = 583 m^3/s
- Spillway Flow = 678 m^3/s

As noted in Section 4.3, the calibration confirmed that the model was replicating the hydraulic conditions during flow conditions when all the river flow is being conveyed through the powerhouse. However, to provide confidence in the model for the simulations in which there is spillway flow, the model results from both the 2006 and 2008 flow conditions were compared to a number of air photos that illustrate the flow conditions for similar river flows with spillway operation. This comparison confirmed that the model accurately predicts the flow patterns over the spillway rapids and downstream towards Eight Foot Falls, as illustrated in the example showing the comparison of the CFD model results in Figure 5 to the air photo in Figure 6. In addition to these air photos, the estimated water levels on the spillway rapids were compared to, and were consistent with water levels that were surveyed for similar spill conditions. Therefore, it can be concluded that the FLOW-3D model accurately represents the flow conditions for powerhouse flow only, as well as for those flow conditions that include spillway flow.

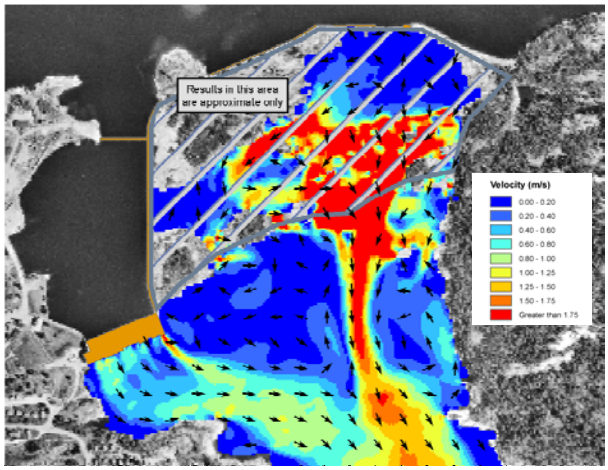

Figure 5: Estimated Hydraulic Conditions for May 29, 2008

Figure 6: Air Photo of Flow Conditions (June 29, 2006)

5 HABITAT SUITABILITY INDEX MODEL

5.1 Application of HSI Models

Habitat suitability approaches have been widely used in fisheries for decades (Bovee 1978; Bovee 1982). This approach can be divided into two basic components: habitat suitability criteria (HSC) which includes generating ranges of fish species utilization for variables of interest and habitat suitability indices (HSI) which are the combined expression, through multiplication, of the derived HSC. HSC have three categories: Category 1 HSC made up by either expert opinion or the Delphi Approach (Crance 1984); Category 2 HSC are developed using occurrence data (Stalnaker et al. 1995); and Category 3 HSC are developed via the relationship of occurrence divided by habitat availability (Stalnaker et al. 1995). Category 3 HSC is essentially considered as a probability of a fish occupying a certain habitat in relation to its availability. Standard HSI model applications have typically utilized depth, velocity, and substrate for characterizing fish habitat.

5.2 Development of Site-Specific HSI Model for Pointe du Bois

The HSI model parameters for the Pointe du Bois site are being developed based on a combination of lake sturgeon spawning habitat suitability information contained in the literature as well as the results of the aquatic studies that were undertaken at Pointe du Bois.

The parameters that promote successful lake sturgeon spawning were reviewed in the literature from available sources where spawning was known to occur, was observed, and/or was described in detail. Category 2 HSC curves were then developed for lake sturgeon as a species for depth, velocity, and substrate. These Category 2 curves were developed from literature by making histograms for each variable based on the ranges described in the literature sources.

The Category 2 curves that were developed based on the literature review were assessed for the Pointe du Bois tailrace and spillway sites using the results of the aquatic studies at both Pointe du Bois and Slave Falls between the spring of 2007 and 2008. The curves were then refined based on this site-specific information on lake sturgeon occurrence and egg mat studies aimed at locating the microhabitats where eggs were deposited. This refinement of the Category 2 curves essentially produced Category 3 HSC for depth, velocity, and substrate. The habitat suitability curves that were adopted for these three parameters are shown in Figures 7, 8, and 9 respectively. These curves show how the various sources of information (literature and site-specific occurrences) were utilized to develop the site-specific habitat suitability curves.

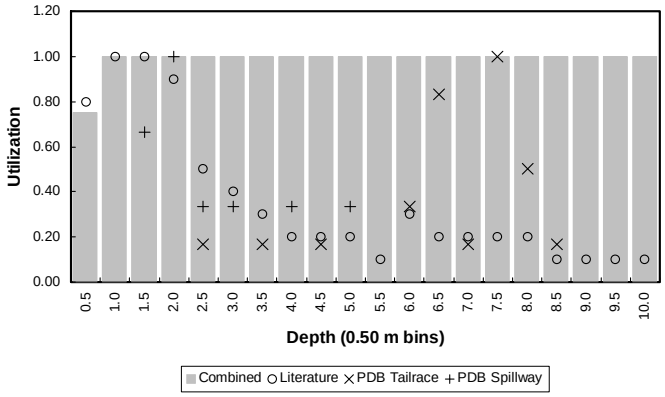

Figure 7: Habitat Suitability Curve for Depth

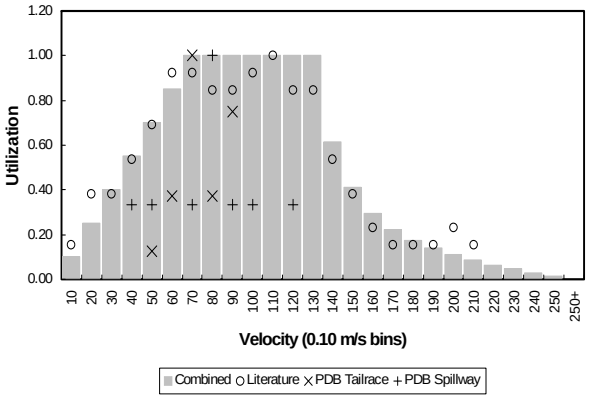

Figure 8: Habitat Suitability Curve for Depth Averaged Velocity

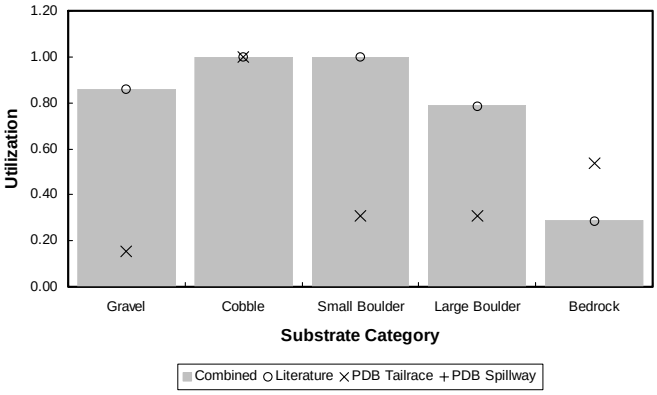

Figure 9: Habitat Suitability Curve for Substrate

Two additional variables were incorporated in the HSI model, based on the knowledge of fish behaviour gained through field studies to better represent the preferred lake sturgeon spawning habitat and include 1) the direction of river flow and 2) distance from an impassable barrier or origin of a supercritical flow boundary.

The utilization of flow direction in the model was in direct response to the strong geological control of the Precambrian Shield bedrock on flow patterns, which sometimes created large back eddies with marked upstream flows as shown in the CFD model results presented in Figure 4. Based on the field observations, fish were known to orient themselves in an upstream location and would not select back eddy areas where they were facing downstream. When the HSI model included use of flow direction, large back eddies or areas of where the flow moved upstream were shown to be unsuitable, which supported the observed egg distributions.

While microhabitat selection was apparent within and among years of the aquatic studies at Pointe du Bois, a macro habitat pattern was clearly evident; 95% of the egg deposition occurred within 85 m downstream of the generating station or spillway rapids, over a range of depth and several hard and clean substratum types. This is shown in Figure 10, shows the abundance of eggs on each egg mat (crosses) and the total abundance of eggs in 20 metre intervals (red line) from the impassable barrier or origin of super critical flow and defines the equation used to model this variable. Consequently, the area modelled as suitable for lake sturgeon egg deposition using only four variables (depth, substrate, depth averaged velocity, and flow direction) was large relative to the area where eggs were observed. This suggests that sturgeon at this site prefer to ascend to near the origin of the attractant flow and are likely to use a fraction of habitat modelled as suitable. Therefore, the distance from an impassable barrier or origin of a supercritical flow boundary was incorporated into the model as a fifth parameter.

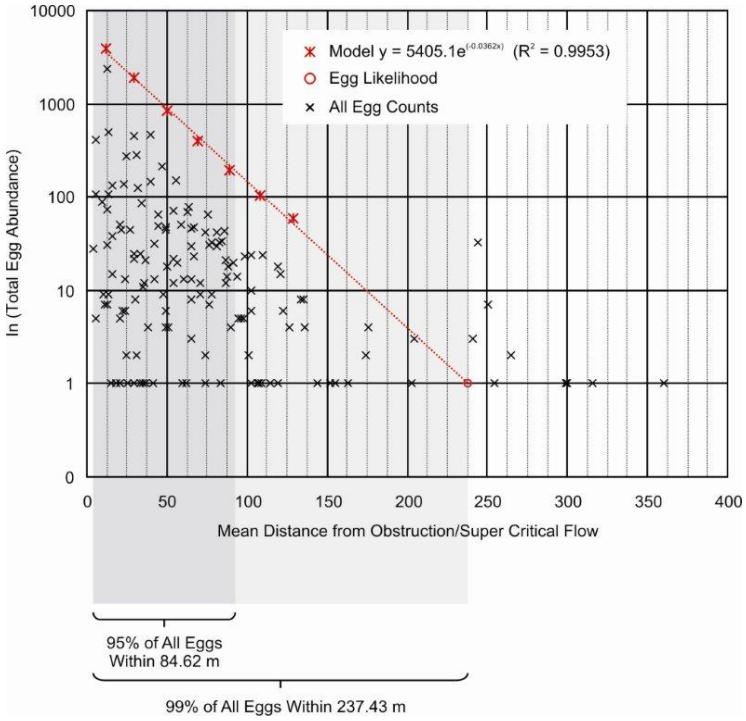

Figure 10: Egg Density versus the Distance from an Impassable Barrier

5.3 Comparison of HSI Model to Observed Spawning Patterns

The two-dimensional grid data output from the CFD model was used with the habitat suitability curves, or distance equation, to map each of the five habitat criteria. An example of the individual spawning habitat suitability for four of the five model parameters associated with the May 19, 2007 flow condition is shown below in Figure 11.

A typical weighted useable area (WUA) approach was then applied to determine the cumulative area of suitable spawning habitat based on the product of HSC curves. This method estimates habitat suitability values by multiplying the individual utilization rates of the different areas for the five parameters. Two-dimensional cells are established containing homogeneous HSI values. A schematic illustrating the WUA for the standard three-parameter HSI model is presented in Figure 12.

The combined lake sturgeon spawning habitat suitability for the May 19, 2007 flow condition is shown in Figure 13. It is shown by comparing the locations of egg deposition for the May 2007 spawning event, shown in Figure 14, that the HSI model provides good agreement to the observed spawning patterns.

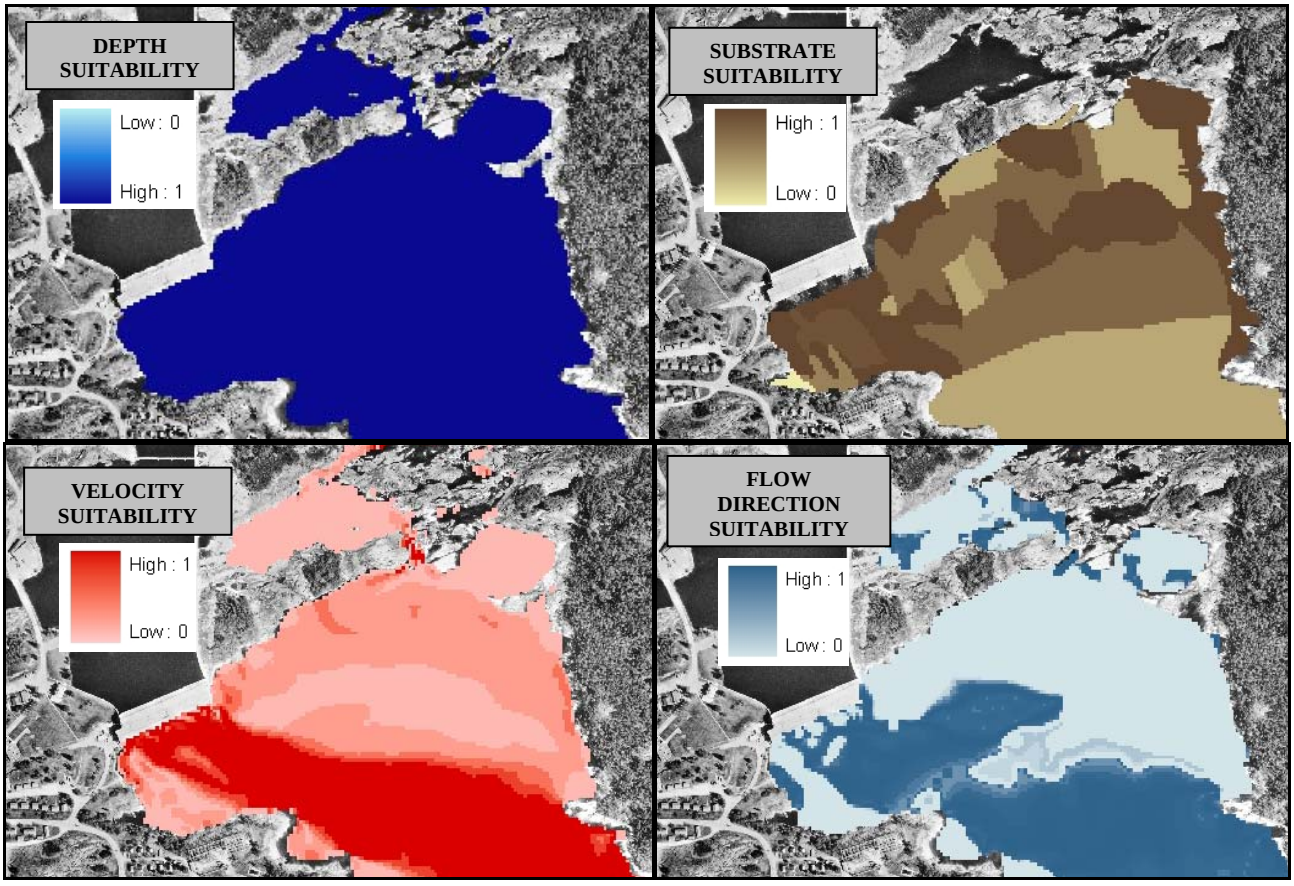

Figure 11: Habitat Suitability for the Model Parameters for the May 19, 2007 Flow Condition

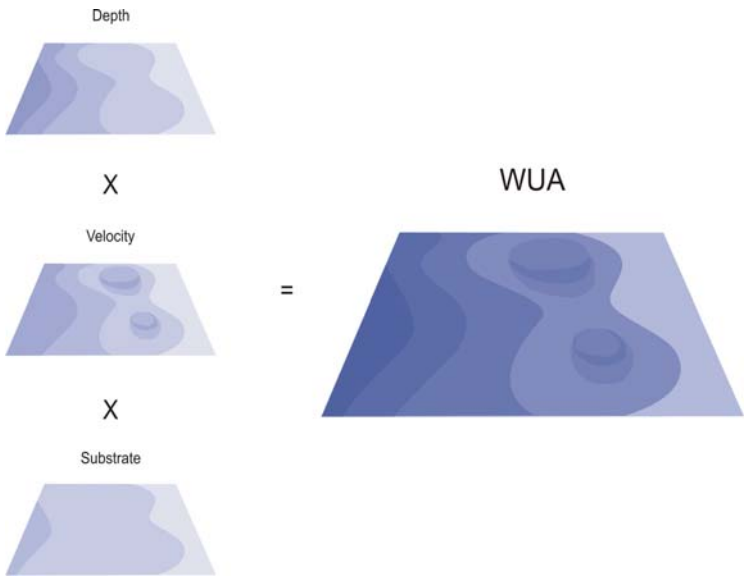

Figure 12: Schematic Diagram of Weighted Usable Area

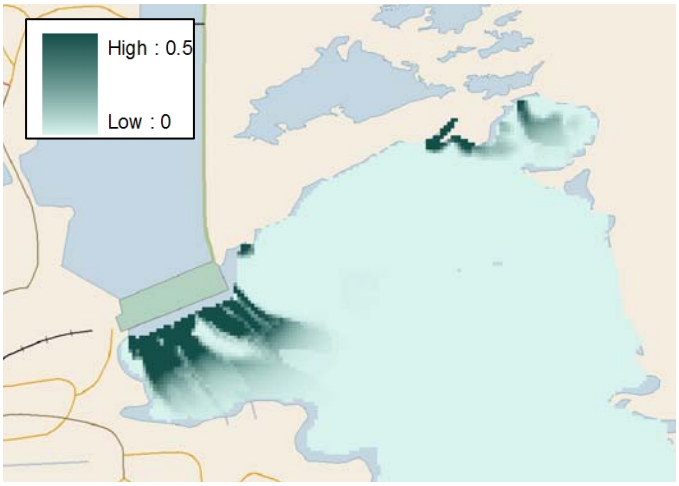

Figure 13: Lake Sturgeon Spawning Suitability for May 19, 2007 Flow Conditions (Five-Parameter HSI Model)

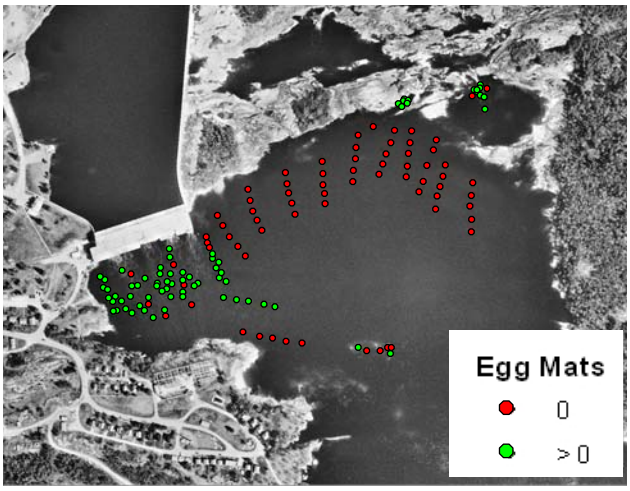

Figure 14: Egg Deposition for May 19, 2007

The five-parameter HSI model was also used to estimate the suitable area for spawning that would have existed during the May 2008 spawning season. The HSI model results were compared to the observed egg deposition characteristics that occurred in May 2008, during a spill condition. As illustrated by comparing the HSI model results shown in Figure 15 and the observed pattern of egg deposition shown in Figure 16, it is clear that the model generally is in good agreement with the observed data. However, it should be noted that additional aquatic studies took place during the lake sturgeon spawning this past spring at Pointe du Bois in May of 2009. Subsequent to a detailed review of this data, the five-parameter HSI model, as presented within this paper, will be reviewed to ensure that it replicates the observed spawning this past year. At this point, the HSI model may be re-calibrated, if required, to even more accurately reflect the observed spawning patterns. As part of this re-calibration, additional parameters, such as turbulence, will be reviewed for applicability for inclusion into the HSI model.

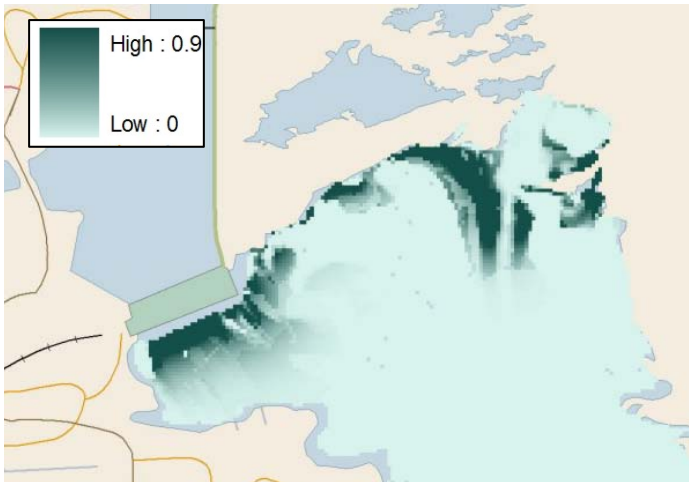

Figure 15: Lake Sturgeon Spawning Suitability for May 29, 2008 Flow Conditions (Five-Parameter HSI Model)

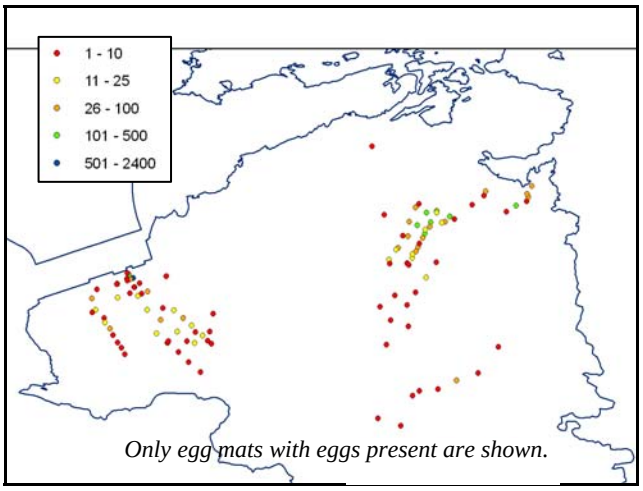

Figure 16: Egg Deposition for May 29, 2008

6 SUMMARY

The Pointe du Bois G.S. is reaching the end of its useful life, and as such, Manitoba Hydro is currently reviewing options for modernization. Since lake sturgeon has recently been designated by COSEWIC as 'endangered' and is being considered for listing under the SARA by the federal government any modernization alternatives for this project must be designed with consideration of the successful lake sturgeon-spawning habitat immediately downstream of the Pointe du Bois powerhouse and spillway rapids.

With this in mind, and in addition to the numerous aquatic studies on lake sturgeon over the past number of years at Pointe du Bois, Manitoba Hydro is working with KGS Acres and North/South Consultants to develop an integrated CFD/HSI model to assess the areas of suitable spawning habitat of the existing environment downstream of the generating station. This integrated CFD/HSI model is being developed based on both information contained within the literature and on site-specific data. The model developed to date has proven to be reasonably accurate in replicating known locations of lake sturgeon spawning activity for a range of flow conditions in the Winnipeg River. Site-specific data continue to be examined for refinement of the model and possible inclusion of additional parameters. The final integrated CFD/HSI model will be used as a design tool in the selection and screening of modernization alternatives, as well as in the design of a preferred alternative. Specifically, the model will be used to assess the post-project change in the availability of lake sturgeon spawning habitat and to incorporate suitable spawning habitats into the design of new structures.

7 ACKNOWLEDGEMENTS

The authors of this paper would like to acknowledge the efforts of all those members of the Manitoba Hydro, KGS Acres, and North/South project team that have provided their input and expertise to the completion of this study. Specific acknowledgements are directed to the members of the Eco-Hydraulic Committee from Manitoba Hydro, hydraulic engineer and numerical model specialist Mr. Junying Qu, Ph.D., P. Eng. from KGS Acres, and aquatic biologists Mr. Paul Cooley, Ph.D., and Mr. Patrick Nelson, Ph.D. from North/South Consultants.

8 REFERENCES

Bovee, K.D. 1978. "The incremental method of assessing habitat potential for coolwater species, with management implications". American Fisheries Society Special Publication 11: 340-346.

Bovee, K.D. 1982. "A guide to stream habitat analysis using the instream flow incremental methodology". Instream Flow Information Paper 12. U.S. Fish and Wildlife Service FWS/OBS-82/26. 248p.

Crance, J.H. 1984. "Habitat suitability index models and instream flow suitability curves: inland stocks of striped bass". U.S. Fish and Wildlife Service FWS/OBS-82/10.85 63p.

Flow Science Inc., 2005. "FLOW-3D User's Manual Version 9.0"

Groeneveld, et al. 2001. "Optimization of Hydraulic Design using Computational Fluid Dynamics". Waterpower XII Conference , July 2001, Salt Lake City, Utah.

Stalnaker, C., Lamb B.L., Henriksen J., Bovee K.D., and Bartholow J., 1995. "The instream flow incremental methodology a primer for IFIM". U.S. Department of the Interior National Biological Service, Biological Report 29. 45p.